NOVEL ATHEROPROTECTIVE MEDIATORS: SPRR3-EXPRESSING VASCULAR SMOOTH MUSCLE CELLS

By

Amanda K. Segedy

Dissertation

Submitted to the Faculty of the

Graduate School of Vanderbilt University

in partial fulfillment of the requirements

for the degree of

DOCTOR OF PHILOSOPHY

in

Pathology

May, 2015

Nashville, Tennessee

Approved:

Professor Larry L. Swift

Professor W. Gray Jerome

Professor Colleen M. Brophy

Professor MacRae F. Linton

Professor Pampee P. Young

To my loving family

and

to Amelia Ruth, my little thesis baby

ACKNOWLEDGMENTS

The journey to completing this body of work has been a long one and could not have been accomplished without help from many kind, generous souls. My heartfelt thanks go to:

- My parents, who have given generously of themselves to share with me a love of learning and of God's glorious creation. Some of my most beloved memories from childhood include: crashing through underbrush, looking for praying mantis egg pouches and counting the hitchhikers on our jeans; changing the salt on the Cornish hen we mummified one summer in a shoebox under our television; late night car rides discussing how things work; bitter cold winter meteorite showers. Their unfailing encouragement and confidence have carried me through challenges big and small and given me the courage to pursue my dreams.

- My husband, who has walked with me through this wilderness of graduate school. His perceptive counsel has helped me develop as a member of a professional community. He seems to see the professional world as a network that can be interacted with and that will respond in predictable ways; his insight has been invaluable. He has been my sounding board, my friend through difficulty and my cheerleader in success.

- My labmates, who have been my teachers, advocates, and friends. Sarika and Bin have given of their time, experience, and patience as they taught me how to design an experiment and, more importantly, to troubleshoot a failed one. Shidrokh, who has since departed for international adventures, was a source of empathy whose resilience inspired me to remain steadfast. Dikshya, who somehow manages to be involved in everything while also pursuing her science, has encouraged me to seek educational experiences outside of the lab and has been an enthusiastic teammate within it.

- Pampee, who chose to invest in my scientific and professional development; who pushed me to grow and provided me with an example of a life that was balanced, ambitious, and always searching for areas to improve.

And, finally, the highest praise and glory go to the God who set the first electrons spinning about the first nucleus and who gave us the curiosity and the wit to search out the mysteries of His creation.

TABLE OF CONTENTS

LIST OF TABLES

LIST OF FIGURES

LIST OF ABBREVIATIONS

AngII Angiotensin II

CT Computed Tomography

CVD Cardiovascular Disease

EC Endothelial Cell

FADD Fas-Associated protein with Death Domain

HDL High Density Lipoprotein

ICAM-1 Intercellular adhesion molecule

IFN-γ Interferon-γ

IL-1 Interleukin-1

IL-6 Interleukin-6

MCP-1 Human Monocyte Chemoattractant Protein-1

MMP Matrix Metalloproteinase

PDGF Platelet-Derived Growth Factor

ROS reactive oxygen species

SPRR Small Proline-Rich Repeat

TGF-β Tissue Growth Factor-β

TNF-α Tumor Necrosis Factor-α

VCAM Vascular Cell Adhesion Molecule

VSMC Vascular Smooth Muscle Cell

CHAPTER 1

Introduction

Atherosclerosis is a disease of the vasculature characterized by the accumulation of lipids and inflammatory cells within the arterial wall. Preferentially developing at curves and branch points of arteries, the earliest stages of atherosclerosis, called fatty streaks, develop within the first decade of life and have even been found in fetal aortas (Nakamura and Ohtsubo, 1992; Napoli et al., 1997). Development of formal, though uncomplicated, atherosclerotic plaques can be found in the aorta beginning at 30-40 years of age (Nakamura and Ohtsubo, 1992). Atherosclerosis typically continues to progress with age and to varying degrees based on a wide variety of risk factors, including family history, chronic inflammatory disease, diet, exercise, and other environmental factors.

The increased risk observed in those who are elderly, sedentary, and consuming a diet high in saturated fat has contributed to the hypothesis that atherosclerosis is a modern disease. To test this hypothesis, a group of archeologists, radiologists, and medical professionals called the HORUS team used whole-body X-ray computed tomography (CT) scanning to search for evidence of arterial calcification as a readout of atherosclerosis in 137 mummies from four distinct groups, dating from between 3100 BCE - 1500 CE. These mummies originated from hunter-gatherer, forager-farmer, and agricultural cultures, had an average age of 36 years, and 36% were female. Of the 137 mummies assessed, atherosclerosis was identified in 38% of mummies from Egypt, 25% of mummies from Peru, 20% of mummies from the Ancestral Puebloan Native Americans, and 80% of mummies from

the Aleutian Islands. While sample sizes were too small to draw statistically significant comparative conclusions between the four distinct groups, arterial calcification burden correlated significantly with increasing age at time of death, though the oldest were estimated to be 44 ± 8 years (Thompson et al., 2013; Clarke et al., 2014). Interestingly, all Aleutian Island mummies have demonstrated evidence of extensive pulmonary anthracosis, probably resulting from the airborne soot in their enclosed, underground homes where seal and whale oil lamps were burned for warmth. The chronic inflammatory state likely associated with constant exposure to irritating inhalants may have accelerated atherosclerosis development, as has been seen in chronic inflammatory conditions such as rheumatoid arthritis and lupus.

In an effort to identify the initiating mechanism behind atherosclerosis, a number of hypotheses have been put forth that fall under one of two main categories: the response to injury hypothesis and the response to retention hypothesis. The response to injury hypothesis postulates that the endothelium is damaged in some way, leading to neointima formation and recruitment of pro-inflammatory cells as a precursor to atheroma formation; proposed causes of injury include turbulent blood flow and oxidative stress (Ross et al., 1977; Dimmeler et al., 1997; Cai and Harrison, 2000; Hahn and Schwartz, 2009; DiCorleto and Soyombo, 1993). The response to retention hypothesis postulates that endothelial activation and inflammatory cell recruitment occur as a consequence of lipoprotein retention in the arterial wall (Williams and Tabas, 1995, 1998; Witztum and Steinberg, 2001). While the initiating factor remains undetermined, arterial wall damage and lipid deposition both occur within the wall, followed by recruitment of monocytes, lymphocytes, and vascular smooth muscle cells (VSMCs) in response. The initiation process is outlined in Figure 1.1.

The monocytes differentiate into macrophages and take up lipoprotein. As the lesion progresses, cholesterol-laden macrophages build up in the intima and VSMCs build a fibrous cap to form a barrier between the thrombogenic atheroma interior and the circulation. The lesion alters fluid dynamics within the lumen, which can aggravate disease progression, and leads to stenosis of the artery.

Atherosclerosis is the driving force behind cardiovascular disease (CVD), the leading cause of death in the United States and world wide (Murphy et al., 2013; Finegold et al., 2013). By 60 years of age, nearly 70% of adults in the US have developed some form of CVD (Mozaffarian et al., 2014). In 2010, an estimated 444 billion dollars, 1 of every 6 dollars spent on health care in the US, went to treatment of CVD (Heidenreich et al., 2011). The major causes of death associated with CVD include myocardial infarction (935,000 incidences/year), stroke (795,000 incidences/year), heart failure (550,000 new patients/year), and sudden cardiac arrest (220,000 incidences/year) (Heidenreich et al., 2011; Association, 2002, 2001). Myocardial infarction most frequently occurs due to rupture of the fibrous cap over an atheroma, which leads to thrombus formation and occlusion of small coronary arteries. Similarly, embolic stroke usually results from rupture and subsequent thrombus formation in the carotid or cerebral arteries. Stenosis, particularly in the small coronary arteries, leads to increased risk of cardiac hypertrophy, heart failure, and sudden cardiac arrest. To counteract this, patients may undergo angioplasty, surgery for stent placement, or a bypass may be performed.

Atheroma-bearing arteries with advanced lesions that have less than 75% cross-sectional luminal narrowing are at risk for increased plaque vulnerability followed by plaque erosion or rupture (Ambrose et al., 1988; Mann and Davies, 1996). Autopsy studies have indicated

that as many as 66% of myocardial infarctions are due to atheroma rupture and subsequent thrombosis (Hong et al., 2004). The development of an atherosclerotic lesion, from initiation to rupture, is summarized in Figure 1.2. Despite the importance of atheroma rupture to human health, however, the mechanisms driving it remain largely theoretical. Moreover, the data that are available focus primarily on the inflammatory cell- and lipid-driven arms of the disease while VSMCs have received relatively little attention. In this document, we will discuss current theories of plaque instability and explore VSMC function in atheroma progression and maintenance of atheroma stability using a mouse model lacking the VSMC- and atheroma-specific protein SPRR3.

1.1 Atherosclerosis Development and Progression

1.1.1 Initiation

The mechanisms behind the increased risk of atherosclerosis in the curves and branch points of arteries, where blood flow over the arterial wall becomes turbulent, have not yet been identified. A number of genes are differentially regulated in areas of turbulent flow versus areas of laminar flow (Ni et al., 2010). Some have hypothesized that laminar flow is itself protective, as restoration of expression levels of some genes to that seen in the laminar flow state delays atheroma progression (Woo et al., 2011). Turbulent blood flow has also been suggested as a cause of endothelial injury and activation, triggering an inflammatory response that began a cascade of events leading to atherosclerosis.

Other causes of endothelial activation have also been hypothesized as initiators of atherosclerosis. Deposition of oxidized low-density lipoprotein and other lipids within the arterial wall can lead to endothelial cell upregulation of cell adhesion molecules VCAM-1

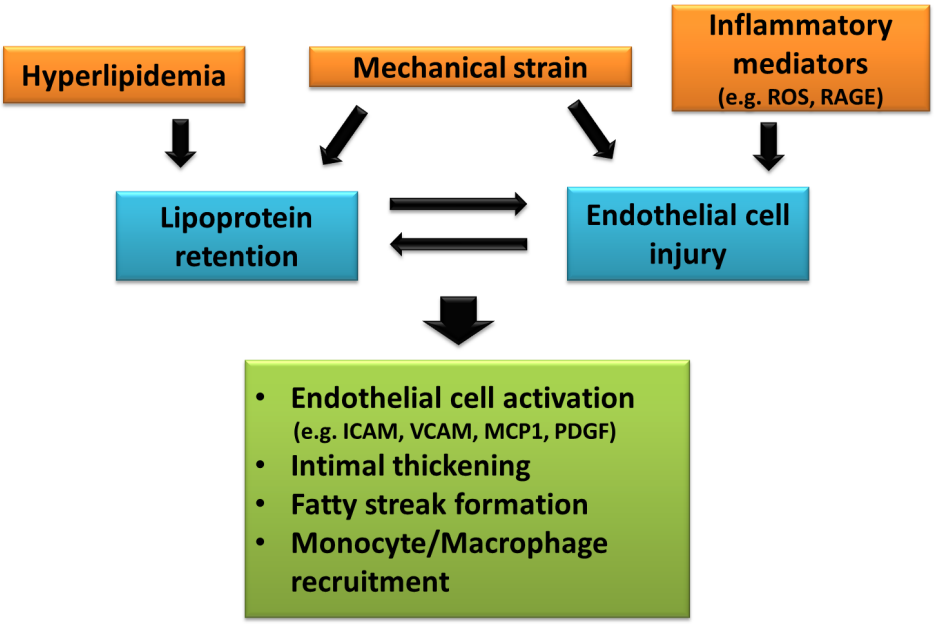

Figure 1.1: **Initiation of atherosclerosis.** While the key initiating factor has not yet been isolated, atheroma initiation occurs in response to endothelial cell injury and lipoprotein retention within the arterial wall. Various hypotheses have been proposed to explain how these occur, but there is evidence that endothelial cell injury, hyperlipidemia, and mechanical strain can all promote lipoprotein retention. Similarly, intimal lipoprotein, particularly if it becomes oxidized, along with mechanical strain and pro-inflammatory mediators such as reactive oxygen species (ROS) and reactive advanced glycation end products (RAGE) may promote endothelial cell injury. These two key events lead to a series of downstream events that together comprise the formation of the fatty streak.

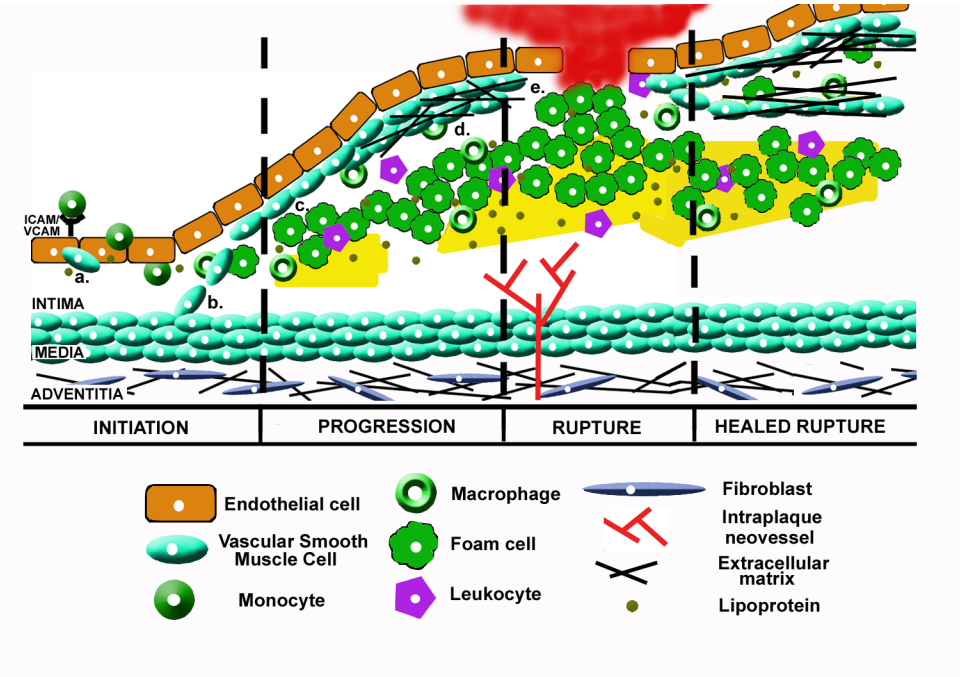

Figure 1.2: **Stages of atherosclerosis progression.** At *initiation*, human arteries contain both endothelial cells and resident vascular smooth muscle cells, or VSMCs, (see a.) within the intima. Lipid deposition or endothelial injury triggers activation of the endothelium, leading to expression of cell adhesion molecules such as ICAM or VCAM . Circulating monocytes are recruited into the artery wall, where they differentiate into macrophages and take up intimal lipoprotein. The activated endothelial cells and macrophages secrete cytokines, such as PDGF, which promote proliferation of VSMCs within the intima and media. In mice and probably in humans, medial VSMCs migrate to the luminal side of the intima (see b.). There, the VSMCs provide a layer of protection, called the neointima, between the early stage atheroma and the circulation. Macrophages and some VSMCs continue to take up lipids deposited within the artery wall and, when laden, are called foam cells. As the atheroma *progresses*, the VSMCs lining the luminal side of the intima secrete extracellular matrix, primarily collagen type I (see d.), which provides added protection between the lipid-rich core of foam cells and extracellular lipoprotein and the circulation. This layer of VSMCs and extracellular matrix is called a fibrous cap and must be continually maintained by the VSMCs, as atheroma macrophages secrete matrix degrading enzymes that will break down the fibrous cap over time. Should the balance between VSMC maintenance and macrophage-driven breakdown of the fibrous cap be lost (see e.), the fibrous cap thins and the atheroma is at increased risk of *rupture*. Rupture has occurred when there is a break in the endothelium allowing contact between the circulation and the lipid-rich core, resulting in thrombogenesis. Intraplaque neovessel formation, found in some more advanced atheromas, has also been associated with increased risk of rupture and is hypothesized to contribute to inflammation within the lesion. Following rupture, retrospective histological studies suggest that VSMC proliferation and matrix deposition is again triggered, leading to a *healed rupture*. A new fibrous cap is built over the old one and the degree of luminal stenosis is increased.

and ICAM-1 and subsequent recruitment of inflammatory cells (Khanicheh et al., 2001; Williams and Tabas, 1998; Tabas et al., 2007). Hyperglycemia and increased circulating free fatty acids may lead to increased advanced glycation end products and reactive oxygen species (ROS) generation within the arterial wall, promoting activation of the endothelium (Brownlee, 2001). Even some infections have been proposed as initiating or aggravating factors in early atherosclerosis (Shah, 2001). Once activated, endothelial cells recruit inflammatory cells, primarily monocytes, to enter the artery wall where they differentiate into macrophages, begin engulfing lipoproteins, and eventually become lipid-laden and are called foam cells.

During the initial stages of atheroma development, VSMC behavior parallels that seen in response to balloon injury or similar trauma to the endothelium. Proliferation is triggered, along with migration from the media, and a VSMC-rich neointima forms over the lesion. In humans, arteries have resident intimal VSMCs from which much of this response is derived while in mice, all VSMCs must migrate from the media. Based on the hypothesis that this neointima formation is a necessary stage in atheroma initiation, much work has been devoted to determining the mechanisms behind VSMC proliferation and/or migration to the intima (Chen et al., 1997; Sawada et al., 2000; Yang et al., 2006; Napoli et al., 2012). Seeking methods to block these responses, researchers have used balloon or chemical injuries to replicate the VSMC behavior patterns seen during atherosclerosis initiation (von der Leyen et al., 1995; Lindner and Reidy, 1991; Law et al., 1996). However, contrary to common assumption, neointima formation remains to be demonstrated sufficient to trigger atherosclerosis.

1.1.2 Progression

Once initiation has occurred and foam cells have begun to concentrate within the arterial wall, this very early stage atheroma is called a fatty streak. Mechanisms to delay progression of the fatty streak and subsequent atheroma to more advanced stages can be generally classified into those related to lipid regulation, inflammation, or VSMCs.

1.1.2.1 Lipid Regulation

Foam cell formation and the buildup of lipid-laden macrophages into an expanding lipid-rich core within the atheroma occurs due to an imbalance in lipid accumulation within the foam cells and arterial wall and lipid efflux. The best tools we have to date for addressing this imbalance are statins, which reduce circulating lipid levels by inhibiting cholesterol synthesis, and successfully reduce the risk of major coronary events by 30% and that of major cerebrovascular events by 19% (Brugts et al., 2009). More recently, the discovery of a heritable loss-of-function mutation in the PCSK9 gene, which causes extremely low levels of plasma cholesterol without evidence of negative side effects, has opened up exciting therapeutic opportunities (Cohen et al., 2006). A comparison of individuals with the PCSK9 loss-of-function allele vs. those expressing wild-type PCSK9 demonstrated a significant reduction ($p = 0.003$) in incidence of coronary heart disease in the loss-of-function group. No difference was observed in risk of stroke or death, however, potentially due to sample size limitations (Cohen et al., 2006). Multiple clinical trials are currently underway in which inhibitors of PCSK9 are being investigated in treated and untreated individuals suffering from high cholesterol (Giugliano et al., 2012; Koren et al., 2012; Sullivan et al., 2012) and in individuals with familial hypercholesterolemia (Raal et al., 2012). While the

efficacy in CVD risk reduction has not yet been determined, PCSK9 inhibitors have been successful in significantly lowering lipid levels in each of these groups.

Among strategies for improving cholesterol efflux from the lesion are methods for raising HDL levels. Attempts to date at increasing circulating HDL levels to reduce CVD risk have provided conflicting results. Niacin reduced adverse cardiovascular events in one trial but was associated with increased risk of stroke in another (Birjmohun et al., 2005; Boden et al., 2011). CETP inhibitors Dalcetrapib and Torcetrapib either failed to confer a reduction in risk or were found to be associated with an increase in all-cause mortality (Barter et al., 2007). Perhaps even more telling, a natural allelic variant of the endothelial lipase gene (LIPG Asn396Ser), which leads to significantly increased plasma HDL levels, failed to associate with reduced risk of myocardial infarction in a large Mendelian randomization analysis (Voight et al., 2012). These studies suggest that, while HDL may yet be leveraged for reduction of risk of cardiovascular injury, a simple increase in HDL levels may be insufficient

1.1.2.2 Immune Cells

A number of immune cell types are implicated in atheroma progression, including neutrophils, monocytes/macrophages, T lymphocytes, and mast cells. Recently, neutrophils have been implicated in monocyte recruitment to the lesion, as mice lacking neutrophil-derived cathelicidins (CRAMP in mouse) experienced an approximately 50% reduction in lesion area after 4 weeks high-fat diet compared with control $ApoE^{-/-}$ mice (Döring et al., 2012). The macrophages accumulating in the artery wall, unable to process or efflux their lipid burdens, can become overloaded and undergo apoptosis, increasing the proinflam-

matory nature of the atheroma environment. This can contribute to further recruitment of inflammatory cells, increase risk of apoptosis in nearby cells, and increase the thrombogenic potential of the atheroma core. CD4+, but not regulatory, T cells have been shown to accelerate atherosclerosis progression (Zhou et al., 2000; Ait-Oufella et al., 2006). A 50% increase in lesion area was observed in immunodeficient scid/scid ApoE$^{-/-}$ mice supplemented with CD4+ T cells compared with untreated controls (Zhou et al., 2000). Lethally irradiated Ldlr$^{-/-}$ mice whose bone marrow was reconstituted using regulatory T cell deficient Cd80$^{-/-}$ Cd86$^{-/-}$ bone marrow experienced a two-fold increase in lesion size compared with mice reconstituted with bone marrow containing regulatory T cells (Ait-Oufella et al., 2006). IFN-γ and Fas secretion by T cells, as well as IL-1β and TNF-α secretion by macrophages have been shown to promote VSMC apoptosis (Geng et al., 1996, 1997). Ldlr$^{-/-}$ mice genetically designed to be mast cell-deficient experienced reduced atherosclerosis ($>$ 60% reduction in aortic atheroma burden) with significantly more (75%) collagen content and thicker (47%) fibrous caps compared with control Ldlr$^{-/-}$ animals (Sun et al., 2007).

As the atheroma progresses, the VSMC role becomes more protective. Pro-apoptotic triggers of VSMCs have been consistently associated with increased atheroma burden and progression (Fernández-Hernando et al., 2007; Mercer et al., 2005; Wang et al., 2014; Li et al., 2011; Martínez-Hervás et al., 2014). Global knockout of Akt1 in ApoE$^{-/-}$ mice, which reduces VSMC survival *in vitro*, leads to a 40% increase in total aorta atheroma burden (Fernández-Hernando et al., 2009, 2007). Similarly, global knockout of p53 in ApoE$^{-/-}$ mice, which increases cleaved caspase-3 expressing atheroma VSMCs by 25%, leads to an approximately 2-fold increase in aortic lesion area (Mercer et al., 2005). Selective in-

duction of VSMC apoptosis in athero-prone ApoE$^{-/-}$ mice has been shown to be sufficient to accelerate progression of atherosclerotic lesions, leading to a 1.8-fold increase in aortic root lesion size (Clarke et al., 2008).

While the cause of this association has yet to be identified, the literature suggests a possible explanation. During atheroma development, increases in pro-inflammatory signaling accelerate atherosclerosis progression (Kirii et al., 2003; Huber et al., 1999; Mallat et al., 2001). Global knockout of IL-1β in ApoE$^{-/-}$ mice led to significantly reduced aortic VCAM-1, ICAM-1, and MCP-1 transcript levels and a 30% reduction in aortic root lesion area after 24 weeks of high fat diet (Kirii et al., 2003). Treatment of high fat diet-fed ApoE$^{-/-}$ mice with weekly injections of 5,000 units of recombinant mouse IL-6 over 9 weeks led to a 1.9-fold increased aortic root lesion area (Huber et al., 1999). Multiple studies have shown that VSMCs undergoing stress secrete pro-inflammatory cytokines. VSMC exposure to FasL and FADD trigger IL-1α secretion (Schaub et al., 2003). Exposure to IL-1α, which can also be released from apoptotic VSMCs and other cells, leads to induction of IL-6 and MCP-1 release by the viable VSMCs nearby (Clarke et al., 2010). FADD-induced apoptosis of SMCs *in vivo* leads to large-scale macrophage recruitment and transcription of MCP-1 and IL-8 by VSMCs (Schaub et al., 2000). In addition, Bennett's study, referenced above, showed increased serum levels of TNF-α and IL-6 after 7 days and IL-12, IFNγ, and MCP1 at 5 weeks of of chronic induction of low level VSMC apoptosis (Clarke et al., 2008).

Advanced atheromas have an additional need for maintenance of VSMC survival. Reduced atheroma VSMC content in humans is correlated with increased risk of atheroma rupture. VSMCs also produce and maintain fibrous cap thickness, the loss of which is cor-

related with atheroma rupture. In support of a protective role in maintenance of atheroma stability, selective induction of VSMC apoptosis in athero-prone ApoE$^{-/-}$ mice promotes key features commonly associated with ruptured atheromas (Clarke et al., 2006), such as increased lipid-rich core size and reduced fibrous cap thickness.

1.2 Theories of Atheroma Instability

1.2.1 Human Studies

Information on atheroma instability in humans is primarily limited to observations of tissue morphology from autopsy studies, carotid atherectomies, and carotid endarectomies (Thim et al., 2008). The majority of heart attacks are attributable to plaque rupture, with a smaller percentage (20-25%) due to superficial erosion of the atheroma (Arbab-Zadeh et al., 2012). Plaque rupture has been defined as loss of endothelial continuity, breakdown of the fibrous cap, and contact between the blood stream and lipid-rich core, ultimately leading to thrombus formation (Schwartz et al., 2007). Superficial erosion is characterized by loss of the endothelium overlying an atheroma with consequent thrombus formation (Virmani et al., 2000).

The majority of plaque ruptures are silent and will not result in infarct. In one angiographic study of patients with ischaemic heart disease assessing non-culprit, or not ischemia-causing, plaques, most (73%) lesions with $> 50\%$ narrowing had an incidence of healed plaque rupture (Mann and Davies, 1999). Moreover, in one autopsy study of 129 individuals who died of noncardiac causes, coronary plaque rupture was found in 15% (Davies et al., 1989). The resulting thrombus is either recanalized or nonocclusive and the rupture is filled in with VSMCs and matrix (Virmani et al., 2000). Following this process,

healed plaque ruptures experience an average stenosis of 80% cross-sectional area luminal narrowing with an estimated pre-rupture average of 66% cross-sectional area narrowing. Culprit ruptured lesions following acute MI average $< 75\%$ luminal narrowing. Therefore, contrary to common belief, there is not a linear relationship between degree of atheroma stenosis and risk of rupture.

The common histological features of ruptured atheromas in humans include: reduced VSMC content, reduced cap thickness, reduced cap collagen content, increased lipid-rich core size, and increased foci of high macrophage numbers in atheroma caps (Arbab-Zadeh et al., 2012; Thim et al., 2008). In fact, the average ruptured plaque in humans is less than 65μm thick (Thim et al., 2008).

The functional effects of the correlative changes observed in human histology studies are most commonly explored using mouse models. However, these functional studies are limited based upon some key differences between mice and humans. Human arteries are larger, contain intimal VSMCs, and develop atheromas in different locations than mice. Most importantly, model organisms currently in use do not, except rarely after greater than one year of age, undergo atheroma rupture (Johnson and Jackson, 2001; Johnson et al., 2005; Williams et al., 2002; Calara et al., 2001).

Given these caveats, however, several contributors to atheroma instability have been proposed and are summarized in Figure 1.3. Rupture may occur due to an imbalance of VSMC synthesis of fibrous cap materials and immune cell release of matrix degrading enzymes, leading to loss of fibrous cap thickness. Intraplaque vascularization, the formation of neovessels observed in advanced atheromas in humans and mice, may promote inflammation and expansion of the lipid-rich core. Additionally, as mechanical strain has

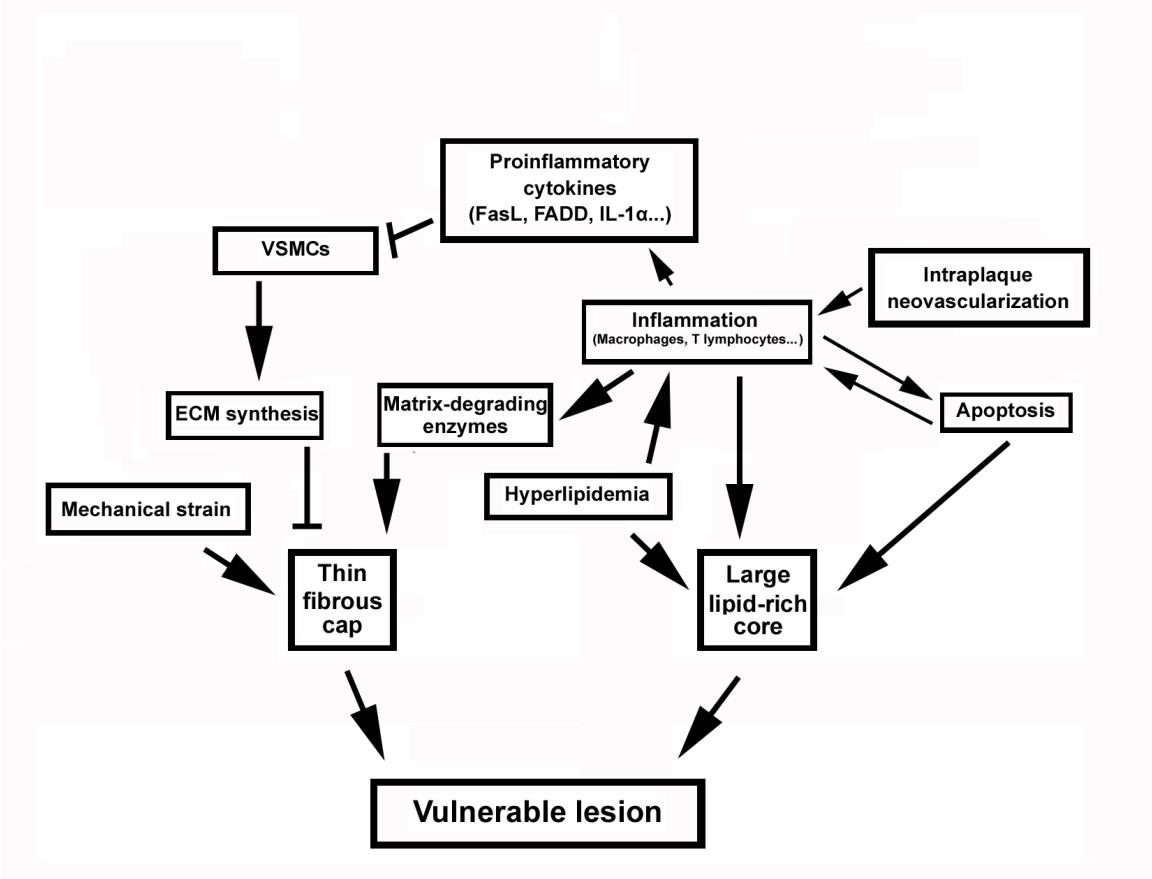

Figure 1.3: **Mechanisms contributing to atheroma instability.** Analysis of culprit lesions have identified two key features that occur with high frequency at sites of atheroma rupture: a thin fibrous cap and a large lipid-rich core. Contributing to each of these is a network of environmental conditions and cellular functions.

proven a contributor to atheroma formation, investigators have mathematically determined the morphology of the atheroma may alter the strain over the cap to induce rupture.

1.2.2 VSMC Survival

Factors that affect VSMC or macrophage content or function within the lesion are likely to contribute to an imbalance of synthesis and degradation of cap materials. VSMC survival has been experimentally identified as a key feature in maintenance of atheroma stability. In an elegant set of experiments using an inducible mouse model of VSMC apoptosis, Bennett

and group demonstrated that in high fat diet-fed ApoE$^{-/-}$ mice, but not in mice with normal lipid regulation, induction of VSMC apoptosis promoted increased lipid-rich core size and thinner fibrous caps (Clarke et al., 2006). Thus, mechanisms that promote VSMC survival may contribute to atheroma stability. The most commonly studied VSMC pro-survival pathway is the PI3K/Akt pathway. This pathway has been shown to be downregulated in atheroma VSMCs compared with those from normal arterial tissue (Allard et al., 2008). While loss of Akt itself has not been investigated in VSMCs alone, global Akt1 knockout has also been shown to promote atheroma instability (Fernández-Hernando et al., 2007). Moreover, Akt activation has a protective effect in the atheroma, reducing lesion vulnerability (Fernández-Hernando et al., 2009). Constitutive activation of Akt has undesirable effects in animal models, however, including cardiac hypertrophy and heart failure (Matsui et al., 2002; Shioi et al., 2000).

1.2.3 Fibrous Cap Maintenance

Collagen expression in atherosclerosis has been shown to be regulated by a myriad of factors, including IL-1, TGF-β, PDGF, angiotensin type II, and IFN-γ (Amento et al., 1991; Belmadani et al., 2008; Mifune et al., 2000). AngII acts via the AT2 receptor to stimulate collagen synthesis associated with MAPK and TGF-β pathway activation (Mifune et al., 2000; Belmadani et al., 2008). Global inhibition of the TGF-β receptor using a TGF-βRII blocking antibody or an inhibitor against TGF-β 1-3 had similar results, both leading to increased atheroma burden and inflammation with a decrease in atheroma collagen content (Lutgens et al., 2002; Mallat et al., 2001). Drawing conclusions from these data is complicated, however, by the massive inflammatory response observed in the TGF-β 1 knockout

mouse model, which develop normally until 2 weeks of age of widespread multifocal inflammatory disease (Kulkarni et al., 1995). Interestingly, adoptive transfer of bone marrow from mice expressing a dominant negative form of TGF-βRII expressed specifically in T cells into Ldlr$^{-/-}$ recipients leads to smaller atheromas with relatively increased T cell and dendritic cell content, reduced VSMC content, and reduced plaque collagen content (Gojova et al., 2003). These histological observations were accompanied by evidence of increased cytokine production in T cells expressing dnTGF-βRII, including IFN-γ. Later work by Libby and group showed that T cell IFN-γ secretion can inhibit VSMC collagen type I synthesis in culture (Amento et al., 1991). Global knockout of the IFN-γ receptor in ApoE$^{-/-}$ mice led to reduced lesion size with increased collagen content but did not appear, based on their representative images, to affect cap thickness (Gupta et al., 1997).

1.2.4 MMP Degradation of Fibrous Cap

When VSMCs migrate, they release matrix metalloproteinases (MMPs), degrading matrix as they travel. MMPs commonly released by VSMCs include MMP-2, MMP-3, and MMP-9, all of which are commonly found in the atherosclerotic lesion. MMP-3 cleaves collagen types III and IV. MMP-2 and -9 both cleave collagen types IV and V. MMP-2 is also able to cleave fibronectin and laminin while MMP-9 targets collagen types I and III.

Despite the ability of atheroma VSMCs to express MMPs, little is known about their regulation or the effect of VSMC-derived MMPs on atheroma stability. Studies have either been general or have focused on macrophage-derived MMPs. In human arteries, MMP-2 expression remains strong independent of atherosclerotic burden (Galis et al., 1994). However, MMP-3 and MMP-9 expression is limited to atherosclerotic lesions and has been

identified by immunohistochemistry in VSMCs and macrophages in the fibrous cap and at the base of the lipid-rich core. MMP9 knockout in athero-prone ApoE$^{-/-}$ mice leads to smaller reduced atheroma size compared with control ApoE$^{-/-}$ mice, in a manner that is at least partly mediated by BM-derived cells (Choi et al., 2005). Transplantation of HSCs with autoactivating MMP9, but not MMP9 overexpression, is sufficient to induce fibrous cap disruption and fibrin deposition in advanced mouse atheromas without altering lesion size, lesional macrophage content, or elastic lamellae morphology (Gough et al., 2006). MMP3$^{-/-}$ApoE$^{-/-}$ mice expressing normal MMP9 develop significantly larger lesions with more fibrillar collagen (Silence et al., 2001). Interestingly, there is evidence both *in vitro* and *in vivo* that MMP3 expression is required for MMP9 activation (Johnson et al., 2011).

1.2.5 Intraplaque Vascularization

Intraplaque vascularization has also been proposed as a mechanism for atheroma destabilization. Neovessels formed within the atheroma are believed to be notoriously leaky, allowing RBC infiltration into the atheroma tissue and promoting inflammation both in response to RBC-mediated tissue damage and due to increased accessibility (Langheinrich et al., 2006). A study in which plaque neovascularization was inhibited by global application of angiogenesis inhibitor angiostatin led to reduced plaque angiogenesis and atheroma size (Moulton et al., 2003). Researchers appear to have mixed views, however, as to whether intraplaque vascularization should be prevented or merely stabilized. Some hypothesize that the presence of a stable source of circulation would reduce hypoxia in advanced atheromas, increase the likelihood of macrophage extravasation, and limit size of and necrosis in the lipid-rich core. However, multiple studies have shown a correlation

in human atheromas between lesion instability and presence of atheroma neovascularization and intraplaque hemorrhage (Hellings et al., 2010; Virmani et al., 2005). Moreover, at least one mouse model has been proposed in which 'tandem stenosis' of carotid arteries in HFD fed ApoE$^{-/-}$ mice leads to intraplaque hemorrhage in 50% of animals, accompanied by evidence of potential intraluminal thrombosis and fibrous cap disruption (Chen et al., 2013).

1.2.6 Mechanical Strain

As atheromas preferentially occur in areas of altered mechanical strain, theoretical models have evaluated the potential role of mechanical forces on the fibrous cap in destabilization of the atheroma. Mathematical modeling in one study suggests eccentric lipid-rich cores are capable of generating altered circumferential strain, with some formations promoting the likelihood of rupture (Richardson et al., 1989). A number of subsequent investigations have explored the impact of changes in the fluid dynamics over the arterial wall caused by atheroma formation (Chèvre et al., 2014; Hetterich et al., 2015; Yap et al., 2014; Nahrendorf et al., 2008). Another model demonstrated that minute spherical calcifications in the fibrous cap can increase local stress around the particle such that rupture may occur in the center of a fibrous cap whose thickness is less than 65 μm (Vengrenyuk et al., 2006).

1.3 SPRR3

SPRR3, part of a family of small proline-rich repeat proteins (SPRRs) found primarily in the cornified envelope of the skin and esophagus, is upregulated in response to mechanical stress (Hohl et al., 1995). SPRRs consist of a head and tail region rich in transglutaminase

domains separated by a flexible, proline-rich central region with repeating units ranging in length between eight and nine residues (Candi et al., 2005). SPRR3 contains three transglutaminase domains and fourteen eight-residue units within the proline-rich flexible internal domain (Steinert et al., 1999).

The structure has proven difficult to model, due to the size and flexibility of the central domain, but the proline-rich flexible linker region is predicted to form a series of beta turns, as each proline would disrupt any alpha-helix or beta-sheet structure that might otherwise occur (Steinert et al., 1999). Modeling of protein-protein interactions for SPRR3 suggest the N- and C-terminal domains are capable of cross-linking with each other and with other cornified envelope proteins such as loricrin and involucrin in order to increase tissue resistance against mechanical stress (Fischer et al., 1999), though this has yet to be shown to occur in tissue.

While little has previously been discovered about SPRR3 function, SPRR family members have been implicated in pro-survival functions in cardiomyocytes (Pradervand et al., 2004), tumor cells (Mizuguchi et al., 2012; Kim et al., 2012), and fibroblasts (Cabral et al., 2001). In cardiomyocytes, SPRR1a has been shown to operate downstream of gp130 in a protective response to cardiac ischemia following TAC (Pradervand et al., 2004). In cholangiocarcinoma cells, SPRR2a interacts with nuclear proteins, leading to p53 and p300 deacetylation, which blocks anti-proliferative and pro-apoptotic signals in cells where it is overexpressed (Mizuguchi et al., 2012).

Using a transcriptional profile screen, we identified SPRR3 upregulation in the aorta of both humans and mice, but not in the internal vena cava (Young et al., 2005). Moreover, arterial SPRR3 upregulation, which is primarily found in VSMCs, is exclusive to areas

of atherosclerotic lesion development. Our lab has also demonstrated SPRR3 expression is triggered in VSMCs by cyclic stress and is dependent upon interactions with collagen 1 and integrin $\alpha 1 \beta 1$ (Pyle et al., 2008). To further investigate the role of SPRR3 in atherosclerosis pathophysiology, we generated an SPRR3 knockout mouse, which we then bred onto an atherogenic ApoE$^{-/-}$ background. The results of this study are described in Chapter 2.

1.4 Concluding Statement

In this document, we explore the role of vascular smooth muscle cells in atherosclerosis progression and maintenance of atheroma stability. As a tool, we use SPRR3, an atheroma- and VSMC-specific protein. We show that loss of SPRR3 reduces atheroma VSMC survival and accelerates atherosclerosis progression. In advanced atherosclerosis, loss of SPRR3 promotes aspects of atheroma destabilization, including reduced lesion VSMC content, thinning of fibrous caps, increased collagen content, and increased lipid-rich core size. Perhaps most excitingly, the SPRR3 knockout mouse demonstrates a unique phenotype of increased coronary atheroma complexity and microinfarcts. In the final chapter, we discuss future directions, including implications of genetic variants of SPRR3 in human disease.

CHAPTER 2

Identification of SPRR3 as a novel atheroprotective factor that promotes adaptive Akt signaling in VSMCs

2.1 Introduction

Cardiovascular disease, the leading cause of death worldwide (Roger et al., 2012), accounts for one in three deaths in the United States (Roger et al., 2012) and is primarily driven by atherosclerosis. Initiation of atherosclerosis is believed to stem from a confluence of injury to the endothelium along with lipid deposition in the vascular wall, which then triggers an ongoing cycle of endothelial cell (EC) activation, inflammatory cell infiltration, hyperplastic vascular smooth muscle cell (VSMC) proliferation, and further lipid accumulation (Zarins et al., 1983). Atherosclerosis progression ultimately results in a toxic microenvironment in which dead or dying lipid-laden foam cells are sequestered from the circulation by a VSMC-derived fibrous cap (Zarins et al., 1983; Kwon et al., 2008). Atheroprotective genes or factors that delay the initiation or progression of the atheroma are of great interest for their potential to delay adverse events (NIH, 2000).

We sought to identify novel, potentially atheroprotective genes in a previous study, in which we conducted a transcript screen for alternately regulated genes in human arteries versus veins and other tissues (Young et al., 2005). The most strongly upregulated of the significantly altered genes was the small proline-rich repeat protein 3 (SPRR3), a member of the small proline-rich repeat protein family. Interestingly, immunofluorescence staining of human thoracic aorta showed that, while expression was high in atheroma, no SPRR3

expression was detected in healthy arterial tissue (Young et al., 2005). SPRRs are primarily expressed in the cornified envelope and stratified epithelium such as skin and, in the case of SPRR3, foregut and esophagus (Fischer et al., 1999). Interestingly, some studies have shown that SPRR3 is also associated with pro-survival functions in colorectal cancer (Cho et al., 2010). However, the mechanism by which SPRR3 promotes cell survival remains undetermined. We have previously investigated the mechanism by which SPRR3 is expressed specifically in VSMCs within atheromas. The mechanism of SPRR3 expression in atherosclerotic plaques requires both cyclic strain and the expression of integrin $\alpha 1\beta 1$, a major receptor for collagen type I; VSMCs isolated from integrin $\alpha 1\beta 1$ knockout mice failed to upregulate SPRR3 transcripts under cyclic strain (Pyle et al., 2008). We confirmed that VSMCs within atheromas expressed integrin $\alpha 1\beta 1$ (Pyle et al., 2008; Schapira et al., 2005). SPRR3 may, therefore, represent a VSMC-derived response to the atheroma microenvironment.

To elucidate the pathophysiological function of SPRR3 in the atheroma, we developed an SPRR3-deficient mouse bred onto an atherogenic ApoE$^{-/-}$ background. Here, we have provided evidence for SPRR3 as an atheroprotective factor that operates specifically in the atheroma and promotes VSMC survival. We also uncovered a novel role for SPRR3 as an atheroprotective protein that regulates lesion development via interaction with the Akt signaling pathway in atheroma VSMCs.

2.2 Methods

2.2.1 Generation of SPRR3$^{-/-}$ Mice

A targeting vector was designed containing a Neo cassette flanked by both LoxP and FRT sites and carrying a 5' long arm of homology to the SPRR3 allele (7.89 kb), a short homology arm of 1.6 kb, along with a combined total of 17.8 kb of flanking genomic sequence on either side. A forward primer (LAN1) targets sequence inside the Neo cassette (5'-CCAGAGGCCACTTGTGTAGC-3') and two reverse primers target sequences 3' of the cassette to aid in genotyping (5'- CGCACACTGGGCATCTGTACATAG -3'; 5'-CAGCAAGGACTCTTCAGAAAGATCC -3').

High fidelity Red/ET recombineering was used to introduce the targeting vector into a hybrid 129SvEv and C57Bl/6J (129/C57) ES cell line. Cells underwent selection by neomycin and appropriate clones were microinjected into 128-cell stage blastocysts and implanted into foster mothers; the resulting chimaeras were bred to homozygosity. Development of SPRR3$^{-/-}$ mice was carried out by inGenious Targeting Laboratories. The Neo cassette was removed by crossing SPRR3$^{-/-}$ mice with ACTB-Flp mice (Jackson Laboratories, stock #005703) as detailed in Figure 2.1, A. Knockout was confirmed by PCR amplification at the genetic level and immunoblot analysis of SPRR3 protein expression levels (Figure 1, B-C). Finally, Neo deleted mice were then backcrossed onto the C57Bl/6 background 15 generations. All mice used in these studies were 6 months old unless otherwise specified. Mice were anesthetized using Isofluorane (HenrySchein).

Mice were maintained in microisolator cages on a rodent chow diet containing 4.5% fat by weight with 13% of calories from fat (diet 5001, St. Louis, MO) or a high fat diet

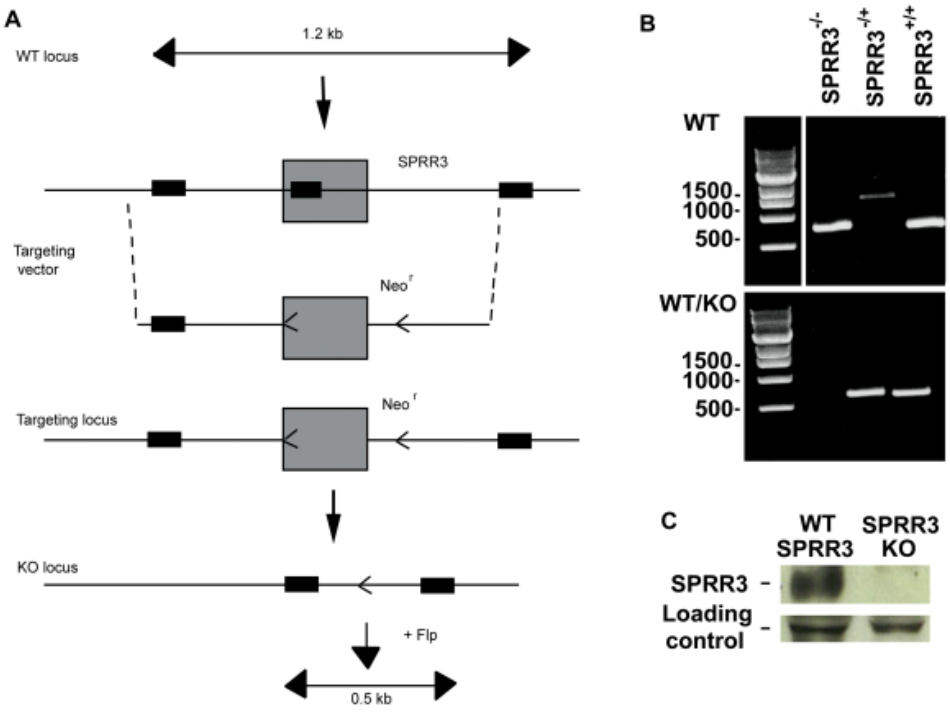

Figure 2.1: **Generation of SPRR3$^{-/-}$ mice.** (A) Targeting strategy used to disrupt the SPRR3 locus. A targeting vector with a Neo selection cassette was used to replace the SPRR3 gene by homologous recombination. SPRR3$^{-/-}$ mice were then crossed with Flp mice to remove the Neo cassette. Arrowhead = Frt site; Bar = forward and reverse primers. (B) SPRR3 knockout was confirmed with PCR using primers against flanking sequences (WT) and a sequence inside the target region (WT/KO). (C) Verification of SPRR3 knockout efficiency by Western against SPRR3 in wild type C57Bl/6 and SPRR3$^{-/-}$ forestomach, which expresses very high levels of SPRR3.

containing 9% fat by weight with 21% of calories from fat, (diet 5021; PMI, St Louis, Missouri, USA). Animal care and experimental procedures were performed according to the regulations of Vanderbilt University's Institutional Animal Care and Usage Committee.

2.2.2 Cells

Immorto-VSMCs were isolated from the aortas of transgenic H-2K^{b}-tsA58 mouse expressing heat-labile T-antigen and maintained as described (Pyle et al., 2008). SPRR3 cDNA subcloned into LZRS-MS-IRES-GFP retroviral expression vector (a kind gift of Alyssa

Weaver, Vanderbilt University) or the empty vector were used for retroviral transduction of T-antigen expressing VSMCs. Transduced GFP- or SPRR3-VSMCs were routinely sorted for GFP expression by flow cytometry to enrich for GFP-positive cells.

Primary VSMCs were isolated from the aortas of SPRR3$^{-/-}$ApoE$^{+/+}$ mice as described and pooled (Pyle et al., 2008). An immortalized line of SPRR3-KO VSMCs was generated. Briefly, pooled VSMCs were isolated from WT C57Bl/6 mice (WT-VSMCs) or from SPRR3$^{-/-}$ApoE$^{+/+}$ mice (SPRR3-KO VSMCs), which we then immortalized using pZipSVtsA58, a retrovirus expressing a heat-labile T-antigen behind the pCMV promoter (a generous gift from Parmjit Jat). These cells were immortalized when cultured at 33° C, but returned to primary phenotype within a week of culture at 37° C. Primary endothelial cells were isolated from the lungs of SPRR3$^{-/-}$ApoE$^{+/+}$ or WT C57/Bl6 mice as described (Pozzi et al., 2000).

2.2.3 Cholesterol Analysis

Mice ($n = 5$ WT mice; $n = 6$ SPRR3$^{+/+}$ApoE$^{-/-}$, SPRR3$^{-/-}$ApoE$^{+/+}$, and SPRR3$^{-/-}$ApoE$^{-/-}$ mice) were fasted for 4 hours before blood was collected for total plasma cholesterol and triglyceride measurements, which were determined as described previously (Babaev et al., 2005).

2.2.4 Aortic Lesion Analysis

En face analysis of aortas was carried out as previously described (Babaev et al., 2005). In brief, aortas were dissected from the ascending aorta to the iliac bifurcation, pinned out, and stained with Sudan IV. Images were captured with a frame grabber and a color video

camera, and then analyzed using the KS 300 system. Surface area of aortic lesions was calculated as a percent of total aortic area in normal chow fed mice ($n = 13$ SPRR3$^{+/+}$ApoE$^{-/-}$ mice and SPRR3$^{-/-}$ApoE$^{-/-}$ mice) and high fat diet ($n = 8$ SPRR3$^{+/+}$ApoE$^{-/-}$ mice and SPRR3$^{-/-}$ApoE$^{-/-}$ mice). For aortic root analysis, aortic valves were dissected as described (Paigen et al., 1987). Briefly, the heart and upper aorta were removed and fixed in OCT (Optimum Cutting Temperature) mounting medium. Hearts were sliced in 10 μm sections and stained with MOMA to quantify plaque macrophage content or CD3 to quantify T-cell content (Santa Cruz). Bright field images were captured using an Olympus DP71 camera, while fluorescent images were collected using a CoolSNAP Hq CCD camera (Photometrics).

2.2.5 Immunoblotting

Ly294002 (25 μM; Sigma) PI3K/Akt inhibitor was used to determine SPRR3 involvement in PI3K/Akt signaling. To identify potential upstream regulators of SPRR3-mediated phospho-Akt signaling, recombinant Insulin-like Growth Factor-1 IGF-1 (insulin-like growth factor-1, 20 ng/mL; R & D Systems) was added to serum-starved cells for five minutes, then cells were washed and incubated one hour in full serum before protein collection. For protein collection, cultured cells were washed twice with PBS and lysed using RIPA buffer supplemented with protease inhibitors and phosphatase inhibitors (Roche). Whole cell lysates were rocked 30 minutes at 4° C then spun 15 minutes at 13,000xg and the supernatant collected. Protein concentrations were determined using a bicinchoninic acid (BCA) kit (Thermo Scientific). Proteins were denatured 10 minutes at 95° C in SDS sample buffer before being resolved by SDS-PAGE electrophoresis and transferred onto a nitrocel-

lulose membrane (PerkinElmer). Blots were blocked in 5% nonfat milk and probed with antibodies to phospho-Akt (Cell Signaling, #4058S), Akt (Cell Signaling, #9272), β-actin (Sigma, #A5441), active caspase-3 (Cell Signaling, #9665), or SPRR3 (Alexis, #ALX-210-902-R100) overnight at 4° C. After washing with 0.1% Tween-20-supplemented TBS, blots were incubated with species specific secondary antibodies for 1 hour at room temperature and chemiluminescence (PerkinElmer, NEL104) was detected by film or visualized using a Syngene GBox (Syngene, Cambridge, United Kingdom). ImageJ version 1.38x (National Institutes of Health) software was used for desitometry analysis of the appropriate lanes; values are normalized to β-actin loading control.

2.2.6 RNA Isolation, cDNA Synthesis, and Real-Time PCR

For RNA isolation from tissue, 3 mice per group were used. Total RNA was isolated using Trizol (Invitrogen) following the manufacturer's instructions. cDNA was generated using iScript cDNA Synthesis kit (Bio-Rad) from 1μg RNA. The cDNA was then used for quantitative real-time PCR (real time qRTPCR) as described (Young et al., 2005). Primers used for real time qRT-PCR were mSPRR3 forward (5'-CCCTTTGTCCCACCTCCT-3') and mSPRR3 reverse (5'-TTGGTGTTTCCTGGTTGTG-3'). A T_m of 59° C was used and a 134bp product was produced.

2.2.7 Immunofluorescent Labeling

For caspase-3 immunofluorescence (IF), GFP-VSMCs and SPRR3-VSMCs grown on coverslips were fixed 10 minutes in cold acetone and permeabilized 5 minutes in 0.2% Triton/PBS. Cells were then stained as described (Alfaro et al., 2010). Briefly, VSMCs were

blocked with 10% goat serum before they were incubated with anti-active caspase-3 antibody (Promega). In the dark, secondary antibody conjugated to Cy3 was incubated with the cells. Vectashield Hard Set mounting medium with Dapi (Vector H-1500) was used to attach coverslips to slides.

For TUNEL IF (Roche), cells grown on coverslips or frozen tissue cryosections were fixed for 1 hour in 1% paraformaldehyde in PBS, pH 7.4. Coverslips were rinsed twice with PBS, then permeabilized 2 minutes at 4° C with 0.1% Triton X-100 in 0.1% sodium citrate. Following PBS rinse, coverslips were labeled with TdT per manufacturer instructions using the *In Situ* Cell Death Detection Kit, TMR red (Roche). To assess apoptosis within the lesion, paraffin-embedded tissue was deparaffinized and labeled with 1:2 TdT:TUNEL dilution buffer per manufacturer instructions (Roche). Smooth muscle α actin (α-SMA; Sigma)-TUNEL colocalization was assessed in $n = 5$ mice/group 6 months HFD. MOMA-2-TUNEL colocalization was assessed in $n = 3$ mice/group 6 months normal diet. vWF (DAKO #A0082, 1:200) and TUNEL colocalization was assessed in $n = 3$ mice/group.

For assessment of VSMC content, frozen sections in OCT were collected as described above from 6 mo. normal diet fed mice. Sections were fixed in acetone for 10 minutes at 4° C, blocked with 10% goat serum for one hour, and then treated overnight at 4° C with primary α-SMA (1:2000) or α-smooth muscle myosin heavy chain (SM-MHC, 1:300; Alfa Aesar #J64817) in 3% goat serum. Coverslips were affixed to slides using Vectashield Hard Set mounting medium with Dapi (Vector H-1500). Staining was assessed by confocal analysis using a LSM510 (Zeiss) microscope to capture 1 μm optical slices (z stack); the images were analyzed with Metamorph v5.0 (Universal Imaging Corp.). VSMC plaque content was calculated as the number of VSMCs divided by plaque cellularity per mm^2

in 8-10 fields of view per mouse using either α-SMA ($n = 8$ SPRR3$^{+/+}$ApoE$^{-/-}$ mice and $n = 5$ SPRR3$^{-/-}$ApoE$^{-/-}$ mice) or α-SM-MHC ($n = 3$ SPRR3$^{+/+}$ApoE$^{-/-}$ mice and $n = 3$ SPRR3$^{-/-}$ApoE$^{-/-}$ mice).

2.2.8 Bone Marrow Transplantation

For BMT, unfractionated BM from donor mice was obtained as described (Babaev et al., 2005). Recipients were preconditioned with 10Gy of γ-radiation from a $_{137}$Cs source before injection through the lateral tail vein with $5x10^6$ nucleated donor cells. PCR confirmed full hematopoietic engraftment. Recipient mice were allowed 2 months for recovery and engraftment post-transplant before high fat diet was initiated.

2.2.9 Proliferation Assays

Proliferation was measured *in vivo* using paraffin-embedded aortic root sections from 6 month high fat diet-fed mice ($n = 3$ SPRR3$^{+/+}$ApoE$^{-/-}$ and SPRR3$^{-/-}$ApoE$^{-/-}$) stained by immunohistochemistry with Ki67 (Novocastra Labs, NCLKi67p). *In vitro* proliferation of GFP-VSMCs and SPRR3-VSMCs was assessed via BrdU incorporation. 96-well plates were seeded at 500 and 1,000 cells/well and cultured in 15% FBS/DMEM. BrdU incorporation assay was carried out according to manufacturer's protocol (BD Biosciences).

2.2.10 Viability Assays

Viability was assessed using MTT. Cells were seeded at 25,000 cells/well in a 96-well plate and allowed 4 hours to adhere. Cells were then serum-starved 24 hours with 0.1% FBS/DMEM and 50ng/mL PDGF. After 24 hours starvation, MTT was added to the wells to a final concentration of 1.2mM and cells were incubated 4 hours at 37° C. The supernatant

was then removed from the cells and they were lysed in DMSO for 10 minutes at 37° C before measuring OD at 540nm. Results represent three independent experiments performed in triplicate.

Cyclic strain was applied in pulse assays as described previously (Pyle et al., 2008). Cells pretreated for 48 hours with 200pM TGFβ were seeded at $1x10^5$ cells/well in a 6 well plate coated with type I collagen and allowed to adhere overnight prior to application of strain.

2.2.11 Statistical Analysis

Statistical significance was determined by Student's *t*-test or ANOVA followed by Tukey's multiple comparison test for parametric data and Mann-Whitney or Kruskal-Wallis for non-parametric data using GraphPad Prism (San Diego, CA). $p \leq 0.05$ were considered statistically significant.

2.3 Results

2.3.1 Atherosclerosis is Increased in ApoE-null Mice Lacking SPRR3

We have shown previously that arterial SPRR3 is expressed in humans and mice at sites of lesion development (Young et al., 2005; Pyle et al., 2008). We verified the atheroma expression pattern of SPRR3 in aortic root atheroma sections from 6 month old ApoE-null mice fed normal diet immunostained for both SPRR3 and a VSMC-specific marker (smooth muscle α-actin, α-SMA). SPRR3 colocalized with α-SMA, indicating that expression was primarily found in VSMCs (Figure 2.2, A). A comparison of SPRR3 transcript levels in atheroma-bearing arterial tissue versus normal arterial tissue indicated a 19-fold increase

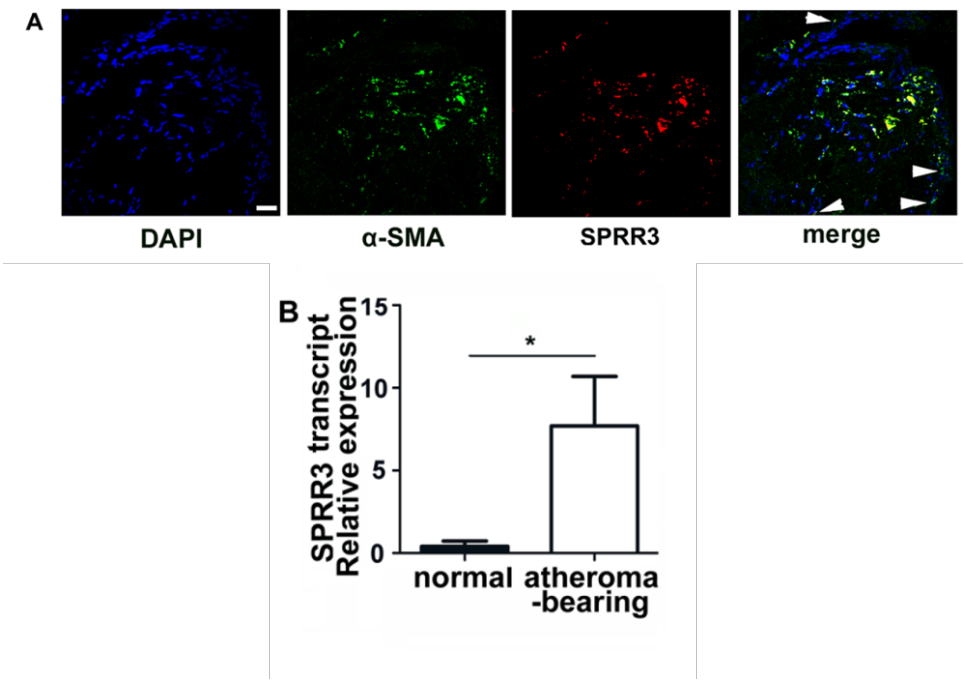

Figure 2.2: **SPRR3 was enriched in atheroma VSMCs but not in normal arteries.** (A) Fluorescent images were acquired by confocal fluorescent microscopy with x40 lens. A representative Z plane shows a high degree of colocalization of α-SMA (green) and SPRR3 (red) in aortic root lesions of 6 month normal diet-fed SPRR3$^{+/+}$ApoE$^{-/-}$ mice. Scale bar, 50 μm. Arrowheads indicate VSMCs not positive for SPRR3 expression. (B) mRNA isolated from atheroma-bearing artery and normal artery (of SPRR3$^{+/+}$ApoE$^{-/-}$ mice) was assessed for SPRR3 expression using real time qRT-PCR ($n = 3$ SPRR3$^{+/+}$ApoE$^{-/-}$ mice and SPRR3$textsuperscript-/-$ApoE$^{-/-}$). Bars represent mean $\pm$SD. *$p < 0.05$.

($p = 0.02$) in SPRR3 mRNA expression (Figure 2.2, B).

To investigate the role of SPRR3 in atherosclerotic lesions, we generated SPRR3 knockout mice (Figure 2.1, A). SPRR3 knockout mice were overtly phenotypically normal and reproduced normally compared with WT C57Bl/6 mice. Serum cholesterol and triglyceride levels (Table 2.1; $n = 6$ SPRR3$^{+/+}$ApoE$^{-/-}$ mice), as well as body weight measurements, were comparable to WT ($n = 5$ SPRR3$^{+/+}$ApoE$^{+/+}$). The lack of an associated phenotype in SPRR3 knockout mice was expected, due to the near total absence of atheroma formation in wild type mice with normal lipid profiles. Therefore, we crossed SPRR3 knockout

Genotype	n	Cholesterol (mg/dL)*	Triglycerides (mg/dL)*
C57BI6	5	78.0 ± 13.1	90.6 ± 4.3
SPRR3$^{-/-}$ApoE$^{+/+}$	6	101.4 ± 9.2	124.9 ± 39.9
SPRR3$^{+/+}$ApoE$^{-/-}$	6	$412 \pm 28.2^{c,d}$	172.9 ± 29.7^{a}
SPRR3$^{-/-}$ApoE$^{-/-}$	6	$455.4 \pm 82.5^{c,d}$	175 ± 31.6^{b}

Table 2.1: **Plasma cholesterol and triglyceride levels in SPRR3$^{-/-}$ApoE$^{-/-}$ mice are not significantly different from SPRR3$^{+/+}$ApoE$^{-/-}$.** *Fasting levels of cholesterol and triglyceride levels were quantified in serum of 6 month old C57/Bl6, SPRR3$^{-/-}$ApoE$^{+/+}$, SPRR3$^{+/+}$ApoE$^{-/-}$, and SPRR3$^{-/-}$ApoE$^{-/-}$ mice fed normal chow. Values are represented as mean $\pm$ SD. $^{a}p < 0.01$ vs C57/Bl6 mice or ^{b} SPRR3$^{-/-}$ApoE$^{+/+}$ mice; $^{c}p < 0.0001$ vs SPRR3$^{-/-}$ApoE$^{+/+}$ mice or ^{d}C57/Bl6.

mice onto the atherogenic ApoE-null background. We assessed atherosclerosis severity in 6 month old ApoE-null (SPRR3$^{+/+}$ApoE$^{-/-}$) and DKO (SPRR3$^{-/-}$ApoE$^{-/-}$) mice fed normal chow (4.5% fat by weight with 13% of calories derived from fat, diet 5001; PMI, St Louis, Missouri, USA). Serum triglyceride and cholesterol levels did not differ between groups (Table 1; $n = 6$ SPRR3$^{+/+}$ApoE$^{-/-}$ mice, and SPRR3$^{-/-}$ApoE$^{-/-}$ mice).

To determine whether SPRR3 loss alters atherosclerosis progression, we compared the extent of atherosclerosis in 6-month-old gender-matched DKO mice with ApoE-null control mice fed a normal chow diet. We used Sudan IV to quantify atherosclerosis by *en face* analysis of aortas, in which DKO mice exhibited a 3-fold increase in lesion area over control ($0.7 \pm 0.14\%$ in SPRR3$^{+/+}$ApoE$^{-/-}$ vs 2.2 ± 0.6 in SPRR3$^{-/-}$ApoE$^{-/-}$; Figure 2.3, A-B; $p = 0.02; n = 13$ per group). Similar results were observed in aortic root lesions stained for lipid levels with Oil Red O (Figure 2.4, A-B; DKO increased 51% over ApoE-null, $p = 0.03$). To determine whether the increased atheroma burden observed on normal chow would be maintained on an atherogenic diet, we fed ApoE-null and DKO mice a high fat diet (9% fat by weight with 21% of calories derived from fat, diet 5021; PMI, St Louis, Missouri, USA) for 6 months. Following the atherogenic diet, a 3 fold greater lesion area

was observed in DKO aortas than in ApoE-null aortas (2.3 ± 0.8 in SPRR3$^{+/+}$ApoE$^{-/-}$ vs 6.8 ± 1.9 in SPRR3$^{-/-}$ApoE$^{-/-}$; Figure 2.5, A-B; $p = 0.048; n = 8$ per group). The significant increase in atheroma burden in DKO mice indicated that loss of SPRR3 resulted in increased plaque burden.

2.3.2 VSMC Survival is Selectively Reduced in Atheromas of SPRR3-Deficient Mice

Since SPRR3 expression was primarily observed in atheroma VSMCs, we sought to determine whether VSMC localization or content was altered in mice lacking SPRR3. An initial stain with anti-α-SMA of aortic root sections from mice fed normal chow suggested DKO mice had lower α-SMA-positive VSMC content than age-matched ApoE-null mice (Figure 2.6, A). To quantify the change in lesion VSMC content, we collected confocal images of anti-α-SMA-stained and anti-smooth muscle myosin heavy chain (SM-MHC)-stained aortic root sections from DKO and ApoE-null mice fed normal chow (Figure 2.6, B-C). VSMC content was quantified as the number of α-SMA-positive or SM-MHC-positive cells normalized to plaque cellularity (cells/mm^2). α-SMA-positive staining indicated that DKO ($n = 8$) lesions had a 37.3% ($p < 0.001$) reduction in lesion VSMC content compared with control ($n = 8$; Figure 2.6, D). Similar results were observed in SM-MHC-stained sections (Figure 2.7, $p = 0.0001; n = 3$ SPRR3$^{+/+}$ApoE$^{-/-}$ and SPRR3$^{-/-}$ApoE$^{-/-}$ mice). When VSMC content was quantified in DKO and ApoE-null mice fed high fat diet for 6 months, lesion VSMC content was reduced by 48.1% ($p = 0.002$) in mice lacking SPRR3.

The reduced atheroma VSMC content in mice lacking SPRR3 could be due to an increase in lesion VSMC cell death or a reduction in proliferation. To determine whether the reduced VSMC content was related to VSMC survival, we compared VSMC death in aortic

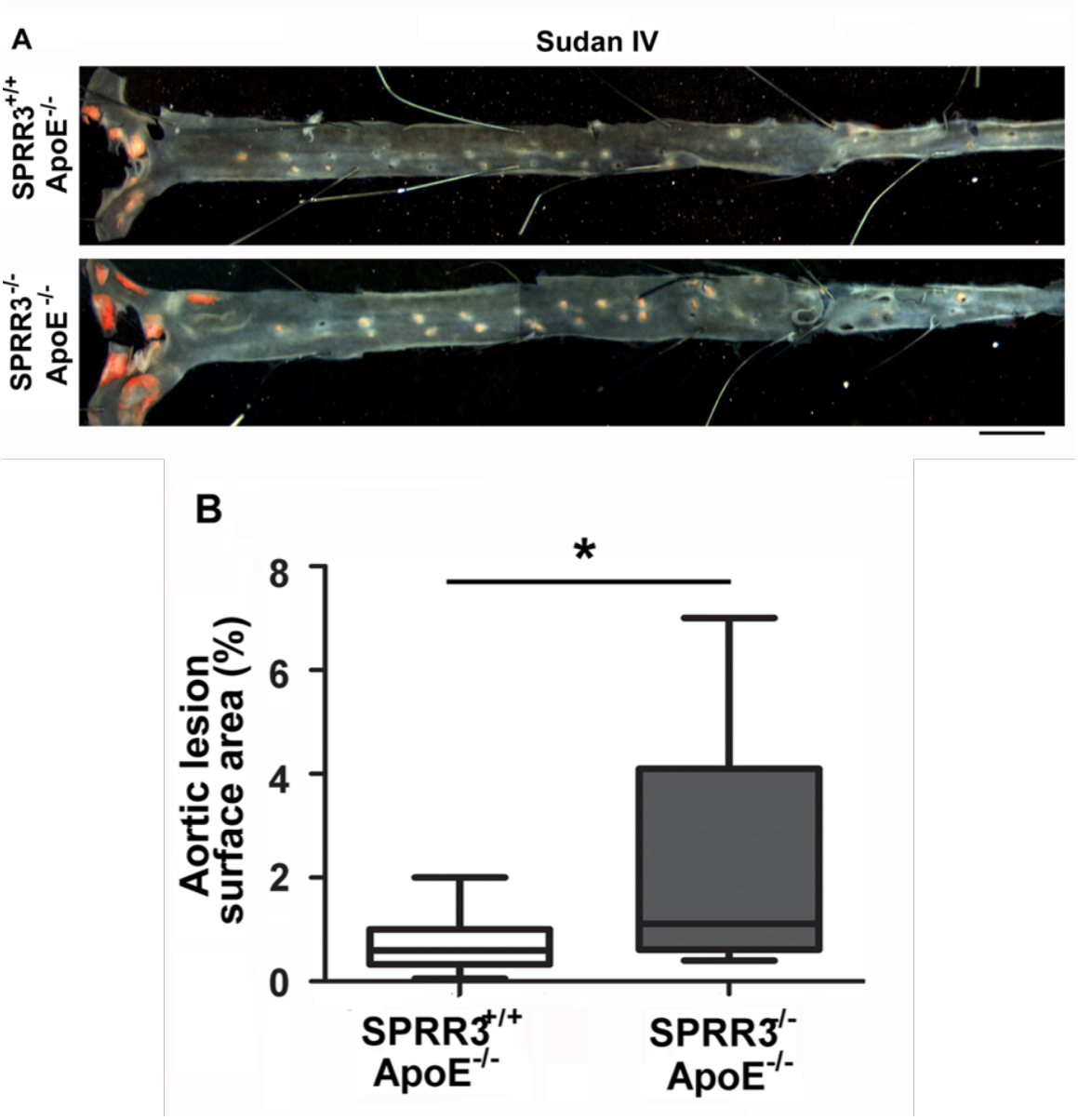

Figure 2.3: **Atherosclerosis progression was accelerated in ApoE-null mice lacking SPRR3.** (A) Representative *en face* images of Sudan IV (red) stained aortas from 6 mo. old gender-matched SPRR3$^{+/+}$ApoE$^{-/-}$ ($n = 13$) and SPRR3$^{-/-}$ApoE$^{-/-}$ ($n = 13$) mice (normal chow). Scale bar, 2mm. (B) Quantification of aortic lesion surface area. Bars represent mean $\pm$ SD. $^{*}p < 0.05$.

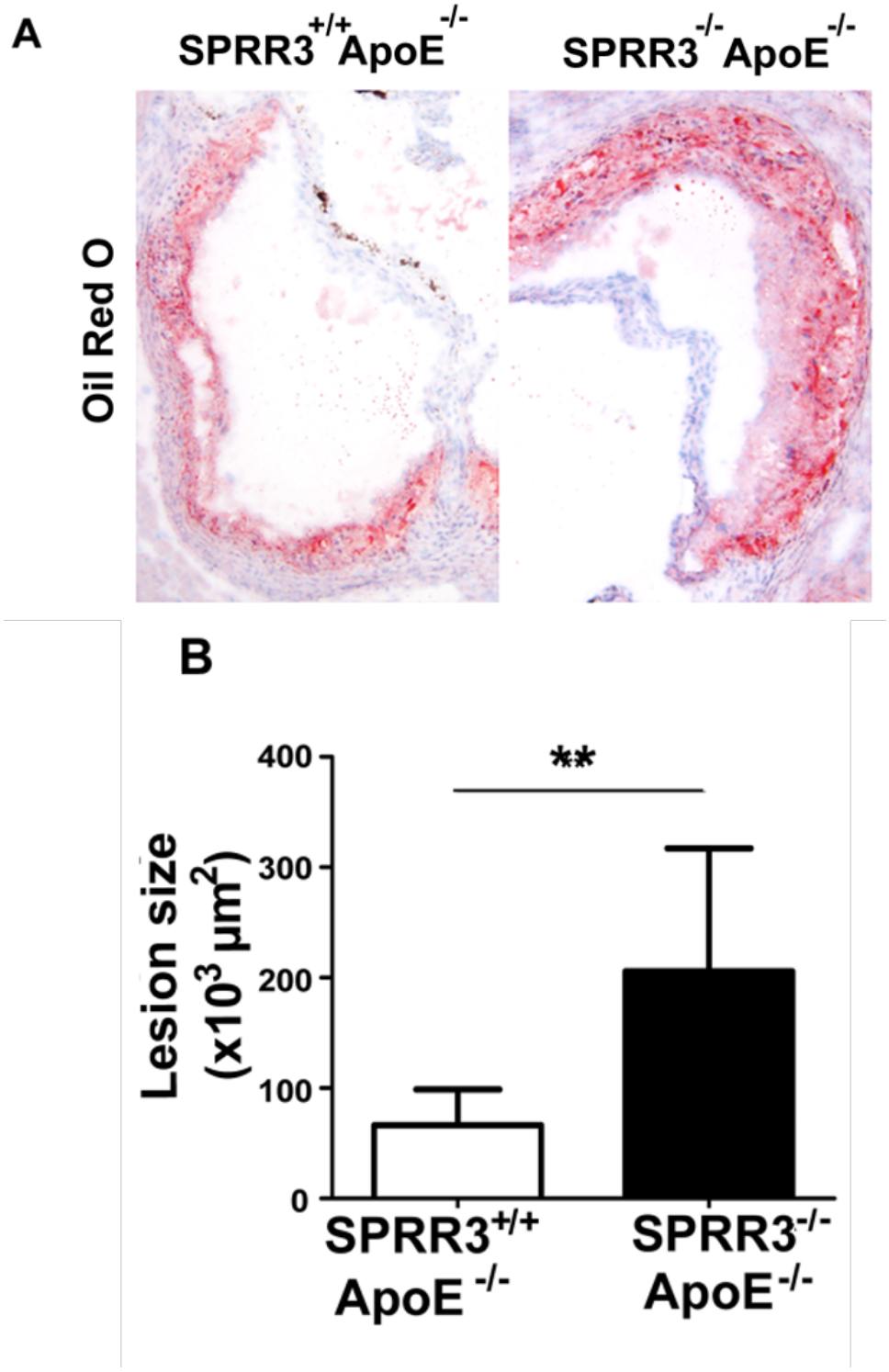

Figure 2.4: **SPRR3-deficient mice have increased aortic root lesion size.** (A) Representative photomicrographs of Oil Red O-stained aortic root sections from age-matched mice fed normal diet ($n = 4$ SPRR3$^{+/+}$ApoE$^{-/-}$ and SPRR3$^{-/-}$ApoE$^{-/-}$ mice). (B) Quantification of Oil Red O staining. Bars represent mean $\pm$ SD. $^{**}p < 0.01$.

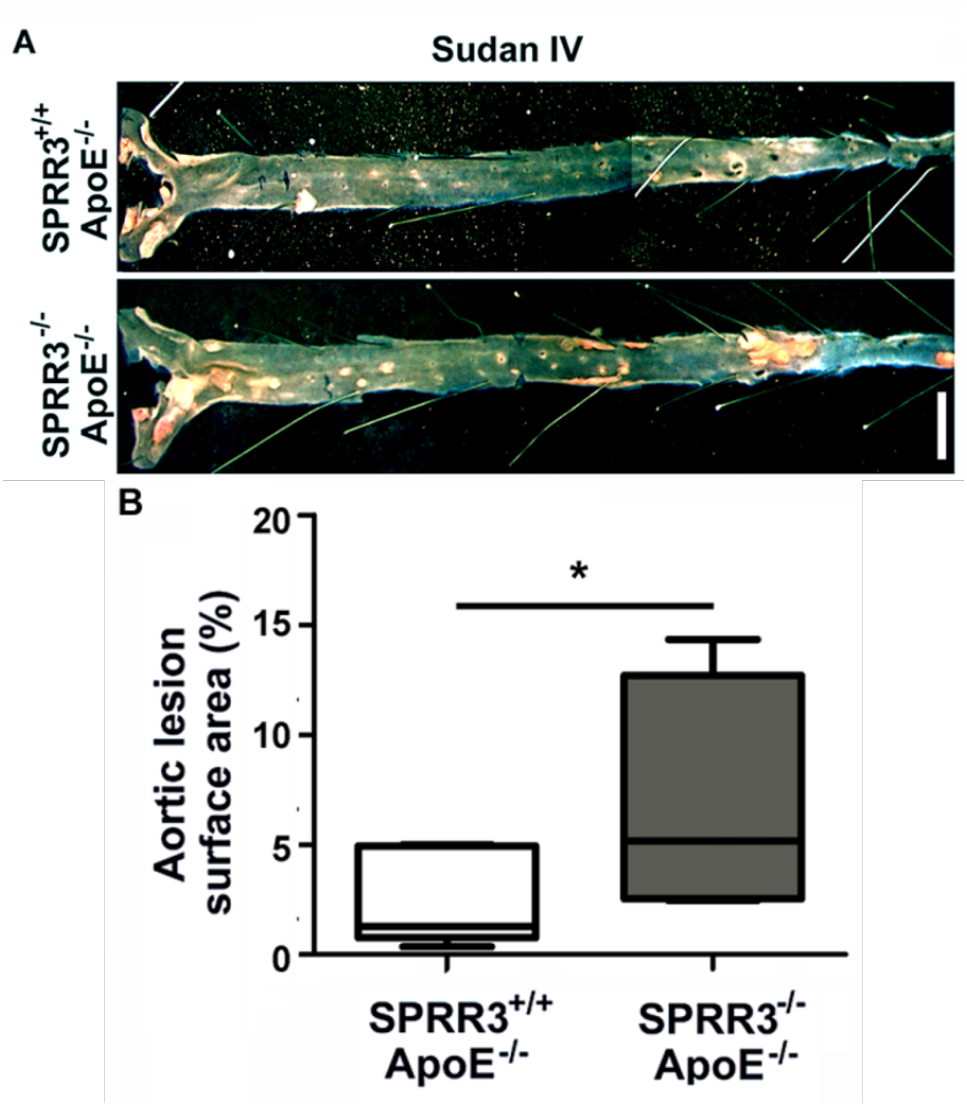

Figure 2.5: **High fat diet leads to aggravated lesion burden in mice lacking SPRR3.** (A) Representative photomicrographs were taken of aortas stained with Sudan IV for *en face* lesion analysis. Scale bar, 2mm. (B) Quantification shows surface area positive for Sudan IV staining in mice ($n = 8$ SPRR3$^{+/+}$ApoE$^{-/-}$ and SPRR3$^{-/-}$ApoE$^{-/-}$ mice). Original magnification, x10 (A). $*p < 0.05$, $**p < 0.01$.

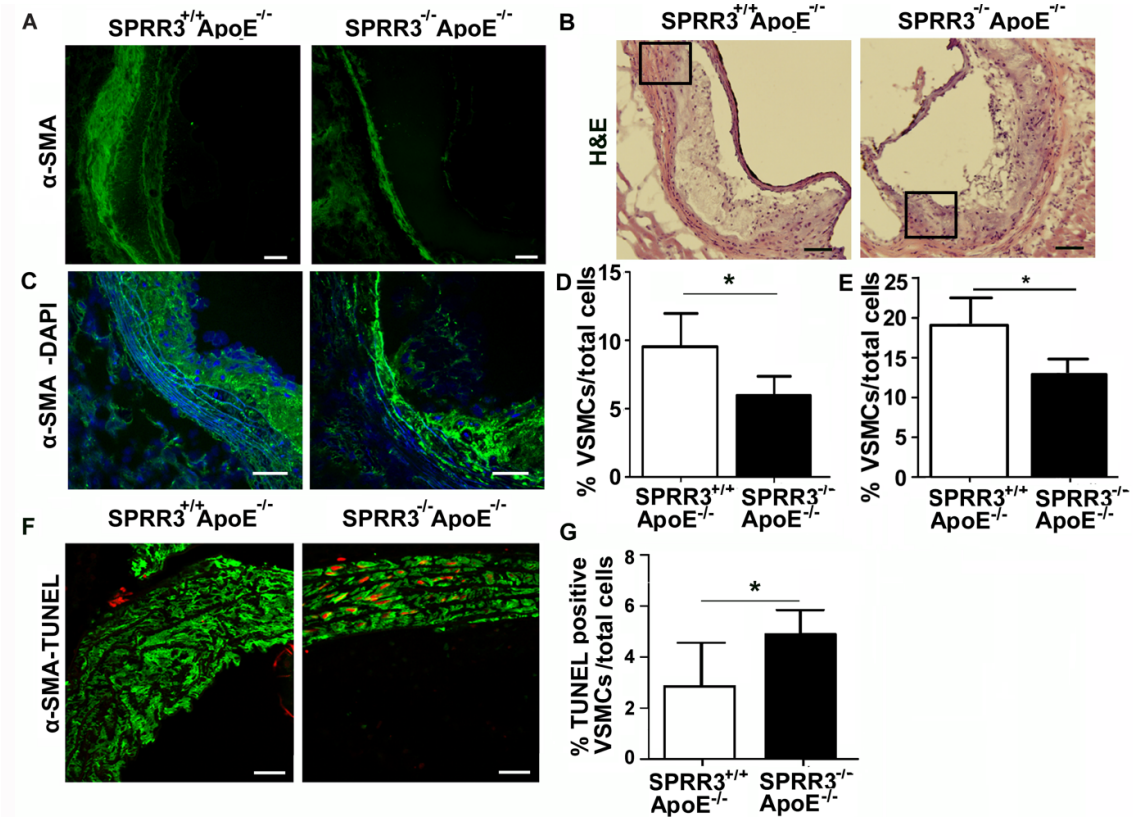

Figure 2.6: **Increased VSMC apoptosis in SPRR3-null atheroma but not in disease-free arteries.** (A) Low magnification photomicrographs of aortic root sections from 6 mo. SPRR3$^{+/+}$ApoE$^{-/-}$ and SPRR3$^{-/-}$ApoE$^{-/-}$ mice fed normal chow stained with α-SMA (green). Scale bar, 100 μm. (B) H&E stained aortic root sections from 6 mo. SPRR3$^{+/+}$ApoE$^{-/-}$ and SPRR3$^{-/-}$ApoE$^{-/-}$ mice (normal chow). Scale bar, 100 μm. Boxed area magnified in C. (C) Representative Z plane from confocal fluorescent microscopy images collected with x40 lens. Sections stained with α-SMA and DAPI (blue). Scale bar, 50 μm. (D) Quantification of %α-SMA positive cap cells in aortic root sections from 6 month old SPRR3$^{+/+}$ApoE$^{-/-}$ ($n = 8$) or SPRR3$^{-/-}$ApoE$^{-/-}$ ($n = 8$) mice fed normal diet. (E) Quantification of % α-SMA positive cap cells in aortic root sections from SPRR3$^{+/+}$ApoE$^{-/-}$ ($n = 6$) or SPRR3$^{-/-}$ApoE$^{-/-}$ ($n = 6$) mice fed high fat diet for 6 months. (F) Representative Z plane from confocal image of α-SMA-TUNEL (red) showed a high degree of colocalization in aortic root of SPRR3$^{+/+}$ApoE$^{-/-}$ and SPRR3$^{-/-}$ApoE$^{-/-}$ mice fed high fat diet for 6 months. Scale bar, 40 μm. (G) Quantification of %fibrous cap α-SMA/-TUNEL colocalization in (F) assessed in 10 fields ($n = 5$ SPRR3$^{+/+}$ApoE$^{-/-}$ and SPRR3$^{-/-}$ApoE$^{-/-}$ mice). Bars represent mean $\pm$ SD. $^*p < 0.05$.

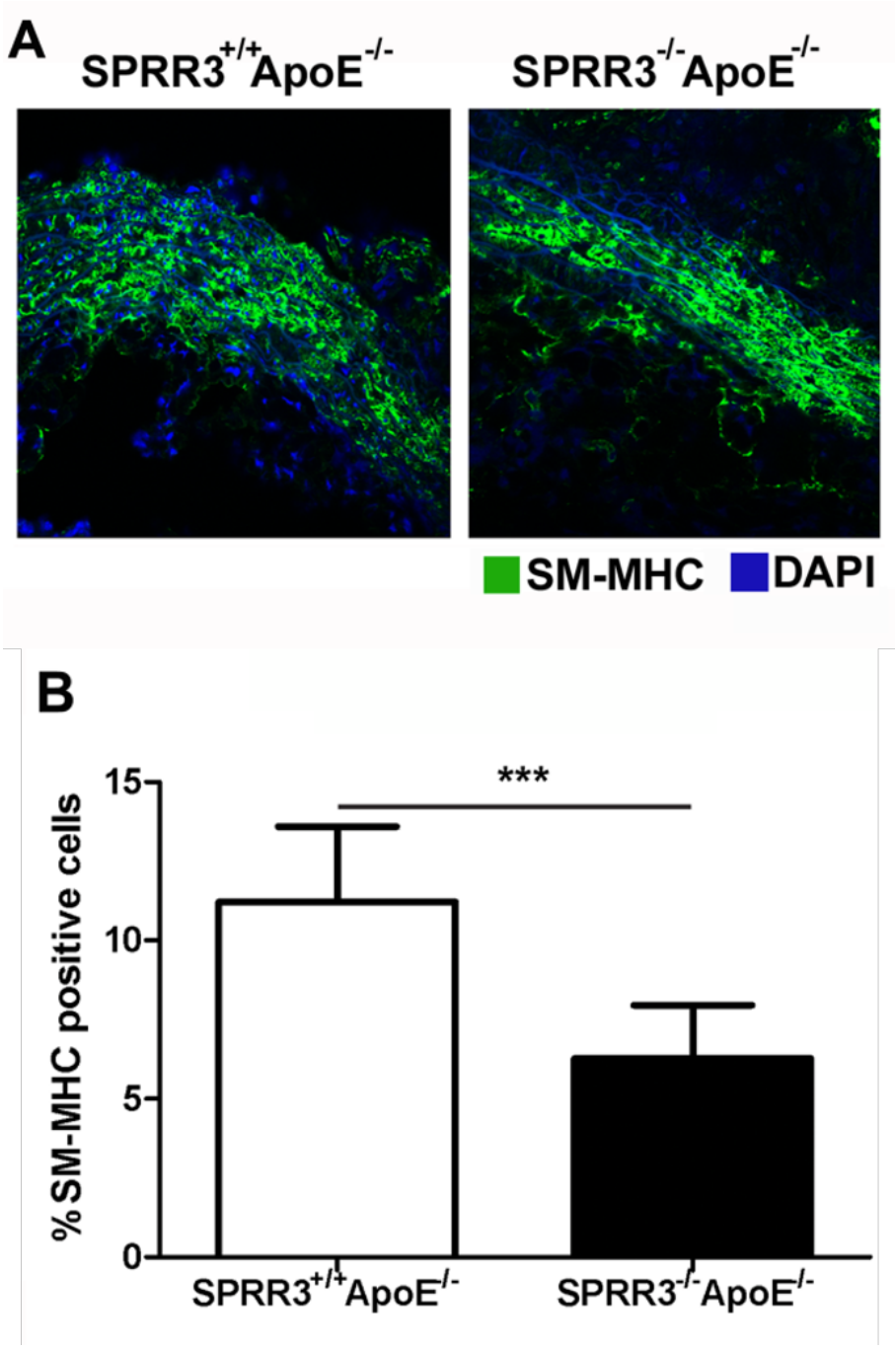

Figure 2.7: **SPRR3-deficient mice have reduced SM-MHC-positive VSMC content when compared with ApoE-null control.** (A) Fluorescent images were acquired by confocal fluorescent microscopy with x40 lens. A representative Z plane shows a reduction in SM-MHC-positive cells (green) in aortic root lesions of 6 month normal diet-fed SPRR3$^{-/-}$ApoE$^{-/-}$ mice compared with control. (B) Quantification of %SM-MHC positive cells in aortic root sections from SPRR3$^{+/+}$ApoE$^{-/-}$ ($n = 3$) and SPRR3$^{-/-}$ApoE$^{-/-}$ ($n = 3$) mice; 35 HPF images evaluated from each cohort.

root lesions of ApoE-null and DKO mice following 6 months on a high-fat diet. In the aortic root, the number of fibrous cap cells co-staining for TUNEL and α-SMA was increased 70.6% in mice lacking SPRR3 (Figure 2.6, E-F; $p = 0.0316$). However, there was no significant difference between groups in basal cell death levels in arterial tissue lacking atheroma, as measured by the percent of cells co-stained for TUNEL and α-SMA ($4.2 \pm 2.3\%$ in SPRR3$^{+/+}$ApoE$^{-/-}$, $n = 7$; $4.32 \pm 3.2\%$ in SPRR3$^{-/-}$ApoE$^{-/-}$, $n = 10$; $p = 0.67$). There was also no significant difference in the number of cells costaining for MOMA-2 and TUNEL or vWF and TUNEL (Figure 2.8, MOMA-2-TUNEL $p = 0.91$).

2.3.3 Proliferation Remains Unchanged in Aortic Roots of Mice Lacking SPRR3

To determine whether changes in proliferation may play a role in reduced VSMC content, we performed immunohistochemistry for Ki67 in aortic root lesions of ApoE-null and DKO mice fed a high fat diet for 6 months. No significant difference was observed in % Ki67-positive cells between groups (Figure 2.9, $p = 0.33$). Our data suggest, therefore, that loss of SPRR3 led to reduced VSMC survival in the atheroma and subsequent reduced lesion VSMC content.

2.3.4 Increased Atherosclerosis in ApoE-null Mice Lacking SPRR3 is not Attributable to Bone-Marrow Derived Cells

Since SPRR3 expression was primarily but not exclusively detected in VSMCs (Pyle et al. (2008); Figure 2.2, A), we sought to identify the affected cell type(s) driving increased atheroma burden in mice with global SPRR3 deficiency. As macrophages are the primary source of foam cells in murine atherosclerosis(Shi et al., 2000; Tabas, 2002), assessments

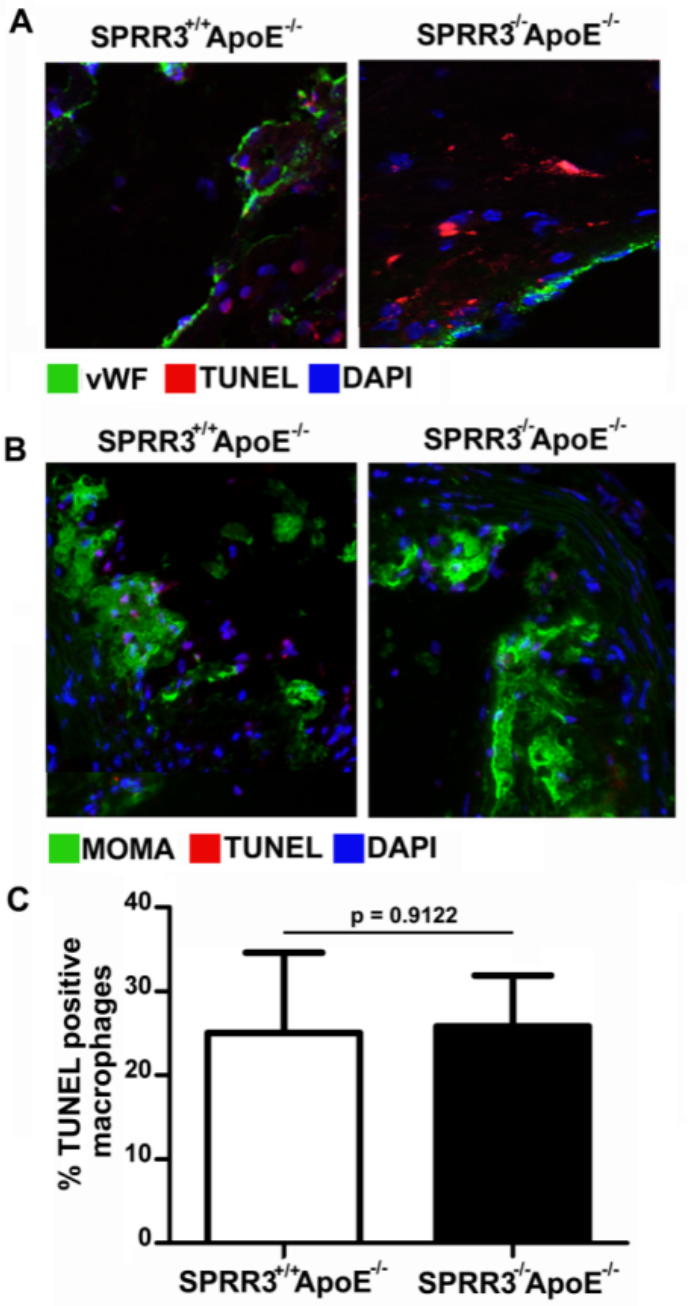

Figure 2.8: **Loss of SPRR3 does not affect cell death in endothelial cells or lesion macrophages.** (A) Aortic root sections from 6 month old, normal diet-fed SPRR3$^{+/+}$ApoE$^{-/-}$ and SPRR3$^{-/-}$ApoE$^{-/-}$ mice were stained with vWF (green) and TUNEL (red). Fluorescent images were acquired by confocal fluorescent microscopy with x40 lens. A representative Z plane shows both groups lacked TUNEL-positive endothelial cells. (B) Serial sections from the aortic root of 6 month old, normal diet-fed SPRR3$^{+/+}$ApoE$^{-/-}$ and SPRR3$^{-/-}$ApoE$^{-/-}$ mice were stained with MOMA-2 (green) and TUNEL (red). (C) Quantification of images from (B) showed no significant difference in %TUNEL-positive macrophages between groups ($n = 4-5$ per group).

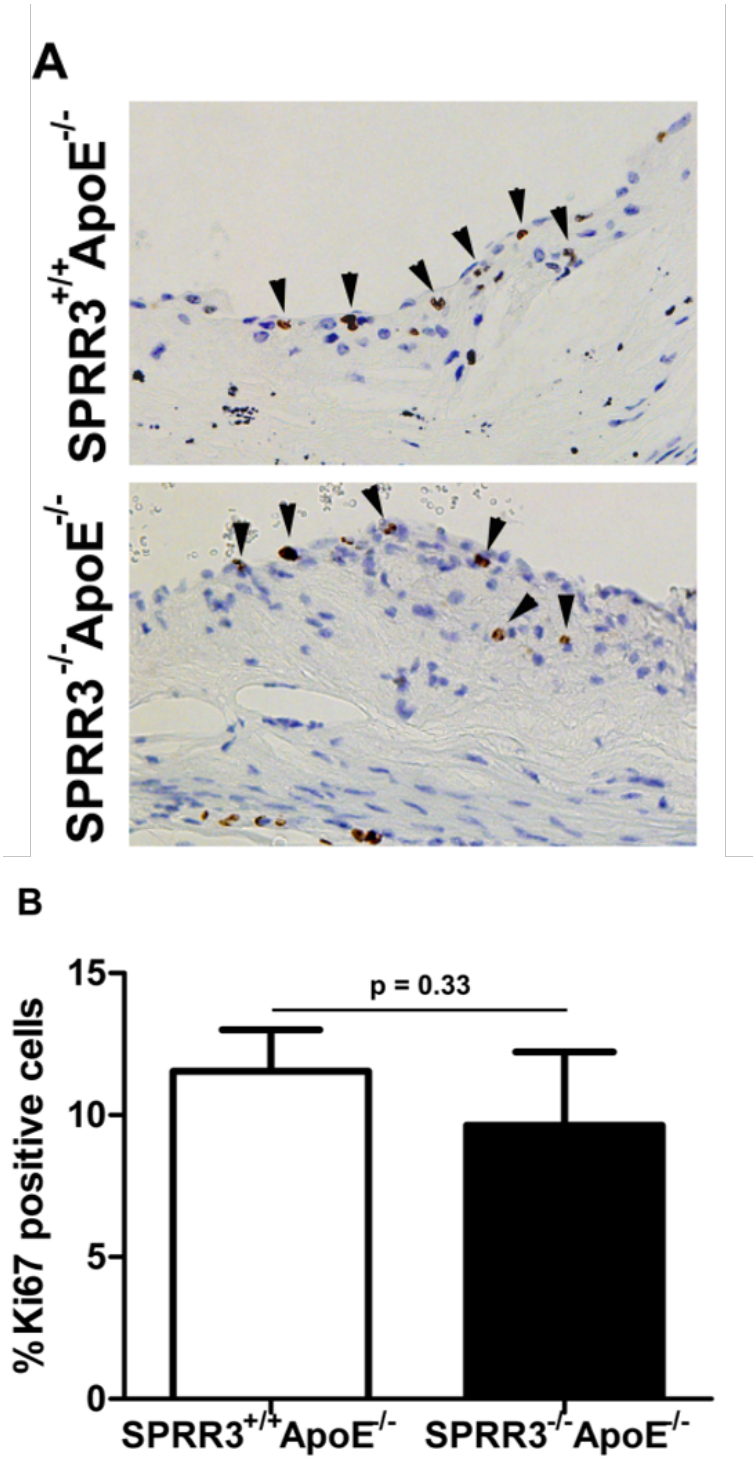

Figure 2.9: **Loss of SPRR3 does not affect proliferation of lesion cells.** (A) Immunohistochemical staining for Ki67 of aortic root sections from 6 month high fat diet-fed SPRR3$^{+/+}$ApoE$^{-/-}$ ($n = 3$) and SPRR3$^{-/-}$ApoE$^{-/-}$ ($n = 3$) mice. (B) Quantification of % Ki67+ cells from (A).

of plaque burden that rely on lipid staining may reflect changes in macrophage recruitment or foam cell formation. We therefore evaluated changes in macrophage content relative to lesion size in aortic root lesions of ApoE-null and DKO mice fed high fat diet for 4 months. Macrophage content was quantified by MOMA-2 staining, which binds an intracellular target in mouse monocytes and macrophages. Although absolute MOMA-2-positive area was increased in DKO mice, after controlling for lesion size, there was no significant difference in MOMA-2-positive staining between ApoE-null ($47.9 \pm 6.2\%$) and DKO ($34.3 \pm 2.1\%$) aortic roots (Figure 2.10, A-B; $n = 8$ SPRR3$^{+/+}$ApoE$^{-/-}$ and SPRR3$^{-/-}$ApoE$^{-/-}$; $p = 0.14$). Similarly, there was no significant difference in CD3-positive staining, an indicator of T cell content, between ApoE-null ($8.07 \pm 3.38\%$) and DKO ($11.4 \pm 0.94\%$) aortic roots ($p = 0.06$) after controlling for lesion size. These data suggested the SPRR3-dependent increase in atheroma burden observed in DKO mice was not mediated by bone marrow (BM) -derived cells.

To further confirm that the effects of SPRR3 loss were mediated through arterial, rather than BM-derived cells, we performed bone marrow transplantation (BMT) experiments. BM from ApoE-null (SPRR3$^{+/+}$ApoE$^{-/-}$), SPRR3 knockout (SPRR3 $^{-/-}$ApoE$^{+/+}$), or DKO (SPRR3 $^{-/-}$ ApoE $^{-/-}$) donor mice was transplanted into 2-week old lethally irradiated DKO recipient mice. The experimental approach and anticipated results are explained in Figure 2.10, C. After 4 months of high fat diet, plaque burden was assessed in aortic root sections and in dissected aortas of each group. Previous studies have demonstrated that rescue of ApoE expression in the BM compartment of ApoE-null mice is sufficient to reduce lesion burden (Linton et al., 1995). We therefore expected that DKO recipients of SPRR3$^{-/-}$ApoE$^{+/+}$ donor cells (positive control) would exhibit significantly reduced atheroma

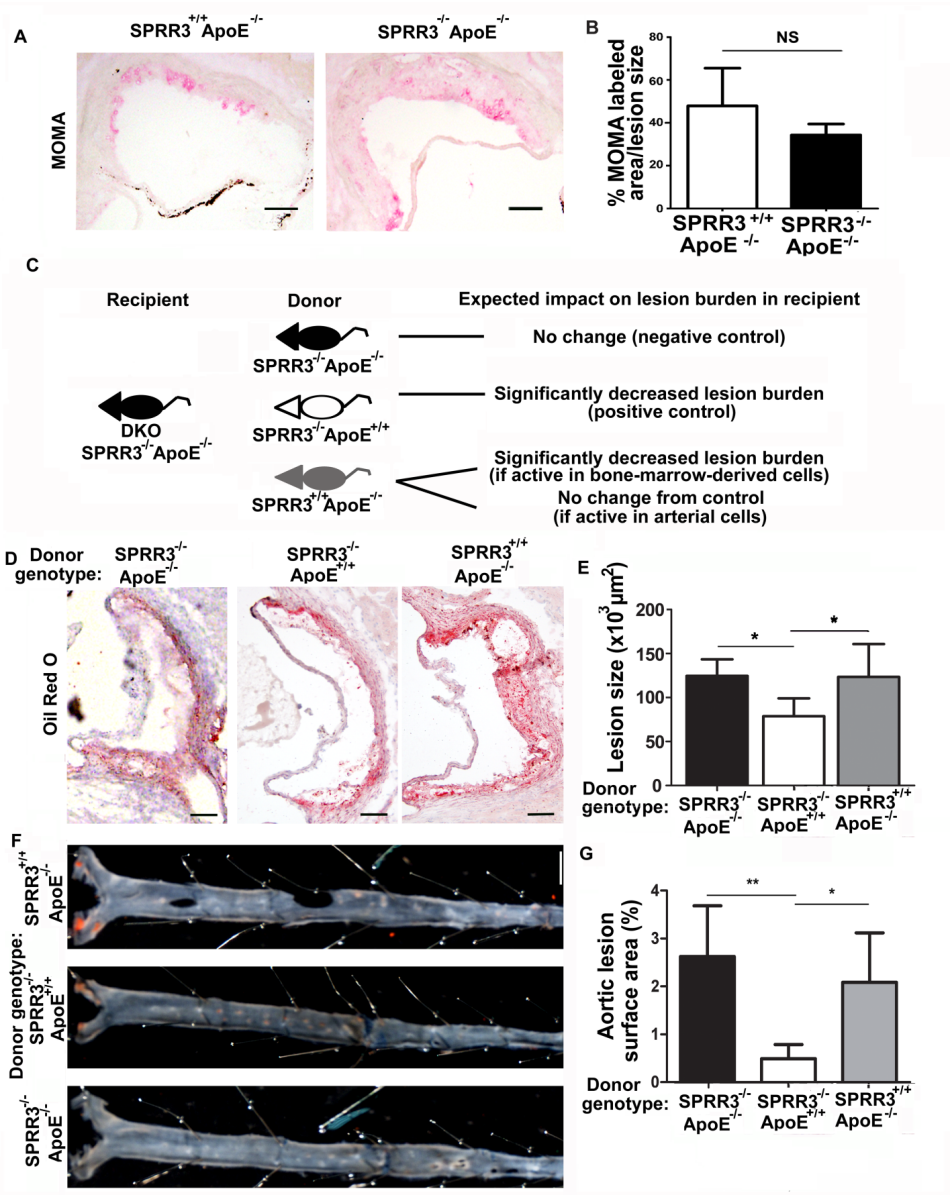

Figure 2.10: **Bone-marrow derived cells did not contribute to SPRR3-dependent effects on atherosclerosis development.** (A) Representative photomicrographs of MOMA-2-stained aortic root sections of 6 mo. mice (normal chow; $n = 8$ SPRR3$^{+/+}$ApoE$^{-/-}$ and SPRR3$^{-/-}$ApoE$^{-/-}$). Scale bar, 100 μm. (B) Quantification of MOMA-2 staining normalized to lesion size (i.e. MOMA-2 positive area/lesion area). (C-G) Donor bone marrow from SPRR3$^{+/+}$ApoE$^{-/-}$ ($n = 6$), SPRR3$^{-/-}$ApoE$^{+/+}$ ($n = 6$), or SPRR3$^{-/-}$ApoE$^{-/-}$ ($n = 6$) were transplanted into SPRR3$^{-/-}$ApoE$^{-/-}$ recipients following lethal irradiation. Mice were allowed 2 months for engraftment followed by 4 months high fat diet prior to evaluation. (C) Schematic depicting BMT experiments and anticipated results (D) Images (scale bar, 100 μm) of ORO-stained (red) lesions in aortic root sections and (E) quantification of lesion area in ORO-stained aortic root sections. (F) Images (scale bar, 2mm) of Sudan IV (red) positive staining in *en face* and (G) quantification of %Sudan IV positive surface area in *en face*. Bars represent mean $\pm$ SD. $^*p < 0.05$.

burden compared with DKO recipients of DKO donor cells (negative control). Should the effects of SPRR3 on atherosclerosis be mediated through the bone marrow compartment, we expected that transplant of SPRR3$^{+/+}$ApoE$^{-/-}$ donor cells into DKO recipients would rescue atheroma burden. Conversely, should the effects of SPRR3 be mediated through arterial cells, we expected to see no significant difference between DKO recipients of SPRR3$^{+/+}$ApoE$^{-/-}$ donor cells and the negative control group. Assessment of plaque burden in the aortic root of DKO recipients of SPRR3$^{+/+}$ bone marrow cells showed that SPRR3$^{+/+}$ bone marrow cells failed to rescue plaque formation, as recipient mice experienced no significant change in lesion size when compared with recipients of DKO bone marrow. In contrast, DKO recipients of ApoE$^{+/+}$ bone marrow experienced a 58.3% reduction ($p < 0.05$) in aortic root lesion size when compared with control recipients (Figure 2.10, D-E). *En face* analysis of dissected aortas showed an 81.3% ($p < 0.01$) reduction in aortic surface area covered by Sudan IV lipid stain (Figure 2.10, F-G) following ApoE$^{+/+}$ BMT and no significant difference in SPRR3$^{+/+}$ BMT recipients. These data demonstrated that increased atherosclerosis observed in DKO mice was not mediated by BM-derived cells but was instead mediated by arterial cells.

2.3.5 EC Survival and Proliferation are not Altered Following SPRR3 Loss

Two arterial cell types, endothelial cells (ECs) and VSMCs, are commonly involved in atheroma development. To determine whether SPRR3 loss affected EC function, we isolated primary ECs from WT C57Bl/6 mice or from SPRR3 knockout mice (Figure 2.11, A). Cell morphology assessment by brightfield microscopy and vWF staining confirmed the purity of our samples (Figure 2.11, A). We compared pooled groups of cells for differences

in survival, proliferation, or SPRR3 mRNA expression (Figure 2.11, B, C, and D, respectively). Quantification of TdT-labeled WT ECs and SPRR3-KO ECs did not show significant survival differences between groups ($25.1 \pm 7.3\%$ WT ECs; $25.6 \pm 8.6\%$ SPRR3-KO ECs; $p = 0.89$). Similarly, BrdU labeling of SPRR3-KO ECs was not significantly different from that of WT (0.08 ± 0.01 WT ECs; 0.02 ± 0.04 SPRR3-KO ECs; $p = 0.04$). Quantitative RT-PCR analysis of SPRR3 transcript expression in ECs isolated from WT C57Bl/6 mice showed little to no SPRR3 transcript expression. These data suggested that altered atheroma pathophysiology in SPRR3-deficient mice was not due to changes in EC function.

To investigate whether increased atheroma burden was associated with an effect of SPRR3 loss on VSMC function, we generated conditionally immortalized VSMCs that were WT or null for SPRR3 expression. Although SPRR3 protein was undetectable in VSMCs at baseline consistent with our previous publications (Pyle et al., 2008), we detected mRNA transcript expression in VSMCs with wild type SPRR3 (Figure 2.11, D).

2.3.6 Loss of SPRR3 Reduces VSMC Survival

To determine the role of SPRR3 in VSMC survival, we isolated primary VSMCs from SPRR3-KO (SPRR3$^{-/-}$ ApoE $^{+/+}$) and WT (C57Bl/6) mice for culture under cyclic strain. As described in our previous work, cyclic strain causes upregulation of SPRR3 expression in VSMCs *in vitro* (Pyle et al., 2008). VSMCs were transferred to collagen-I treated elastomer membranes and subjected to 72 hours of cyclic strain to promote SPRR3 expression. Treatment with 0.5 mM H_2O_2 for 2 hours resulted in a $54.4 \pm 0.23\%$ increase in TdT-labeling in primary SPRR3-KO VSMCs as measured by TUNEL staining compared with

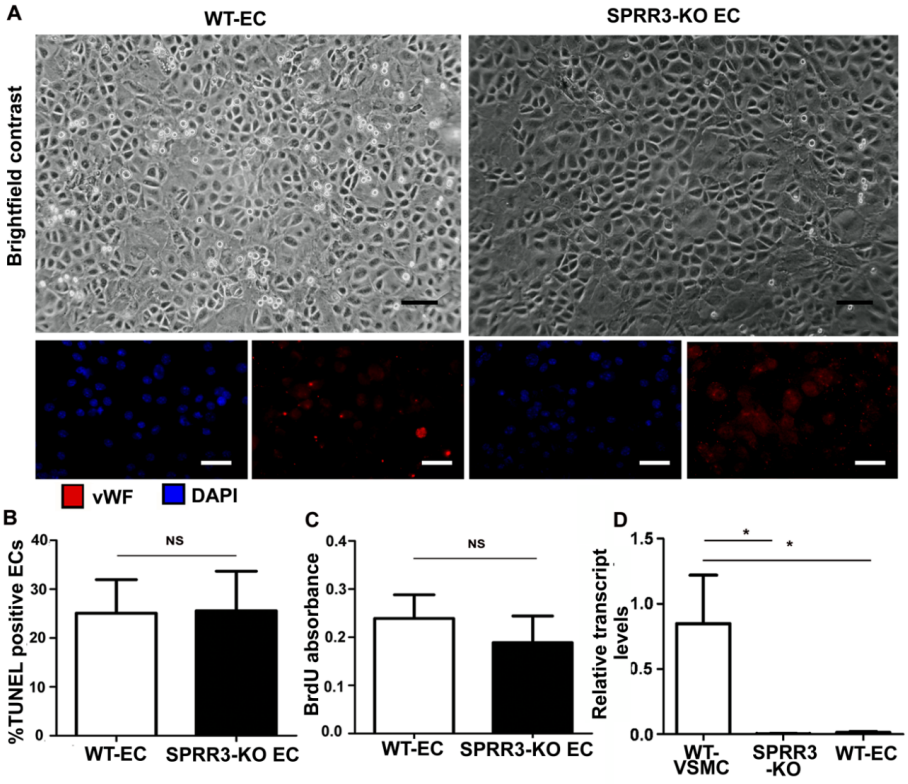

Figure 2.11: **Characterization of primary lung endothelial cells from wildtype and SPRR3 knockout mouse.** (A) Primary endothelial cells in culture (brightfield contrast) and stained by DAPI (blue) and vWF antibody (red). Scale bar, 100 μm (brightfield), 50 μm (IF). (B) Loss of SPRR3 does not affect EC apoptosis. Cells were exposed to 0.5mM H_2O_2 for 2 hours prior to TUNEL assay. (C) Loss of SPRR3 does not affect EC proliferation as measured by BrdU staining. (D) Relative transcript levels of SPRR3 in WT compared to SPRR3-KO ECs as measured by real time RT-PCR. Bars represent mean $\pm$ SD. $*p < 0.05$.

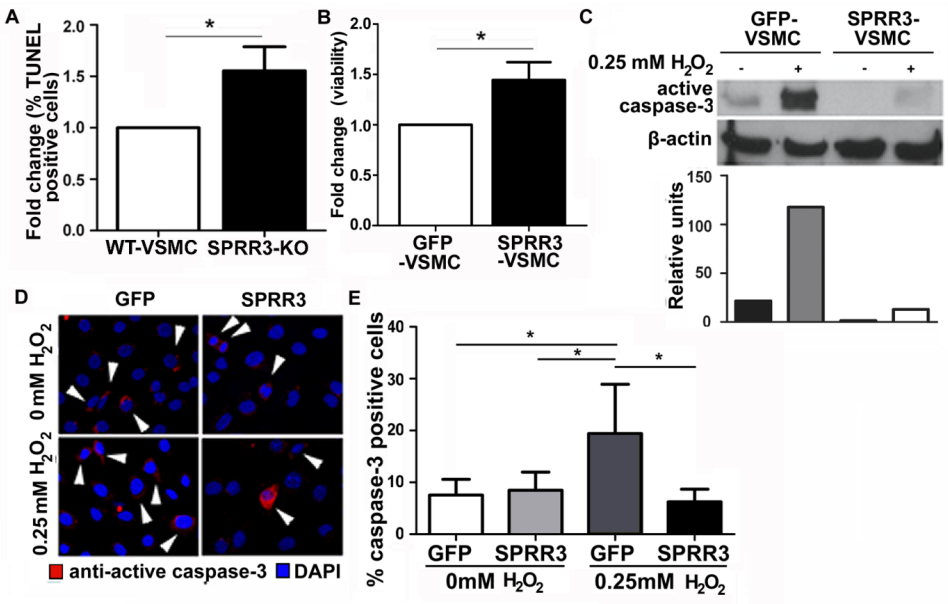

Figure 2.12: **SPRR3 modulates VSMC survival.** (A) Primary VSMCs isolated from SPRR3$^{-/-}$ ApoE $^{+/+}$ or WT mice exposed to 2 hours of oxidative stress (0.5mM H_2O_2) under cyclic strain were stained with TUNEL. %TUNEL-positive VSMCs were calculated among $>$ 200 cells/treatment in 3 replicates. (B) Viability in 24 hour serum-starved VSMCs overexpressing vector or SPRR3 measured by MTT. (C-E) SPRR3 overexpression enhances VSMC survival under 4 hours oxidative stress (0.25mM H_2O_2). (C) Western blot and analysis of active caspase-3 expression. (D) Photomicrograph showing IF staining of VSMCs expressing active caspase-3 (red); DAPI (blue) stains nuclei. Scale bar, 50 μm. Arrows indicate examples of caspase-3 positive cells. (E) Quantification of active caspase-3 IF in $>$ 200 cells/treatment ($N = 3$). Bars represent mean $\pm$ SD. *$p < 0.05$.

primary WT VSMCs (Figure 2.12, A; p=0.02) while no difference was observed in unchallenged groups under strain or between WT VSMCs and SPRR3-KO VSMCs not exposed to cyclic strain (Figure 2.13, A-B). This finding demonstrated a protective role for SPRR3 in VSMCs exposed to oxidative stress under cyclic strain.

2.3.7 VSMCs Overexpressing SPRR3 Exhibit Reduced Apoptosis and Proliferation

If loss of SPRR3 leads to increased VSMC apoptosis, we hypothesized a pro-survival phenotype would be observed with SPRR3 overexpression. To generate SPRR3-overexpressing VSMCs, we isolated VSMCs from transgenic H-2K^b-tsA58 mice that we then retrovirally

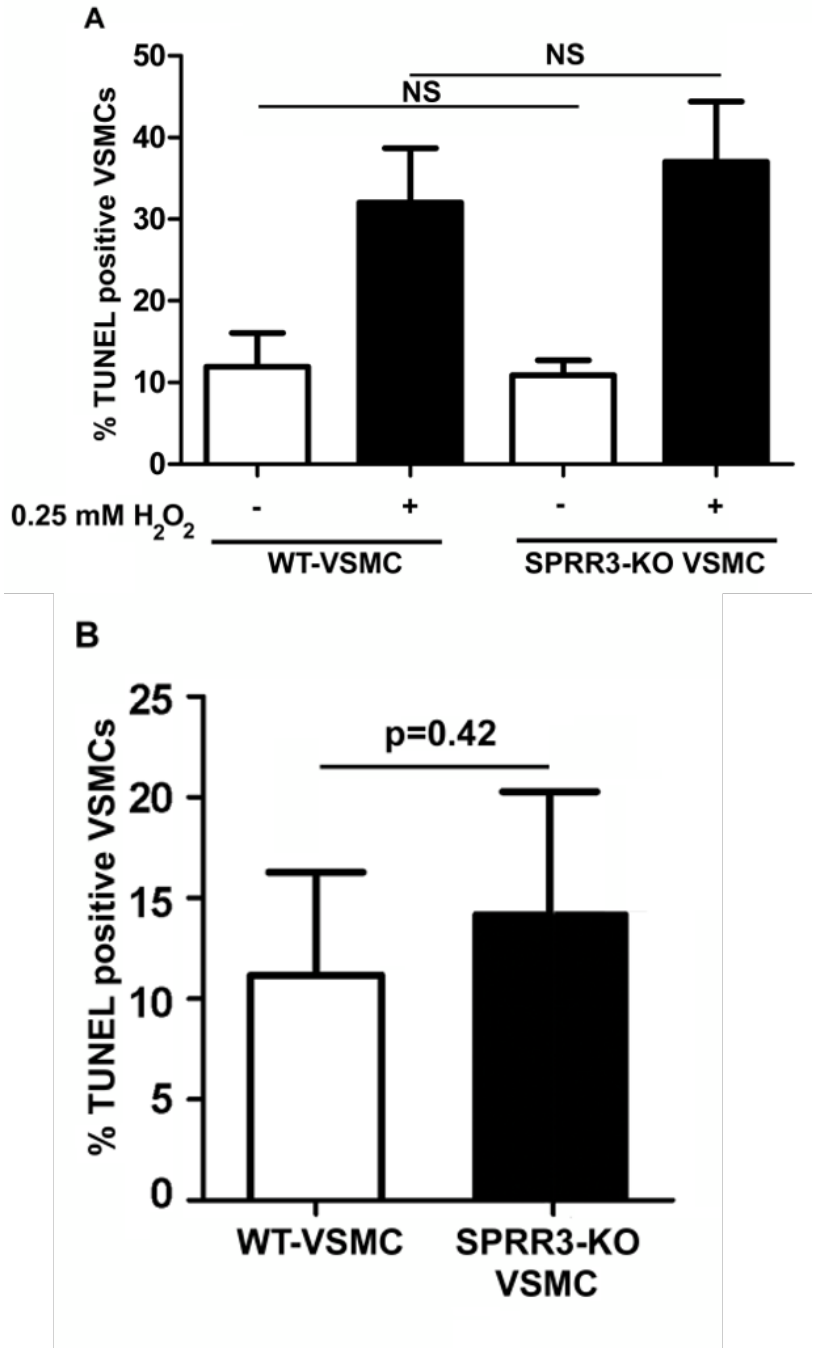

Figure 2.13: **SPRR3 loss in VSMCs does not confer protection from cell death in static conditions or in the absence of oxidative stress.** (A) WT- and SPRR3-KO VSMCs were cultured under static conditions and treated with 0.25mM H_2O_2 for 4 hours before staining with TUNEL. TUNEL-positive VSMCs were quantified as a percent of total in > 50 cells/treatment in 3 replicates. No difference in survival was observed with or without oxidative stress from WT cells (B) Primary VSMCs isolated from SPRR3$^{-/-}$ ApoE $^{+/+}$ or WT mice exposed to cyclic strain were stained with TUNEL. %TUNEL-positive VSMCs were calculated among > 50 cells/treatment in 3 replicates.

transfected with LZRS plasmid expressing GFP alone (GFP-VSMCs) or expressing human SPRR3 and GFP (SPRR3-VSMCs). Cells from the H-2K^b-tsA58 mouse expressing heat-labile T-antigen behind the mouse major histocompatibility complex H-2K^b are immortalized at 33° C and return to primary phenotype after a week at 37° C (Pyle et al., 2008).

We evaluated the effect of SPRR3 overexpression on VSMC survival using MTT dye reduction assays in serum-starved cells and both immunoblot and immunocytochemical staining analysis of active caspase-3 expression in cells exposed to oxidative stress. MTT dye reduction assays conducted under serum deprivation conditions indicated a 20% increase ($p = 0.03$) in survival of SPRR3-VSMCs compared with control GFP-VSMCs (Figure 2.12, B). This increase in VSMC viability observed with SPRR3 overexpression was not due to increased proliferation. WT-VSMCs and SPRR3-KO VSMCs treated with bromodioxyuridine (BrdU) stain revealed no significant difference in proliferation of VSMCs lacking SPRR3 when compared with control VSMCs (Figure 2.14, $p = 0.43$). To determine whether the increase in VSMC number observed in SPRR3-VSMCs was due to reduced apoptosis, we evaluated active caspase-3 levels by immunoblotting (Figure 2.12, C) or immunofluorescence (Figure 2.12, D-E) following oxidative stress (via 0.25mM H_2O_2), a pro-apoptotic trigger frequently observed in atherosclerotic lesions. Both methods demonstrated that SPRR3-VSMCs expressed less active caspase-3 in response to oxidative stress.

2.3.8 Akt Phosphorylation is Increased in VSMCs Expressing SPRR3

A myriad of signaling changes takes place in VSMCs associated with plaque development and progression. Many of these signaling changes are associated with the functional

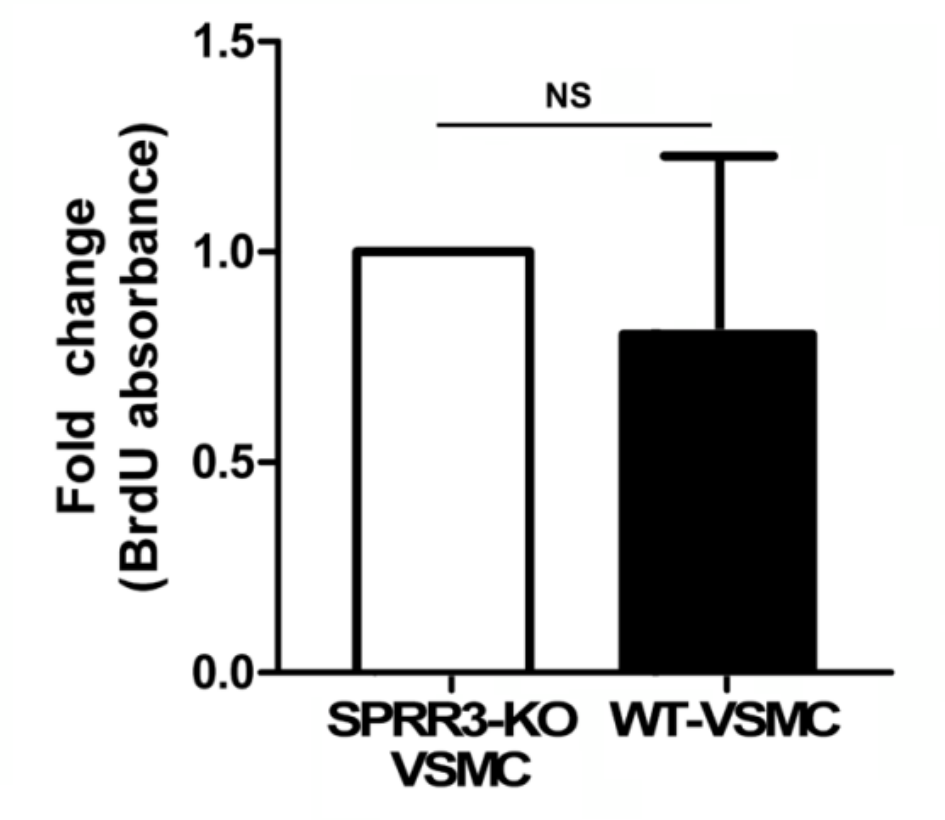

Figure 2.14: **Loss of SPRR3 does not affect VSMC proliferation *in vitro*.** WT-VSMCs and VSMCs overexpressing SPRR3 were assessed for BrdU incorporation. Colorimetric measurements were collected for 4 experiments with 3 replicates/treatment.

changes observed in VSMCs during plaque progression (e.g. proliferation, migration, synthesis of cap material) and with responses to novel interactions and stressors in the plaque microenvironment (e.g. altered mechanical strain, pro-inflammatory signals, ROS, growth factors). Signaling pathways with pro-survival functions frequently observed to be activated in plaque VSMCs include p38, ERK1/2, and Akt (Allard et al., 2008; Bass and Berk, 1995; Lehoux et al., 2000; Xu et al., 1996; Ip et al., 1990). We investigated the activity of each of these kinases by immunoblot analysis of whole cell lysates from control GFP-VSMCs and SPRR3-VSMCs. Western blot analysis indicated that Akt phosphorylation at Ser473 was increased in SPRR3-VSMCs relative to GFP-VSMCs (Figure 15, A) and in WT-VSMCs relative to SPRR3-KO VSMCs (Figure 2.15, B). However, there was no difference in phosphorylated p38 or phosphorylated ERK1/2 levels in GFP-VSMCs or SPRR3-VSMCs, indicating that SPRR3 was not a downstream effector of these pathways (Figure 2.16).

Several growth factors have been implicated in phosphorylated Akt (pAkt) activation in lesion VSMCs, including IGF-1 (Bennett and Boyle, 1998; Bennett et al., 1995). We investigated whether IGF-1 may enhance SPRR3-mediated increases in pAkt levels. Treatment of GFP- or SPRR3-VSMCs with IGF-1 triggered a proportionally equal increase in pAkt levels, indicating that SPRR3 was not a downstream effector of IGF-1 (Figure 2.15, C). Addition of a PI3K/Akt inhibitor (Ly294002) abolishes pAkt in both GFP-VSMCs and SPRR3-VSMCs, indicating that SPRR3 increases pAkt levels in a canonical, PI3K/Akt-dependent manner (Figure 2.15, C). To assess whether the observed SPRR3-mediated survival benefits were dependent on Akt activity, we evaluated GFP- and SPRR3-VSMCs with and without Ly294002 and assessed cell death using TUNEL staining. The pro-survival ef-

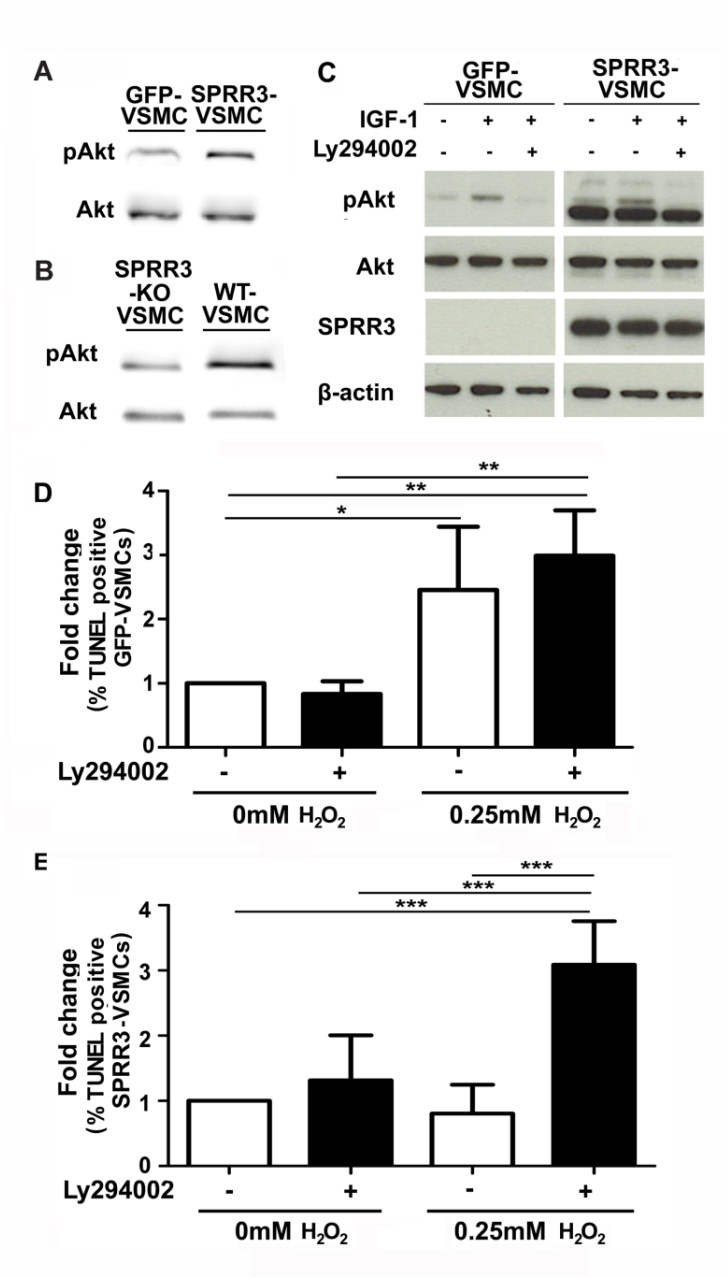

Figure 2.15: **SPRR3 mediated a PI3K-dependent increase in Akt activation required for SPRR3-dependent VSMC survival benefits.** (A) Immunoblot analysis of pAkt in cell lysate from 24 hour serum-starved VSMCs overexpressing vector or SPRR3. (B) Immunoblot analysis of pAkt in cell lysate from 24-hour serum-starved VSMCs isolated from wildtype or SPRR3 KO mice. (C) Addition of IGF-1 (20ng/mL) increased pAkt levels proportionally in VSMCs overexpressing vector or SPRR3. The SPRR3-dependent pAkt increase was ablated with addition of Ly294002 (25μM). (D-E) Quantification of TUNEL-positive VSMCs overexpressing vector (D) and SPRR3 (E) with and without Ly294002 applied at the same time as oxidative stress challenge. Apoptosis was measured following 4 hours of oxidative stress (0.25mM H_2O_2). %TUNEL positive VSMCs calculated among $>$ 100 cells/treatment in 4 replicates. Bars represent mean $\pm SD$. *$p < 0.05$; **$p < 0.01$.

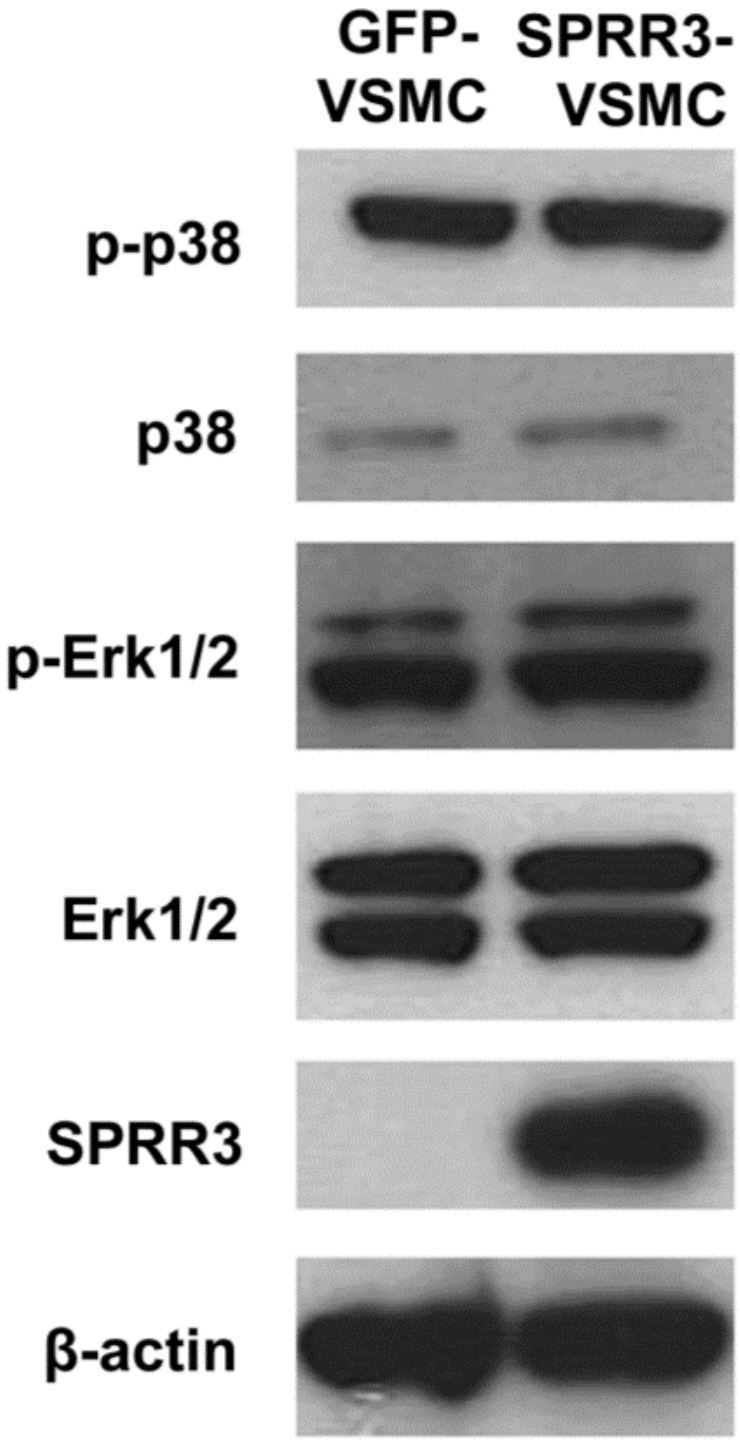

Figure 2.16: **SPRR3 overexpression in VSMCs does not affect activation of p38 or ERK1/2.** Cell lysates from SPRR3-overexpressing VSMCs or GFP-expressing controls were subjected to immunoblot analysis using anti-p-p38 (43 kDa), anti-p38 (43 kDa), anti-pErk1/2 (42/44 kDa), anti-ERK 1/2 (42/44 kDa), anti-SPRR3 (35 kDa), or loading control anti-β-actin (42 kDa).

fect of SPRR3-overexpression was abolished in cells treated with Ly294002, in which we detected a 49% increase ($p = 0.005$) in TdT-labeling compared to untreated cells (Figure 2.15, D-E).

2.4 Discussion

We have identified SPRR3 as an atheroprotective factor in VSMCs that is uniquely upregulated in mouse and human atherosclerotic lesions. Global knockout of SPRR3 in the mouse led to significantly increased atheroma burden along with reduced survival of VSMCs, but not of endothelial cells (ECs). Additionally, transplantation of SPRR3$^{+/+}$ bone marrow cells into mice lacking SPRR3 did not alter atherosclerosis development. Intriguingly, SPRR3 expression in cultured VSMCs was positively associated with Akt activity. *In vitro* studies in VSMCs challenged with oxidative stress indicated an SPRR3-mediated survival benefit. When these studies were conducted in the presence of a PI3K/Akt inhibitor, the SPRR3-mediated survival benefit was lost. Our findings indicated that SPRR3 expression in VSMCs played a critical role in Akt-mediated survival signaling in atherosclerotic lesions, protecting the atheroma from excessive VSMC apoptosis and leading to higher VSMC content in the fibrous cap.

Most studies intent on identification of atheroprotective genes have investigated ECs or immune cells. In ECs, studies have focused on key differences between gene expression in arterial tissue exposed to laminar versus turbulent flow, as exposure to turbulent flow is associated with increased risk of atheroma initiation (Dai et al., 2010; Dimmeler and Zeiher, 2003; Hahn et al., 2009; Hergenreider et al., 2012; Park et al., 2011; Surapisitchat et al., 2001). In immune cells, studies have investigated the role of genes that either reduce

inflammation or improve cholesterol homeostasis, both interventions leading to reduced lesion size and complexity (Ding et al., 2012; Kyaw et al., 2011; Langlois et al., 2011; Navab et al., 2011). Less is understood, however, about VSMC-specific atheroprotective genes. A few studies have investigated regulation of VSMC proliferation and intima-media thickness, mechanisms most critical at atheroma initiation (Boucher et al., 2007; Doran et al., 2010; Karas et al., 2001). More work is needed in investigating later stages of atheroma development where VSMC survival and maintenance of a synthetic phenotype may be more important, as these characteristics are critical for regulation of atheroma progression and fibrous cap stability (Clarke et al., 2006).

Previously, Bennett's group demonstrated accelerated atheroma progression and a vulnerable phenotype in an inducible diphtheria toxin-driven mouse model of chronic, low level VSMC apoptosis (Clarke et al., 2008). A potential explanation for this effect may be that an increase in VSMC apoptosis within the lesion will, in turn, increase cellular debris and other pro-inflammatory stimuli, recruiting macrophages and other immune cells to the lesion and accelerating foam cell formation. The effect may also suggest a protective role of VSMCs in the lesion, either through an unidentified secreted factor(s) or through delay of lipid deposition or macrophage entry. While the mechanism(s) driving atheroma progression in lesions experiencing chronic VSMC apoptosis remains uncharacterized, Bennett's model emphasizes the importance of reducing VSMC apoptosis in regulation of atheroma size and composition. Despite the potential for use in delaying atheroma progression, no one has previously identified a lesion-specific regulator of VSMC survival.

SPRR3 knockout mice demonstrated altered VSMC survival in atheromas, while VSMCs in normal arterial tissue remained unaffected. Cells residing in the atheroma microenviron-

ment encounter a myriad of stressors, putting them at increased risk of cell death. Stressors in the atheroma milieu include extracellular cholesterol and oxidized fatty acids, hypoxic conditions, rising ROS levels, and an array of inflammatory cytokines released by both activated ECs and macrophages (Deguchi et al., 2009; Geng et al., 1997, 1996; Harada-Shiba et al., 1998; Reid et al., 1992). The critical role VSMCs play in synthesis and subsequent maintenance of the barrier between these atheroma components and the circulation makes them an indispensible part of a stable plaque. Our data suggested that SPRR3 activity specifically in the atheroma may be part of an adaptive response to the injurious atheroma microenvironment by protecting VSMCs from death.

The PI3K/Akt pathway is an important regulator of cell survival. We showed that upregulation of SPRR3 in VSMCs was positively associated with increased Akt phosphorylation; and the reverse was also true, as VSMCs lacking SPRR3 had reduced pAkt levels. The SPRR family has, until recently, been recognized solely as a family of structural proteins providing support against high levels of mechanical strain. Some evidence has been published showing an association between increased SPRR3 levels and increased colorectal or breast cancer cell proliferation and Akt activity (Cho et al., 2010; Kim et al., 2012), however the mechanism for this phenotype or whether SPRR3 plays a role in oncogenesis has not yet been studied. Previous work has not identified a kinase-interacting role for SPRR family members. Thus, our current study uncovered a novel function for SPRR3 through activation of Akt to promote VSMC survival. Consistent with our hypothesis, other groups have identified pro-survival activity for SPRR family members. One investigation suggested that SPRR2a may modulate p53 transcription and p300 acetylation status in cholangiocarcinoma cells leading to reduced apoptosis (Mizuguchi et al., 2012). Another

group demonstrated that SPRR1a is upregulated downstream of the gp130 pathway in cardiomyocytes and protected against ischemic stress-induced apoptosis (Pradervand et al., 2004). Future studies will focus on elucidation of the precise molecular mechanism by which SPRR3 may activate Akt specifically in plaque VSMCs, allowing a targeted intervention aimed at VSMC protection within the lesion.

Our survival studies, in which cultured VSMCs under oxidative stress were treated with a PI3K/Akt inhibitor, showed that pAkt upregulation was required for an SPRR3-mediated survival benefit. The SPRR3-dependent increase in Akt activity occurs independently of the insulin-like growth factor signaling pathway, as treatment with IGF-1 results in a proportional increase in pAkt across cell types. Tissue-specific activators of Akt are rare. To our knowledge, the only other protein that promotes Akt activity in a tissue-specific manner is T-cell leukemia/lymphoma 1 (TCL1). Expressed only in lymphoid tissue, TCL1 was discovered due to its proto-oncogene activity in human T cell malignancies (Laine et al., 2000). TCL1 increases Akt activation by binding the PH domain of Akt and causing a conformational change to promote Ser473 phosphorylation (Laine et al., 2002). SPRR3 represents, to our knowledge, the first VSMC-specific activator of Akt and one that has the potential to mediate the VSMC atherosclerosis response.

Since chronic VSMC apoptosis leads to accelerated atherosclerosis, and SPRR3-mediated protection was lost following PI3K/Akt inhibition, the increase in atheroma burden in SPRR3 knockout mice may be at least partly attributable to altered Akt activity. Global knockout of Akt1 (the most widely expressed isoform of Akt) or Akt3 in ApoE-null mice leads to accelerated atheroma progression (Ding et al., 2012; Fernández-Hernando et al., 2007). Global Akt2 knockout on an LDLR-deficient background, meanwhile, leads to

smaller, more complex atheromas with a 6-fold increase in % TUNEL-positive cells and reduced cap VSMC content (Rensing et al., 2014). Bone marrow transplantation studies revealed that Akt1 deficiency in the BM alone is insufficient to increase the atherosclerotic phenotype in ApoE-null mice, indicating the increased atherosclerosis is probably due to changes in the arterial cells (Fernández-Hernando et al., 2007). $Akt1^{-/-}$ mice experience reduced survival of ECs, macrophages, and VSMCs, and Akt1 loss is associated with increased inflammatory molecule expression (e.g. IL-6, TNF-α) in the artery wall (Fernández-Hernando et al., 2007, 2009). Mice experiencing a global knockout of Akt3 also exhibit increased atherosclerosis on an ApoE-null background (Ding et al., 2012). Loss of Akt3 did not affect macrophage survival, but foam cell formation was increased in $Akt3^{-/-}$ macrophages *in vitro* and rescue of Akt3 in the BM of Akt3-null mice was atheroprotective. While both the Akt1 and Akt3 studies examined the specific role of BM-derived cell expression of Akt relative to arterial expression, neither study attempted to separate the role of VSMC expression of Akt from that of ECs. *In vitro* studies have indicated that VSMCs isolated from atheroma in humans and mice have downregulated activity of Akt pathway members (e.g. FoxO3, GSK3-β) and are more prone to apoptosis (Allard et al., 2008). In our study, upregulation of Akt activity by SPRR3 may be stabilizing atheroma VSMCs and thereby slowing plaque progression.

Altogether, we show loss of SPRR3 in the plaque accelerates atheroma progression while reducing VSMC pro-survival signals. While atheroprotective signaling has been identified in areas of shear stress, these pathways are generally downregulated in atheroma-prone regions experiencing turbulent mechanical stress. Our findings demonstrated that atheroprotective signals also occur in atheroma-resident cells. Moreover, the atheroma-

specific expression pattern provides a unique opportunity for targeted intervention in atheroma VSMCs. Our data suggests lesion VSMC expression of SPRR3 may provide a defense mechanism in atherosclerotic plaques, in which pro-survival Akt signaling is promoted to stabilize these cells under mechanical strain, slowing plaque progression. Identification of intermediary signaling interactions may provide key targets for future therapy of patients with early onset or advanced stages of CVD. In the next chapter, we explore the implications of SPRR3-dependent changes in VSMC function, including reduced atheroma VSMC content and increased VSMC apoptosis, on atheroma stability.

CHAPTER 3

Loss of SPRR3 in ApoE$^{-/-}$ Mice Leads to Increased Atheroma Vulnerability

3.1 Introduction

In the previous chapter, we presented evidence that loss of SPRR3 expression reduces atheroma VSMC content and survival, accelerating atheroma progression. As was discussed in the Introduction, research of plaque rupture has primarily utilized data collected during autopsy studies and carotid endarectomies (Thim et al., 2008; Arbab-Zadeh et al., 2012; Virmani et al., 2003). These studies have revealed that an increase in artery obstruction is not correlated with risk of rupture. In fact, plaques that are less than 80% stenotic are the most likely to be associated with occlusion due to plaque rupture (Giroud et al., 1992; Glaser et al., 2005). A set of common characteristics is observed in all culprit plaques. They have a large lipid-rich core (Schwartz et al., 2007) and a thin fibrous cap, usually consequent to reduced extracellular matrix in VSMC-poor caps (Libby, 2013; Lutgens et al., 1999). The association of reduced VSMC content within the atheroma has prompted us to explore whether mice lacking SPRR3 may also be at increased risk of vulnerable atheromas.

Fibrous cap thinning is hypothesized to result from an imbalance between MMP release, primarily from macrophages, usually found at higher concentration near a rupture in the cap, and VSMC synthesis of matrix for cap maintenance (Libby, 2013). Moreover, though this set of common characteristics has been identified among culprit plaques, myocardial infarction patients from these studies are also shown to have multiple vulnerable

but unruptured plaques with the same common characteristics observed in the culprit ruptured plaque (Mann and Davies, 1999). The molecular trigger causing one such vulnerable plaque to rupture thus remains unclear.

SPRR3, which is expressed in atheroma VSMCs but not in healthy arterial tissue, is necessary to modulate atherosclerosis progression (Young et al., 2005; Pyle et al., 2008; Segedy et al., 2014). Loss of SPRR3 leads to increased atheroma burden and reduced atheroma VSMC content associated with increased VSMC death in an Akt-dependent manner (Segedy et al., 2014). Previous work has indicated that chronic, low level VSMC apoptosis over 10 weeks is sufficient to promote some characteristics of plaque instability, such as thinning fibrous caps and increased percentage of lipid-rich core size (Clarke et al., 2008).

In this study, we use SPRR3$^{-/-}$ ApoE$^{-/-}$ mice to explore the effect of SPRR3 loss on long-term atheroma stability. We show that loss of SPRR3 reduces stability in brachiocephalic artery atheromas, leading to larger lipid-rich cores and thinner fibrous caps with reduced collagen content, and leads to an unprecedented increase in coronary artery atheroma complexity. *In vitro*, we show that SPRR3 loss itself reduces VSMC collagen type I expression in an Akt-dependent manner. Our study demonstrates that SPRR3 promotes stability of advanced atheromas in addition to its role in slowing atheroma growth.

3.2 Methods

3.2.1 Histology

Brachiocephalic artery sections (10 μm) were collected from SPRR3$^{+/+}$ ApoE$^{-/-}$ and SPRR3$^{-/-}$ ApoE$^{-/-}$ mice fed high fat diet for six months and stained with Masson's trichrome. Mor-

phometry calculations were performed using ImageJ (NIH). The relative lipid-rich core area was determined by dividing the area of the lipid-rich core, as defined by the colorless area within the lesion, by the total area of the lesion. Percent cap collagen content was determined by dividing the area of connective tissue along the luminal surface of the lesion by the total cap area, which was determined by measuring the area between the luminal surface and the lipid-rich core (Seimon et al., 2009). For evaluation of lipid-rich core size, cap thickness, and cap collagen content, five sections per mouse were assessed. Sections not containing lesions with detectable lipid-rich core or fibrous cap were discarded, and the remaining images were quantified as described. For quantification of cap macrophage content, brachiocephalic artery atheroma sections from 6 month high fat diet-fed ApoE-null and DKO mice were immunohistochemically stained with antibody against F480. Using ImageJ, the area of F480+ staining was measured and normalized against cap area to determine %macrophage area within the cap.

Cardiac apices collected from ApoE-null and DKO mice were divided into three large transverse sections before being paraffin embedded for serial sectioning. A single 10μm section from each large transverse section MOVAT stained left ventricular coronary arteries were categorized according to Stary's classification (Stary et al., 1995, 1994) as no lesion, fatty streaks (AHA type II), intermediate atheromas (AHA type IV), or advanced atheromas (AHA type V). In brief, lesions categorized as fatty streaks were characterized by foam cell accumulation as represented by a small amount of blue mucin-type buildup on the luminal surface of the artery. Lesions categorized as intermediate atheromas were characterized by pooled lipid/foam cells, represented by colorless areas associated with the blue mucin buildup within the lesion and are covered by a thin intimal layer of cells. Lesions catego-

rized as advanced atheromas are more complex, with well-delineated lipid-rich cores and thicker caps.

3.2.2 Immunoblotting

For protein collection, cultured cells were washed twice with PBS and lysed using RIPA buffer supplemented with protease inhibitors and phosphatase inhibitors (Roche). Whole cell lysates were rocked 30 minutes at 4° C then spun 15 minutes at 13,000xg and the supernatant collected. Protein concentrations were determined using a bicinchoninic acid (BCA) kit (Thermo Scientific). Proteins were denatured 10 minutes at 95° C in SDS sample buffer before being resolved by SDS-PAGE electrophoresis and transferred onto a nitrocellulose membrane (PerkinElmer). Blots were blocked in 5% nonfat milk and probed with antibodies against collagen type I (MDBioproducts, #203002) or β-actin (Sigma, #A5441).

3.2.3 Real Time Reverse Transcription Polymerase Chain Reaction

For real time RTPCR measurements of MMP-2 and -3 levels, SPRR3-KO and WT-VSMCs were plated at a density of $5x10^4$ cells/well in a 12 well plate. Cells were serum starved in 1% FBS overnight and allowed to recover in normal serum for 18 hours. A subset of cells was also treated with 25 μM PI3K inhibitor Ly294002 (Sigma). Total RNA was isolated using Trizol (Invitrogen) following the manufacturer's instructions. cDNA was generated using iScript cDNA Synthesis kit (Bio-Rad) from 1μg RNA. The cDNA was then used for quantitative real-time PCR (real time qRTPCR) as described (Young et al., 2005). Primers used for real time qRT-PCR were procollagen type IaI forward (5'-GCC AGA TGG GTC CCC GAG GT -3'), procollagen type IaI reverse (5'-GGG GGT CCA GCA GCA CCA

AC-3'), MMP2 forward (5'-GTC CCG AGA CCG CTA TGT-3'), MMP2 reverse (5'-GTT GCC CAG GAA AGT GAA-3'), MMP3 forward (5'-CAT GGA GAC TTT GTC CCT TTT GAT-3'), and MMP3 reverse (5'-CGT CAA AGT GAG CAT CTC CAT TA-3').

3.3 Results

3.3.1 Advanced SPRR3-Deficient Brachiocephalic Atheromas Have Thin Fibrous Caps with Reduced Collagen Content and Large, Lipid-Rich Cores

Our previous work demonstrated reduced VSMC content and increased TUNEL-positive VSMCs in aortic root lesions of DKO ($SPRR3^{-/-}ApoE^{-/-}$) mice when compared with ApoE-null controls ($SPRR3^{+/+}ApoE^{-/-}$) (Segedy et al., 2014). To determine the role of SPRR3 loss in atheroma vulnerability, brachiocephalic artery sections were collected from ApoE-null ($n = 12$) and DKO ($n = 12$) mice fed high fat diet for 6 months. The sections were stained with Trichrome Blue and compared for lipid-rich core size, collagen content, and cap area. DKO mice exhibited significantly larger lipid-rich cores when calculated as a percent of lesion area ($50.4 \pm 2.8\%$ in DKO and $36.6 \pm 5.4\%$ in ApoE-null mice; Figure 3.1, A-B). Percent cap collagen content is reduced in DKO mice when compared with ApoE-null controls ($32.3 \pm 4.1\%$ in DKO and $57.7 \pm 12.8\%$ in ApoE-null; Figure 3.1, C). Cap area, when controlled for lesion area, is also reduced in DKO mice (0.08 ± 0.03 in DKO and 0.24 ± 0.02 in ApoE-null; Figure 3.1, D). Immunohistochemistry for F480, a macrophage marker, was then performed on brachiocephalic artery sections from 6 month high fat diet-fed ApoE-null ($n = 3$) and DKO ($n = 5$) mice (Figure 3.2, A-B). When evaluated for % F480 positive cap area, no significant difference was observed between groups (2.6 ± 0.4 $SPRR3^{+/+}ApoE^{-/-}$, 1.5 ± 0.5 $SPRR3^{-/-}ApoE^{-/-}$; Figure 3.2, C). These data indicate that char-

acteristics of vulnerable plaques are increased in advanced atheromas of DKO mice when compared with ApoE-null controls.

3.3.2 SPRR3 Deficient Mice Develop Advanced Coronary Artery Atherosclerosis

To determine the effect of SPRR3 loss on the development of coronary artery atherosclerosis, cardiac apex sections from ApoE-null ($n = 15$) and DKO ($n = 15$) mice fed high fat diet for 6 months were stained with MOVAT and assessed for coronary artery atherosclerosis. Atheroma burden in coronary arteries were classified according to severity as (1) no lesion, (2) fatty streak, (3) atheroma, or (4) advanced atheroma (Figure 3.3, A-F) and, in one instance, coronary artery intraplaque hemorrhage was observed (Figure 3.3, G). To allow for sufficient space to distinguish features of atheroma progression, only arteries larger than 25 micrometers were included in the quantification. DKO mice demonstrated significantly more atheroma-containing coronary arteries per apex (DKO = 13.8 ± 7 and ApoE-null = $3.2 \pm 5.3; p = 0.013$), but no significant difference in lesion-free coronary arteries, fatty streaks, or atheromas (Table 3.1). Interestingly, trichrome blue staining of cardiac apex tissue sections from DKO mice fed high fat diet for 6 months also showed regions of infarction (Figure 3.4), whereas these are not found in ApoE-null control tissue sections.

Preliminary studies investigating changes in cardiac function using echocardiography in DKO mice ($n = 5$) compared with ApoE-null ($n = 2$) and SPRR3-KO ($SPRR3^{-/-}ApoE^{+/+}$, $n = 5$) mice over time were also performed (Figure 3.5, A-D). Percent difference between measurements at baseline and after 8 months high fat diet were calculated for fractional shortening (FS), ejection fraction (EF), left ventricular internal dimension at diastole (LVIDd), and left ventricular internal dimension at systole (LVIDs). This preliminary study

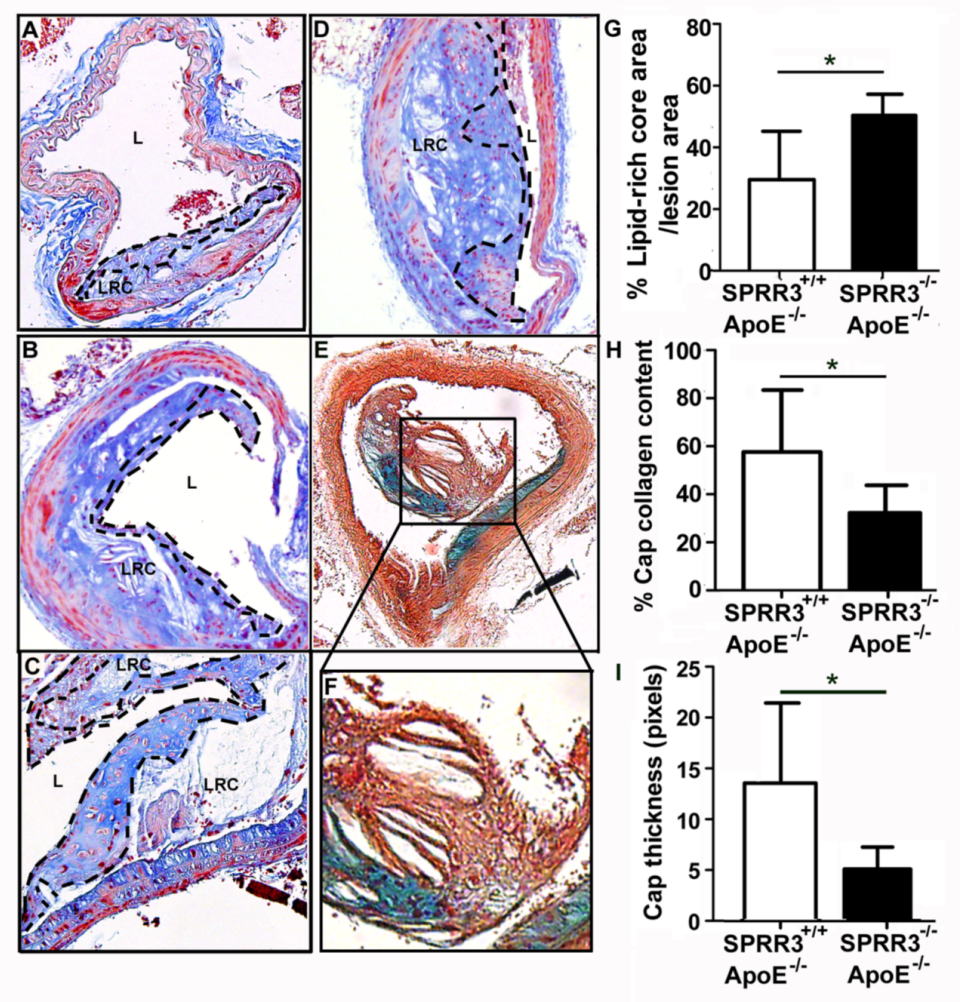

Figure 3.1: **Advanced SPRR3-deficient brachiocephalic atheromas have reduced cap collagen content and larger lipid-rich cores.** Brachiocephalic artery tissue sections collected from SPRR3$^{+/+}$ ApoE$^{-/-}$ (A) or SPRR3$^{-/-}$ ApoE$^{-/-}$ (B-F) mice fed high fat diet for 6 (A-E; Masson's trichrome) or 4 (F; H&E) months. Features of plaque vulnerability were increased in the SPRR3$^{-/-}$ ApoE$^{-/-}$ lesions, including one incidence of an organized thrombus (F), as well as significantly larger lipid rich cores and reduced cap collagen content (G-H). Original magnification, x20 (A-F). $*p < 0.05$.

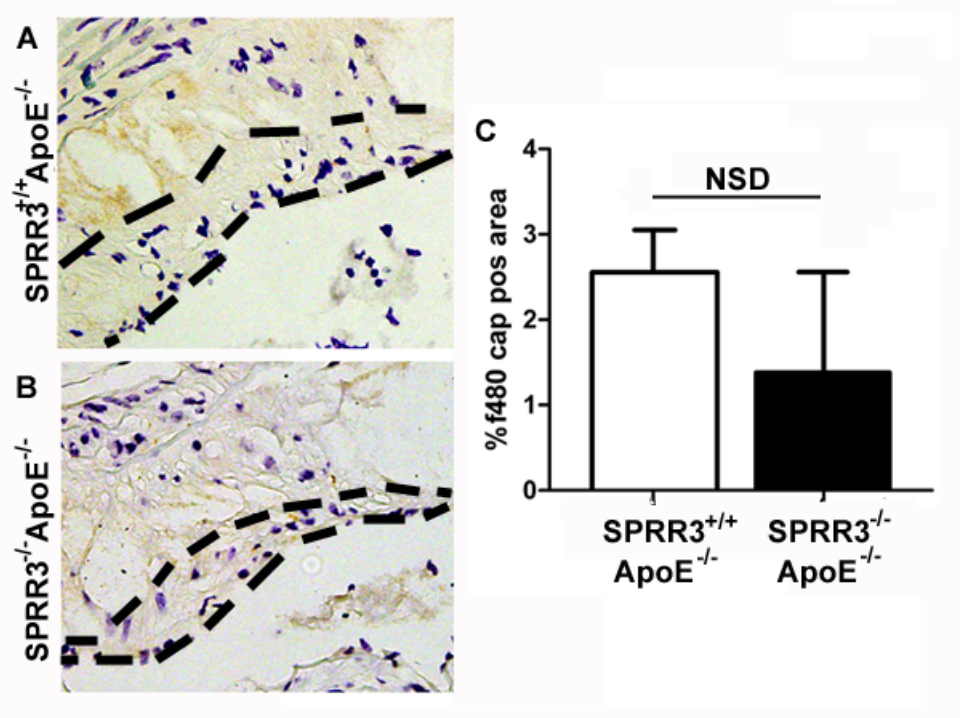

Figure 3.2: **Advanced SPRR3-deficient brachiocephalic atheromas do not demonstrate altered cap macrophage content.** Brachiocephalic artery tissue sections collected from SPRR3$^{+/+}$ ApoE$^{-/-}$ ($n = 3$; A) or SPRR3$^{-/-}$ ApoE$^{-/-}$ ($n = 5$; B) mice fed high fat diet for 6 months were probed with an antibody against F480. Quantification of % F480+ cap area identified no significant difference between groups (C). Original magnification, x40 (A-B).

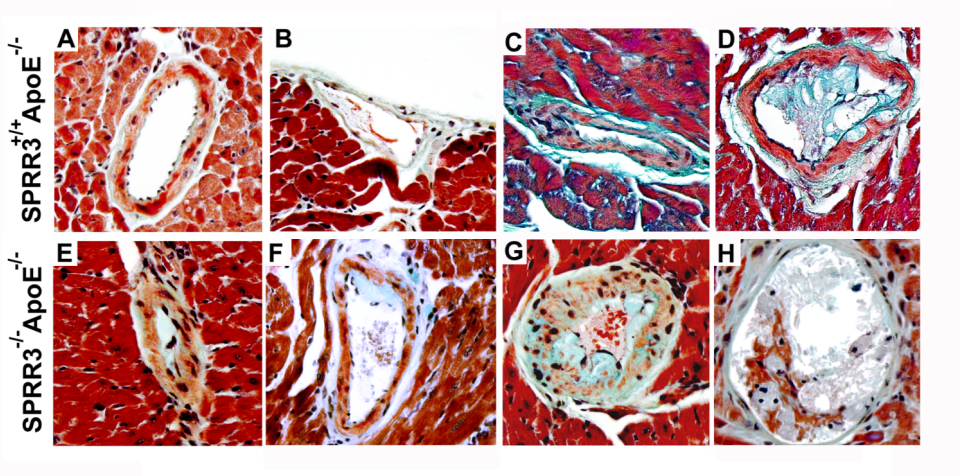

Figure 3.3: **SPRR3-deficient ApoE$^{-/-}$ mice develop advanced coronary artery atherosclerosis.** Left ventricular tissue sections collected from cardiac apices of SPRR3$^{+/+}$ ApoE$^{-/-}$ or SPRR3$^{-/-}$ ApoE$^{-/-}$ mice fed high fat diet for 6 months were stained with MOVAT pentachrome. Representative images are shown for arteries containing no lesion (A), fatty streaks (B, D), intermediate lesion (E), advanced atheroma (C, F), and intraplaque hemorrhage (G). Original magnification, 40x.

	ApoE-null	**DKO**
no lesion	$80.5\% \pm 18.8$	$72.4\% \pm 11.5$
fatty streaks	$9.3\% \pm 9.7$	$14.4\% \pm 9$
advanced atheroma	$4.3\% \pm 5.2$	$13.8\% \pm 7$*
$^*p < .05$		

Table 3.1: **Loss of SPRR3 leads to increased coronary artery atheroma complexity.**

identified a significant reduction in %difference in fractional shortening between SPRR3-KO mice and ApoE-null mice, as well as between SPRR3-KO mice and DKO mice (Figure 3.5, A). There was also a significant reduction in %difference in ejection fraction between SPRR3-KO mice and DKO mice (Figure 3.5, B). However, no significant differences were observed between ApoE-null and DKO mice for any measurement. Additional animals are needed to determine whether loss of SPRR3 in atherogenic mice is associated with reduced cardiac function.

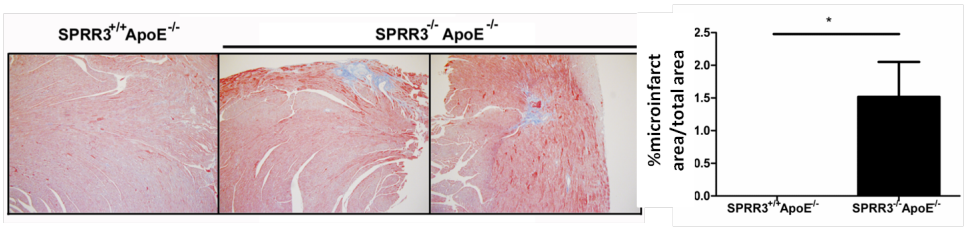

Figure 3.4: **Loss of SPRR3 in ApoE$^{-/-}$ mice leads to spontaneous cardiac microinfarctions.** Left ventricular tissue sections collected from cardiac apices of SPRR3$^{+/+}$ ApoE$^{-/-}$ or SPRR3$^{-/-}$ ApoE$^{-/-}$ mice fed high fat diet for 6 months were stained with Masson's trichrome. (A) Representative images of healthy cardiac tissue in SPRR3$^{+/+}$ ApoE$^{-/-}$ mice and microinfarcts observed in SPRR3$^{-/-}$ ApoE$^{-/-}$ mice. (B) Quantification of percent infarcted area in SPRR3$^{+/+}$ApoE$^{-/-}$ versus SPRR3$^{-/-}$ ApoE$^{-/-}$ mice. Original magnification, 10x. $^{**}p < 0.01$.

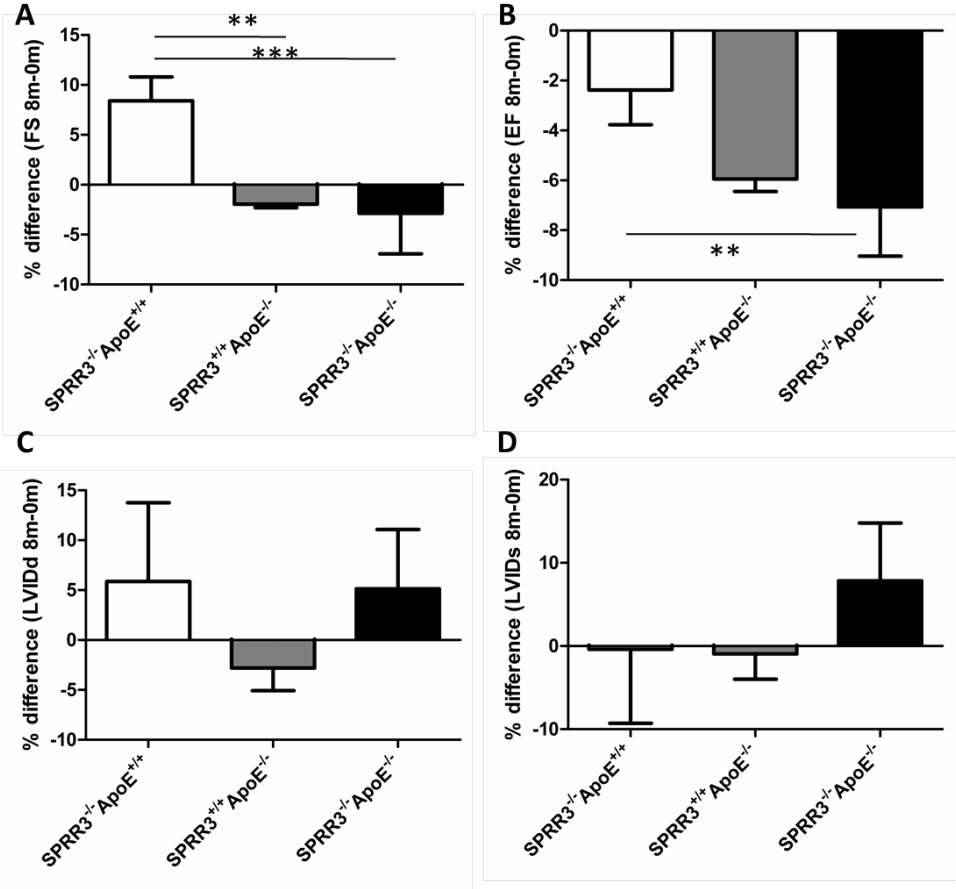

Figure 3.5: **SPRR3-deficient atherogenic mice may not experience reduced cardiac function** Percent difference between measures of cardiac function was calculated in 8 month high fat diet-fed SPRR3-KO (SPRR3$^{-/-}$ApoE$^{+/+}$, $n = 2$), ApoE-null ($n = 5$), or DKO ($n = 5$) mice compared with the same mice at baseline. (A) Fractional shortening, (B) Ejection fraction, (C) Left ventricular internal dimension at diastole (LVIDd), (D) Left ventricular internal dimension at systole (LVIDs). ** $p < 0.01$, *** $p < 0.001$

3.3.3 SPRR3 Promotes Procollagen Type I mRNA and Protein Synthesis in an Akt-Dependent Manner

To determine whether the reduced collagen content observed in SPRR3-deficient lesion caps may be due to an SPRR3-dependent change in collagen synthesis, we tested whether collagen mRNA and protein levels were affected in VSMCs isolated from SPRR3 knock-out mice (SPRR3-KO VSMCs) or in VSMCs expressing wild-type levels of SPRR3 (WT-VSMCs) (Figure 3.6, A). Real-time RTPCR showed that, when compared with wild type VSMCs (WT-VSMCs), SPRR3-KO VSMCs express significantly less procollagen type IaI mRNA. Similar results were observed when cell lysates from SPRR3-KO and WT-VSMCs were compared by immunoblotting for collagen type I protein levels (Figure 3.6, B). This increase in collagen type I precursor expression was dependent on Akt activity, as treatment with PI3K inhibitor Ly294002 reduced procollagen type IaI protein levels in SPRR3-OE VSMCs (Figure 3.6, C).

3.3.4 MMP-2 and -3 Transcript Levels are Unaffected by SPRR3 in Cultured VSMCs

To determine whether MMP expression is alternately regulated in SPRR3-deficient cells, mRNA was collected from SPRR3-KO VSMCs, WT-VSMCs, and SPRR3-OE VSMCs either untreated or treated with 25μM Ly294002. There was no significant difference between groups in response to SPRR3 expression level or in response to PI3K inhibitor treatment for either MMP-2 (Figure 3.7, A) or MMP-3 (Figure 3.7, B). These data suggest that MMP-2 and MMP-3 mRNA is not regulated by SPRR3 or PI3K/Akt in VSMCs.

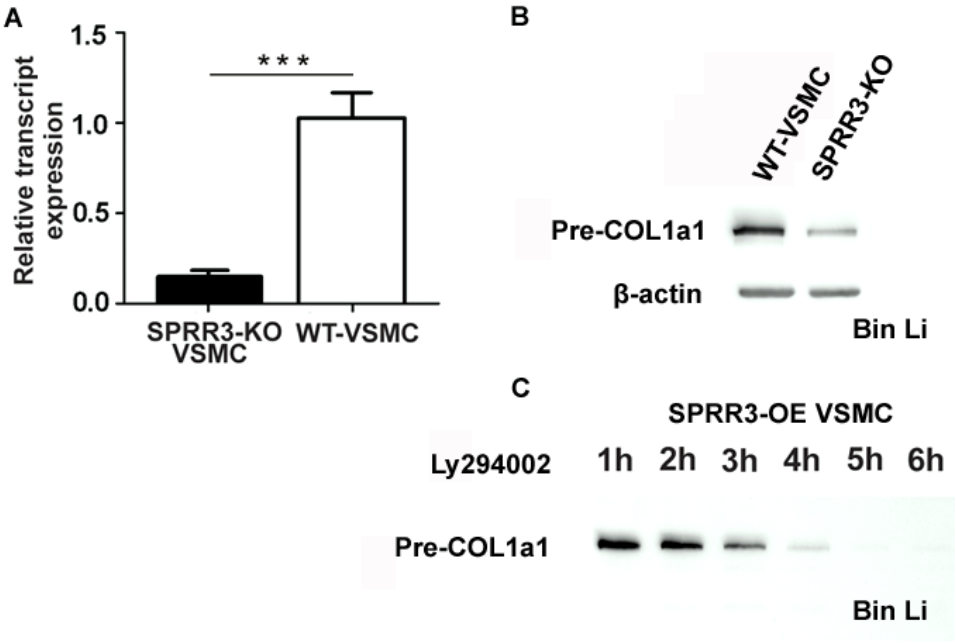

Figure 3.6: **Collagen type I mRNA and protein expression are positively associated with SPRR3 expression in VSMCs *in vitro*.** (A) Real time RTPCR assessment of procollagen type 1a1 relative transcript levels in SPRR3-KO VSMCs compared to WT-VSMCs. (B) Cell lysates from WT-VSMCs and SPRR3-KO VSMCs were subjected to immunoblot analysis using anti-Pre-collagen type 1a1 (200kDa) or loading control ant-β-actin (approximately 42kDa). (C) Cell lysates from SPRR3-OE VSMCs that were treated with 25μM Ly294002 were collected at 1 hour intervals between 1 and 6 hours and were subjected to immunoblot analysis using anti-Pre-collagen type 1a1. *** $p < 0.001$.

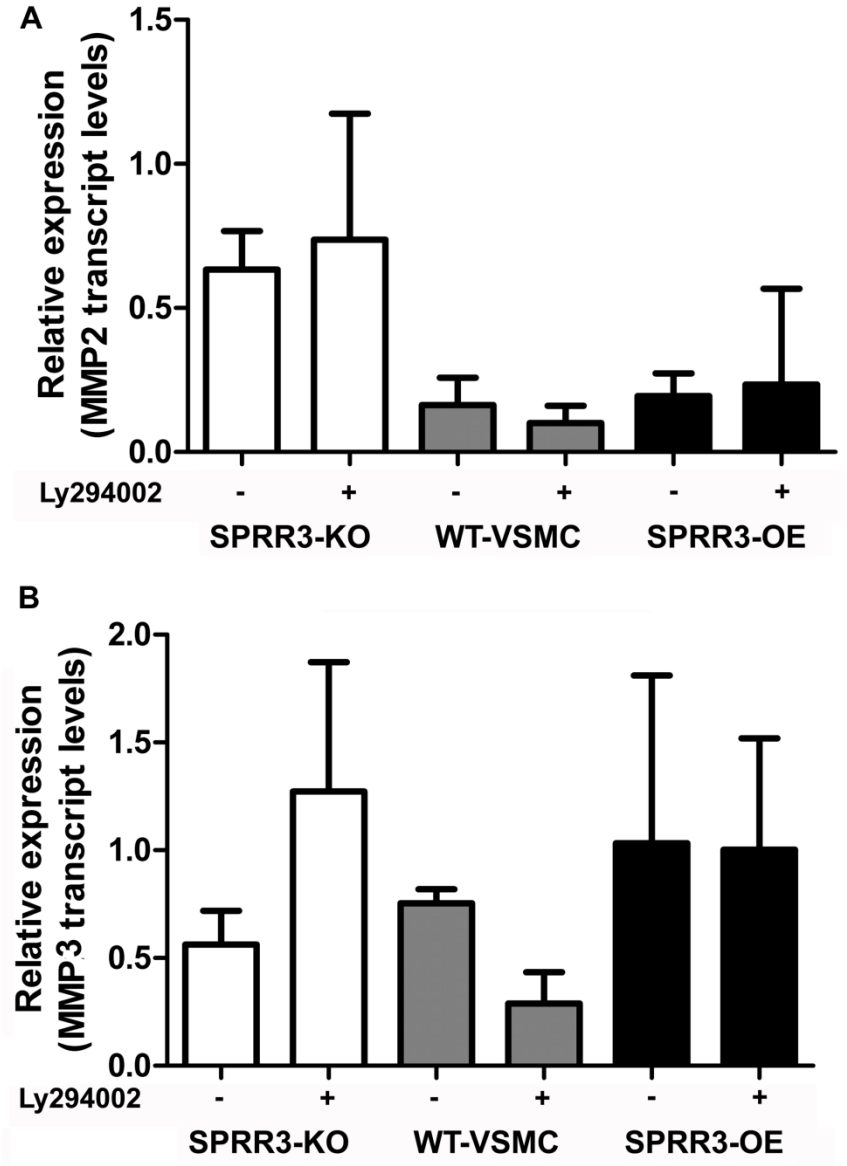

Figure 3.7: **VSMC expression of MMP-2 and -3 transcripts are unchanged with SPRR3 expression.** (A) Relative transcript levels were assessed in SPRR3-KO VSMCs, WT-VSMCs, and VSMCs overexpressing SPRR3 that are untreated or treated with 25μM Ly294002 for MMP-2 levels. (B) Relative transcript levels were assessed in SPRR3-KO VSMCs, WT-VSMCs, and VSMCs overexpressing SPRR3 that are untreated or treated with 25μM Ly294002 for MMP-3 levels.

3.4 Discussion

This study was designed to investigate the effect of SPRR3 loss on atheroma stability. The specificity of expression of SPRR3 in atheroma VSMCs makes it a useful tool for exploring VSMC-specific effects in atherosclerosis progression and stability. Our study shows that atheroprone ApoE-null mice lacking SPRR3 over 6 months of high fat diet are significantly more likely to develop unstable brachiocephalic atheromas. This is likely due to a confluence of reduced VSMC content, as was observed previously (Segedy et al., 2014), and reduced VSMC synthesis of collagen type I.

Extracellular matrix production within the fibrous cap of advanced atheromas, of which collagen type I is the principal component, is dependent on VSMCs. During atherosclerosis progression, the fibrous cap is laid down over the increasingly thrombogenic atheroma contents. Regulators of VSMC collagen synthesis have been little explored. Expression of procollagen type I chains, which are transcribed from two different chromosomes, are coordinately regulated at the transcriptional level through competitive binding of Nkx2.5, which acts as an activator, and δEF1/ZEB1, which acts as a repressor (Vuust et al., 1985; Ponticos et al., 2004). Most studies of collagen regulation in VSMCs point to TGF-β as the principal regulator. Treatment of VSMCs in culture with TGF-β promotes transcript levels and activity of the collagen catabolic pathway, increasing the metabolism of L-arginine to the collagen precursor L-proline (Durante et al., 2001). TGF-β, PDGF, and IL-1 have each been shown to increase collagen type I and type III production *in vitro*. This same study demonstrated that IFNγ inhibits basal and IL-1-, PDGF-, TGF-β-stimulated collagens type I and III production (Amento et al., 1991). Angiotensin II stimulates synthesis of collagens

type I and type III, as well as fibronectin, in a dose-dependent manner via the MAPK signaling pathway (Mifune et al., 2000; Kato et al., 1991).

Our *in vitro* assessment of procollagen type 1 transcript and protein production indicated an interaction between Akt pathway activity and collagen synthesis in SPRR3-deficient VSMCs. While Akt has not been noted as a regulator of collagen synthesis in VSMCs, a few studies have suggested mechanisms by which this may occur. In hepatic stellate cells, PDGF treatment increases focal adhesion kinase (FAK) activity, leads to increased PI3K/Akt activity, and promotes collagen type I mRNA and protein production. Inhibition of PI3K by Ly294002 or a dominant negative form of Akt reduced collagen type I mRNA and protein production, while constitutively active Akt leads to increased collagen type I mRNA and protein (Reif et al., 2002). Inhibition of PI3K or Akt in cardiac fibroblasts blocks TGF-β-induced or lysyl oxidase-induced collagen type I synthesis (Voloshenyuk et al., 2011). It is possible that SPRR3 may operate through one of these mechanisms to influence collagen synthesis in VSMCs.

Despite the consistent association observed in histological studies of CVD patients between ruptured atheromas and VSMC loss, relatively little is known about the molecular mechanisms by which VSMCs support atheroma stability (Thim et al., 2008; Arbab-Zadeh et al., 2012). Most studies have investigated the role of inflammatory cells in atherosclerosis stability. Bennett's group has shown that VSMC apoptosis in established atheromas is sufficient to promote features of atheroma vulnerability (Clarke et al., 2006). Here, we show that SPRR3 expression is required for VSMC maintenance of fibrous cap collagen content and thickness as part of a protective arterial response to atheroma conditions.

This study introduces SPRR3 as a VSMC-specific modulator of collagen synthesis that

may be leveraged in future studies for promoting maintenance of fibrous cap thickness in atheroma VSMCs. Moreover, the previously identified role of SPRR3 in maintenance of VSMC cellularity within the fibrous cap (Segedy et al., 2014) would itself affect cap thickness. We also show that SPRR3 deficiency leads to an intriguing phenotype of increased coronary artery complexity and microinfarcts within the cardiac left ventricle, emphasizing the importance of VSMC function in maintenance of a stable atheroma phenotype. In the following chapter, we will discuss future directions for our exploration of the involvement of SPRR3 in mediating VSMC behavior to promote atheroma stability and the mechanisms by which this occurs. We will also explore the potential for use of the SPRR3-deficient mouse as a unique model of atheroma vulnerability.

CHAPTER 4

Atherosclerosis Development in Humans and Mice

In the previous chapter, we investigated the consequences of SPRR3 loss on features of atheroma stability in advanced atherosclerotic plaques. Our data emphasize the importance of VSMC behavior within the atheroma as part of a protective arterial response. In this chapter, we will explore the effects of VSMCs and SPRR3 loss on other areas of interest to atherosclerosis development including the role of intimal VSMCs in initiation of atherosclerosis, the effects of SPRR3-deficiency and its associated VSMC loss and reduced atheroma collagen synthesis on risk of aneurysm formation, and the importance of SPRR3 in human myocardial infarction and stroke risk.

Animal models of atherosclerosis allow researchers to study the disease at an accelerated rate compared with human lesion development. Mouse models are most frequently used due to the relative ease of genetic manipulation and low cost of maintenance. To prompt atherosclerosis development in mice, hyperlipidemic models have been generated in which LDL cholesterol is boosted in genetic knockouts. However, some key differences remain between mouse and human atherosclerosis. Of interest to us was the lack of intimal VSMCs in healthy mouse arteries. Intimal vascular smooth muscle cells are found in human arteries within the first decade of life (Nakamura and Ohtsubo, 1992). As may be recollected from Chapter 1, there has been some controversy over the initiating factor of atherosclerosis, which has carried on for the past 2-3 decades (Ross et al., 1977; Dimmeler et al., 1997; Cai and Harrison, 2000; Hahn and Schwartz, 2009; DiCorleto and Soyombo,

1993). Does atherosclerosis occur as a result of intimal injury, usually endothelial cell injury, then followed by lipoprotein retention or is the converse true?

4.1 Is VSMC apoptosis sufficient to cause atherosclerosis initiation in a humanized mouse artery?

Previous work has shown that VSMC apoptosis alone is sufficient to accelerate atherosclerosis progression in ApoE$^{-/-}$ mice, but their model showed no evidence of atherosclerosis development in mice wild-type for ApoE (Clarke et al., 2006, 2008). However, the experiment did not account for the lack of intimal smooth muscle cells found in mice compared with human arteries. Interested in investigating whether VSMC apoptosis is sufficient to induce atherosclerosis in a setting of resident intimal VSMCs, we chose to generate a model in which neointima formation could be stimulated using $FeCl_3$ treatment of carotid artery tissue and VSMC apoptosis could subsequently be triggered in a specific manner. We replicated the model used in Bennetts study in which the human diphtheria toxin receptor was expressed specifically in VSMCs via the SM22α promoter. Upon treatment with low levels of diphtheria toxin, VSMC apoptosis can then be triggered. Our mouse, which expressed wild type ApoE, was fed high fat diet for two weeks before induction of neointima formation. A two week recovery period allowed time for neointima formation, which peaks at 14 days post injury (Lindner and Reidy, 1993). Mice were then treated with 1ng/g diphtheria toxin three times over one week to trigger VSMC apoptosis, then maintained on high fat diet for two months and evaluated for initiation of atherosclerosis.

While we were able to confirm neointima formation was successfully induced at the 7 day time point (Figure 4.1) using H&E staining of tissue sections collected from the

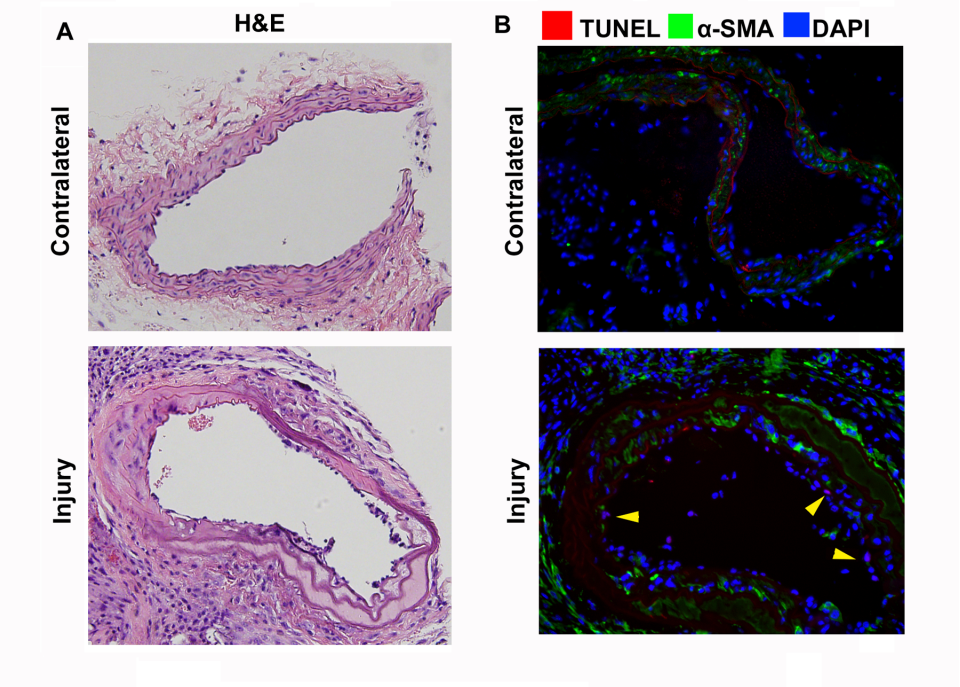

Figure 4.1: **Neointima formation and VSMC apoptosis at 7 days post injury.** Carotid arteries injured with $FeCl_3$ treatment and their contralateral controls were harvested at 7 days post injury. Sections were collected and stained with (A) H&E or (B) probed with antibodies against TUNEL (red), -smooth muscle actin (green), or DAPI (blue).

injured area and the contralateral artery, we found this model to be technically challenging in multiple ways. First, 10-20% of mice were lost due to complications of the surgery and $FeCl_3$ artery burn. Those which survived to be treated with diphtheria toxin experienced a second, more severe round of mortality with at least 50% of the remaining mice from each group dying either due to toxicity from the diphtheria toxin treatment or to hemorrhage near the site of $FeCl_3$ injury. After multiple cohorts, we successfully gathered 5 mice with carotid $FeCl_3$ injury and subsequent VSMC apoptosis. The injured and contralateral artery were collected from each mouse and assessed by *en face* for atheroma burden. Interestingly, none of the injured carotids showed Sudan IV positive staining for lipids.

These data suggest that VSMC apoptosis alone is insufficient to induce atherosclerosis,

even in a model with intimal VSMC content. There are some limitations to our analysis, however. The high levels of mortality incurred by the surgery and subsequent trigger of widespread VSMC apoptosis suggest that the survivors may have experienced reduced recombination efficiency of the SM22α-Cre with the hDTR-expressing gene, leading to milder VSMC apoptosis levels (Hara-Kaonga et al., 2006). Alternatively, two months of high fat diet may not have been sufficient in a wild-type background for a lesion initiated through VSMC apoptosis to accumulate intimal lipid levels that are measurable by Sudan IV staining. Our choice of time point was based on observations of time to low levels of lesion development in ApoE-null mice fed high fat diet. To address these concerns, multiple time points should be considered and VSMC apoptosis in another arterial site should be measured against diphtheria-toxin treated mice without $FeCl_3$ injury to control for variation in Cre recombination efficiency.

4.2 SPRR3 loss does not promote aneurysm formation

Another consequence of increased VSMC loss in the aorta is increased risk of aneurysm formation. To investigate whether SPRR3-deficient ApoE$^{-/-}$ mice are at increased risk of aneurysm formation, five SPRR3$^{+/+}$ApoE$^{-/-}$ (ApoE-null) and five SPRR3$^{-/-}$ApoE$^{-/-}$ (DKO) mice were implanted subcutaneously with Alzet osmotic minipumps (model 1002; Durect Corporation) at 8 weeks old. These pumps released angiotensin II (Ang II) at 1000 ng/kg/min. Using a tail cuff, blood pressure measurements were collected at baseline (SPRR3$^{+/+}$ApoE$^{-/-}$ = 107.9 ± 9 mmHg; SPRR3$^{-/-}$ApoE$^{-/-}$ = 107.4 ± 11 mmHg) and at 6 days (SPRR3$^{+/+}$ApoE$^{-/-}$ = 148.9 ± 13 mmHg; SPRR3$^{-/-}$ApoE$^{-/-}$ = 167.5 ± 19 mmHg) and 8 days (SPRR3$^{+/+}$ApoE$^{-/-}$ = 159.3 ± 21 mmHg; SPRR3$^{-/-}$ApoE$^{-/-}$ = 161.6 ± 21 mmHg) following Ang II treatment

(Figure 4.2, A).

No significant difference was observed between groups at any time point, however, the range of SPRR3$^{-/-}$ApoE$^{-/-}$ (DKO) blood pressures at later time points was large, with some mice experiencing blood pressures as high as 193 mmHg. Following three weeks of treatment, the aortas of these mice were collected and assessed for evidence of aneurysm formation. Three of the ApoE-null mice and one of the DKO mice demonstrated evidence of aneurysm formation, suggesting that SPRR3-deficiency in ApoE$^{-/-}$ animals is not sufficient to increase risk of aneurysm in hypertensive conditions (Figure 4.2, B). This study, although performed in accordance with standard protocols for measuring aneurysm formation, may not have tested SPRR3 function under ideal conditions. At eight weeks of age, SPRR3-deficient ApoE$^{-/-}$ mice have developed little measurable atherosclerosis and therefore would not yet be experiencing the atheroma-related consequences of SPRR3 loss. This experiment establishes, rather, a baseline effect of SPRR3 deficiency on response to hypertension. An additional group of animals at 16 weeks of age fed high fat diet for 2 months would be of interest in determining whether atherosclerosis-associated VSMC loss observed in ApoE-null mice lacking SPRR3 may influence aneurysm risk.

4.3 SPRR3 as a risk factor for human embolic vascular disease

The data presented in Chapters 2 and 3 demonstrating increased atherosclerosis progression and vulnerability in mice lacking SPRR3 led us to hypothesize that there may be an association between certain human SPRR3 variants and embolic stroke and myocardial infarction. SPRR3 has not itself been recorded as a gene of interest at genome-wide significance. To investigate this hypothesis, we made use of a clinical repository of DNA samples linked to

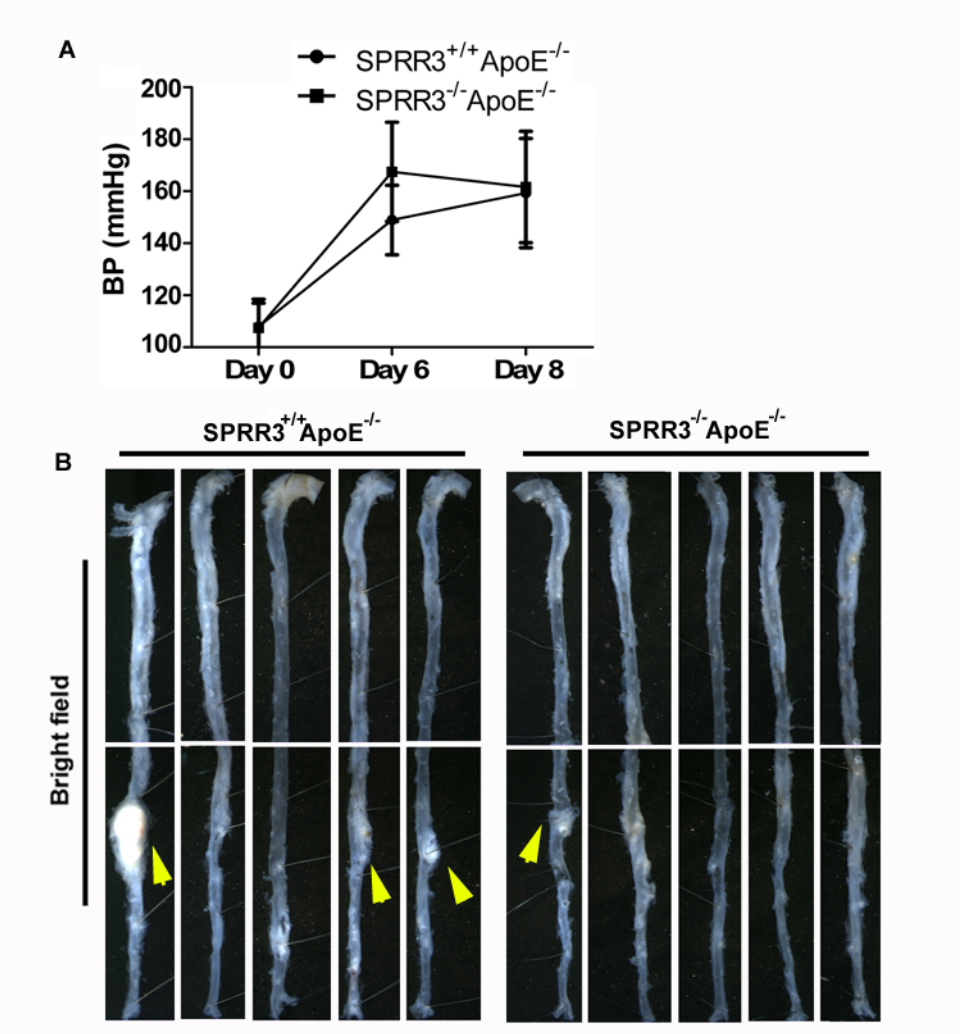

Figure 4.2: **SPRR3 loss does not promote risk of aneurysm formation in AngII-treated mice.** (A) Mean systemic blood pressure measurements collected from SPRR3$^{+/+}$ApoE$^{-/-}$ (n=5) and SPRR3$^{-/-}$ApoE$^{-/-}$ (n=5) mice using a tail cuff system (Model MK-2000, Muramachi Kikai Co.) at baseline and on days 6 and 8 following treatment with 1000 ng/kg/min AngII. (B) Bright field images of intact SPRR3$^{+/+}$ApoE$^{-/-}$ (n=5) and SPRR3$^{-/-}$ApoE$^{-/-}$ (n=5) aortas. Atherosclerotic lesions appear white. Yellow arrowheads indicate areas with aneurysm formation.

de-identified electronic medical records (EMRs) established for genetic association studies of complex traits (Ritchie et al., 2010). This DNA biorepository contains over 2 million patient samples, some of which have been genotyped in previous GWAS (genome-wide association study) platforms. Using these previously genotyped samples, we selected a case group of $\tilde{1}$,600 individuals with a medical history of embolic stroke or myocardial infarction and a control group of $\tilde{5}$,000 individuals with no history of cardiovascular disease. To expand our available sample set, we chose not to limit our study to early-onset myocardial infarction patients. An estimation of available power using the power calculation software Quanto indicated that a sample size of $\tilde{1}$,600 cases at 80% power would be sufficient to detect significance at $p < 0.05$ at an odds ratio of 1.4 and a minor allele frequency minor allele frequency (MAF) of 5% (see Figure 4.3. Previously published odds ratios for cardiovascular disesases range from 1.1 to 3. From among the sites genotyped in the GWAS studies (Illumina 1M, Illumina OmniQuad, and Illumina 660W), we selected 97 SNPs from within 50kb up- and downstream of SPRR3 (De la Cruz et al., 2010) with an r^2 threshold of 0.8 using a cosmopolitan tagSNP search of the HapMap and Environmental Genome Project (EGP) databases on the Genome Variation Server and the Exome Sequencing Project (ESP) database on the Exome Variant Server (both managed by the University of Washington). Covariate adjustment was made for age at onset, sex, HDL, LDL, and TG levels, and median BMI.

Samples were evaluated using logistic regression and stratified by race/ethnicity unadjusted and adjusted for the above mentioned covariates. Given our data in the mouse model indicating the importance of this gene, we set our significance threshold at $p < 0.05$ with Bonferroni correction. While no variants were identified as significantly associated with

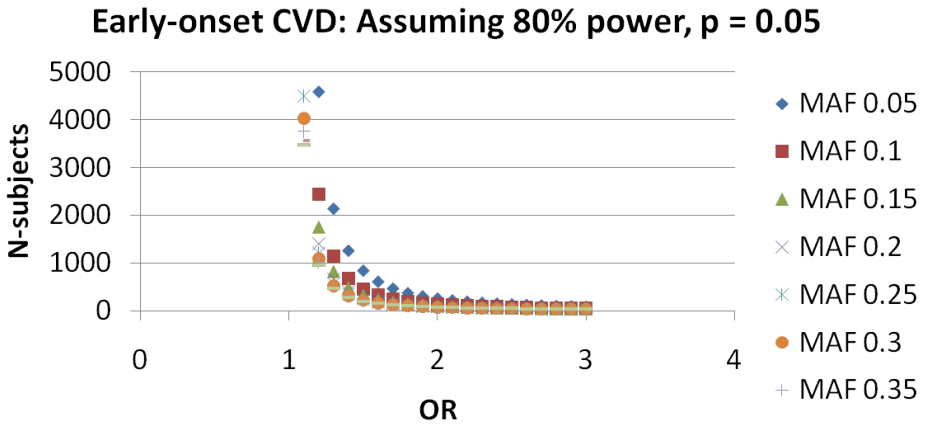

Figure 4.3: **Power calculations assuming 80% power.** Preliminary power calculations demonstrate that, for a variety of minor allele frequencies (MAFs), our available pool of potential CVD patients ($\tilde{1}$,600 individuals) is sufficient to detect the expected association at relatively low odds ratios (ORs).

risk of embolic stroke or heart attack with Bonferroni correction, two alleles did reach significance in the group of individuals who suffered from an MI alone (rs10494289 and rs 883810). These SNPs were located at 28kb and 32kb upstream of SPRR3, respectively. While still within the 50kb fixed window of SPRR3, they are well outside the known functional range. These variants may indicate the existence of an enhancer or repressor region that regulates SPRR3 expression levels, may be acting solely as markers of SPRR3, or may be false positives. However, the existence of these highly suggestive variants indicate that our study would benefit from expansion and confirmation through use of another dataset, such as that available from the Framingham Heart Study.

A PheWAS (phenome-wide association study) was also performed investigating missense mutations in the exon region of SPRR3. The analysis adjusted for age and gender and evaluated only individuals identifying as white. False positives were limited by filtering the results to variants with a MAF of 1% or higher and with at least 10 individuals carrying

Disease Trait	Odds Ratio	P-value	Associated allele	Location
Intracranial hemorrhage (injury)	1.88	0.027	exm101823_A	Exon, missense G105D
Abnormality in fetal heart rate or rhythm	1.45	0.017	exm101837_C	Exon, missense L149V
Other cardiac conduction disorders	1.39	0.037		
Elevated C-reactive protein	1.32	0.033		
Hypertensive heart disease	1.11	0.046		
Hypotension	1.08	0.024		
Atrial fibrillation	1.07	0.047		
Atrial fibrillation & flutter	1.06	0.049		

Table 4.1: **SPRR3 missense mutations associated with disease phenotype risk by PheWAS**

the variant. While no variants associated with embolic heart attack or stroke risk, we found that 2 variants were significantly associated with cardiovascular-related disease phenotype risk (exm101823_A and exm101837_C; see Table 4.1). Software for the prediction of the probable impact of a mutation on protein function (SIFT and PolyPhen) suggested that these variants would be probably damaging and tolerated, respectively. While these data are suggestive, it is important to remember that PheWAS indicate associations, rather than cause-and-effect relationships. Further work is needed to determine whether these associations are due to a biological function of SPRR3 or whether the variant and phenotype are co-occurring in individuals due to a third common factor.

4.4 Discussion

Linkage analysis and positional cloning identify low hanging fruit, genes with large effect and strong genotype-phenotype correlations. In diseases like cardiovascular disease that have complex, multifactorial patterns of inheritance, associated genes are likely to be many in number with a small effect size and would be less likely to be identified by this type of study (Risch, 2000). Genome-wide association studies (GWAS), when sufficiently powered, are able to identify genes with somewhat smaller effect size. However, to be recorded

as a gene of interest at genome-wide significance, a threshold of $p < 5x10^{-8}$ due to multiple comparisons adjustments is still required. Under such conditions, candidate gene studies may identify associations that have been missed by larger scale studies (Myocardial Infarction Genetics Consortium, 2009). GWAS and candidate gene studies have identified eleven risk loci for early-onset myocardial infarction (Myocardial Infarction Genetics Consortium, 2009; Morray et al., 2007), which is hypothesized to have a stronger genetic component than more common forms of CVD. Most of these loci are near candidate genes that have not yet been characterized. Those that have been characterized include LDLR, PCSK9, PHACTR1, NOS3, and PON1. LDLR, PCSK9, and PON1 and are involved in lipid balance (Hobbs et al., 1992; Linsel-Nitschke et al., 2008; Abifadel et al., 2003; Getz and Reardon, 2004). PHACTR1 has been strongly associated through a previous GWAS with coronary artery calcification (Schunkert et al., 2011). NOS3 mediates synthesis of nitric oxide in endothelial cells and affects vasodilation, VSMC migration, and adhesion in both platelets and leukocytes (Hibi et al., 1998). Those associated with other aspects of atherosclerosis development and progression remain less well explored. An association between SPRR3 and embolic vascular disease would provide a marker for risk in cardiovascular disease patients.

CHAPTER 5

Discussion and Future Work

In this dissertation, we have explored the role of VSMCs in atheroma progression and stability using the atheroma- and VSMC-specific protein SPRR3. We have identified SPRR3 as a novel atheroprotective factor, the loss of which accelerates lesion progression and impairs VSMC maintenance of fibrous cap thickness. These phenotypes are associated with changes in VSMC function; specifically, we show that VSMCs lacking SPRR3 experience reduced survival both *in vitro* and *in vivo*, fail to sustain their cellularity within the lesion, and experience reduced collagen type I expression both *in vitro* and *in vivo*. Future work will investigate the mechanism(s) by which SPRR3 mediates these VSMC functions and whether SPRR3 or its downstream effectors may be used to rescue the accelerated, unstable atherosclerosis observed in SPRR3-deficient ApoE$^{-/-}$ mice. The atheroma-specific expression pattern of SPRR3 situates this protein as an ideal target for therapeutic interventions intended to reduce risk of rupture.

5.1 Mechanisms of SPRR3 activity

The studies described in the preceding chapters demonstrate that SPRR3 expression mediates an increase in Akt activity which, in turn, modulates many of the identified functions of SPRR3. However, the mechanism by which SPRR3 promotes Akt activity remains a mystery. Chapter 1 outlines the current understanding of the general structure of SPRR3. Little is known due to the flexibility of the SPRR3 central domain, which has prevented its crystallization and subsequent characterization of its tertiary structure. Moreover, the

only published studies on SPRR3 functional domains describe the transglutaminase substrate domains, a standard characteristic of SPRR family members. Since experiments performed by previous members of our lab have determined that inhibition of transglutaminase enzymes did not affect SPRR3 function in VSMCs, we are left without the aid of confirmed structural domains.

To our knowledge, there is also no published evidence indicating kinase activity or phosphorylation of an SPRR family member. However, assessment of the amino acid sequence indicates a total of 14 potential serine/threonine/tyrosine phosphorylation sites with a NetPhos predicted output score of greater than 0.7 (Blom et al., 2004). The predicted phosphorylation sites, transglutaminase substrate domains, and some additional sites with homology to known protein domains are shown in Figure 5.1. These potential phosphorylation sites are distributed across the protein with sites in both the N and C-terminal ends and are found at the highest concentration in the central flexible region. One of the predicted phosphorylation sites is found within a sequence that has homology with SH3 ligand domains, is predicted by NetPhosK1.0 (Blom et al., 2004) as a potential DNA-PK interactor. While DNA-PK has been shown to phosphorylate Akt (Stronach et al., 2011), this direct interaction would bypass PI3K, which our data shows to be involved in SPRR3-mediated increase in Akt activity. Based on the previous studies in our lab indicating that SPRR3 regulation is dependent on integrin $\alpha 1 \beta 1$ interaction with collagen type I matrix, we have hypothesized that a downstream mediator of integrin $\alpha 1 \beta 1$ signaling that operates upstream of PI3K, such as FAK, may be involved. SPRR3 may act as a mediator between FAK and PI3K or it may act as a cofactor to promote PI3K phosphorylation by FAK. Indeed, preliminary data generated by others in our group have indicated that SPRR3 and

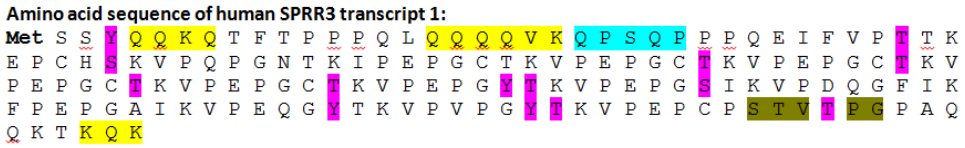

Figure 5.1: **Predicted functional domains of human SPRR3.** Yellow = transglutaminase substrate domains; Blue = possible SH3 ligand domain; Pink = predicted phosphorylation (S/T/Y) sites; Green = WW domain.

FAK immunoprecipitate together, lending support to this hypothesis. It is conceivable that either the SH3 ligand domain or the WW domain, both of which are involved in mediating protein-protein binding interactions, may be a binding site for FAK or one of its complex members. More work is required to determine whether this is a direct interaction, however, or whether SPRR3 is part of a complex with FAK, interacting with a third protein.

Another unexplored avenue by which SPRR3 may regulate VSMC activity may be through direct interaction with nuclear transcription factors. While there are no predicted DNA binding domains on SPRR3, another SPRR family member, SPRR2a has been shown to translocate to the nucleus of human cholangiocarcinoma cells and deacetylate p53 and p300, suppressing p53 transcriptional activity (Mizuguchi et al., 2012). While our lab has only seen perinuclear staining by immunofluorescence (Pyle et al., 2010), preliminary work using immunoblotting for SPRR3 following membrane fractionation of cell lysates from control GFP-VSMCs and SPRR3-overexpressing VSMCs indicated that SPRR3 may localize to the nucleus under conditions of excess (Figure 5.2). To determine whether this is an artifact of SPRR3 overexpression, fractionated protein samples from GFP-VSMC controls should be concentrated and loaded at a high concentration (40μg) for visualization of SPRR3 localization when expressed at wild type levels. If localization to the nucleus is confirmed, a previously unexplored mechanism of action for SPRR3 would be indicated.

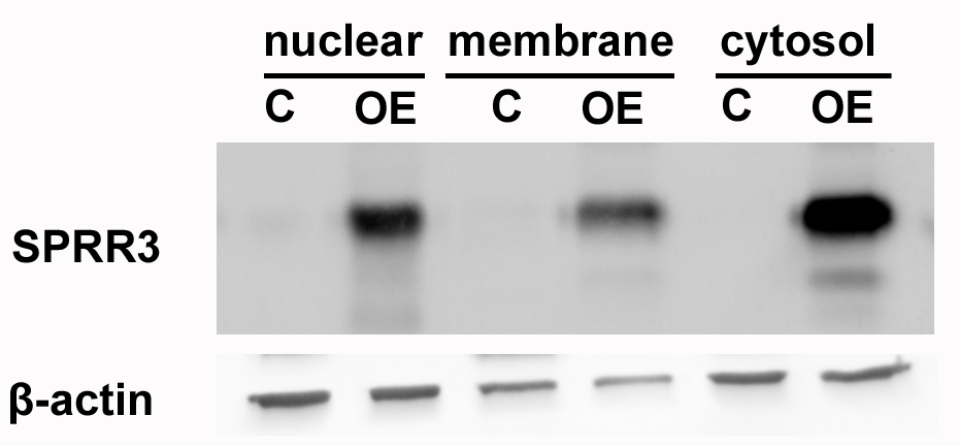

Figure 5.2: **SPRR3 localizes to the nucleus when in excess.** Control GFP-VSMCs (C) and VSMCs overexpressing SPRR3 (OE) were separated into nuclear, membrane, and cytosolic fractions. Immunoblotting for anti-SPRR3 (22kDa) and anti-?-actin (42kDa) was performed using these protein fractions.

5.2 Future Directions

5.2.1 Akt as a Mediator of SPRR3 Effects *in vivo*

Multiple *in vitro* experiments discussed in the previous chapters have indicated that SPRR3 affects VSMC survival and collagen type I synthesis through the Akt pathway. These experiments do not preclude the activity of other, as yet unidentified factors and more importantly, they do not show whether increased Akt pathway activity is sufficient to compensate for SPRR3 loss *in vivo*. To determine whether the atherosclerosis phenotype observed in the SPRR3 deficient ApoE$^{-/-}$ mice are dependent on Akt activity, we sought a model in which we could modulate Akt activity specifically in VSMCs. There are multiple isoforms of Akt, however, and it is unclear which is most important in VSMCs. As described in the discussion of Chapter 2, studies have been performed with global Akt-1 knockout, as well as Akt-2 and Akt-3 (Ding et al., 2012; Fernández-Hernando et al., 2007; Rensing et al., 2014; Fernández-Hernando et al., 2009). However, none of these studies attempted

to isolate the *in vivo* effects of a particular isoform in VSMCs. One study used RTPCR to evaluate multiple tissue types and showed relatively lower Akt-2 expression in VSMCs isolated from human aortic VSMCs and human coronary artery VSMCs than in tissues taken from human liver, skeletal muscle, or ovary. Akt3 levels were relatively higher than Akt1 or Akt2. However, transcripts were observed for each isoform and the study did not attempt to explore differences in function between the isoforms (Sandirasegarane and Kester, 2001). To address this difficulty, we will utilize the role of PTEN as a general regulator of Akt phosphorylation (see Figure 5.3). By generating a mouse expressing an inactive form of PTEN in which exon 5 has been deleted, all three isoforms of Akt will be phosphorylated.

PTEN has previously been deleted specifically in smooth muscle cells with some limited success. In this model, PTEN was reduced and phosphorylated Akt increased in major vessels, hearts, and lungs. The $PTEN^{loxP/loxP}$SM22α-Cre mice also exhibited medial SMC hyperplasia, vascular remodeling, pulmonary hypertension, increased bone marrow cellularity, and expansion of red pulp in the spleen, as well as reduced body size. These mice all died between 3 and 6 weeks of age (Nemenoff et al., 2008, 2011). Another group successfully circumvented the lethal phenotype observed in the VSMC-specific PTEN-null mice by using a global $PTEN^{+/-}$ $ApoE^{-/-}$ mouse. A 50% reduction in PTEN protein expression and a corresponding 50% increase in phosphorylated Akt levels was confirmed by immunoblot analysis. However, following 6 weeks of high fat diet, no significant difference in extent of atherosclerosis, VSMC content, cellularity, proliferation rate, or apoptosis levels was detected between PTEN haploinsufficient mice and ApoE-null control groups (Andres et al., 2006). Additionally, while neither of the above groups reported spontaneous cancer development, PTEN acts as a tumor suppressor and is frequently subject to

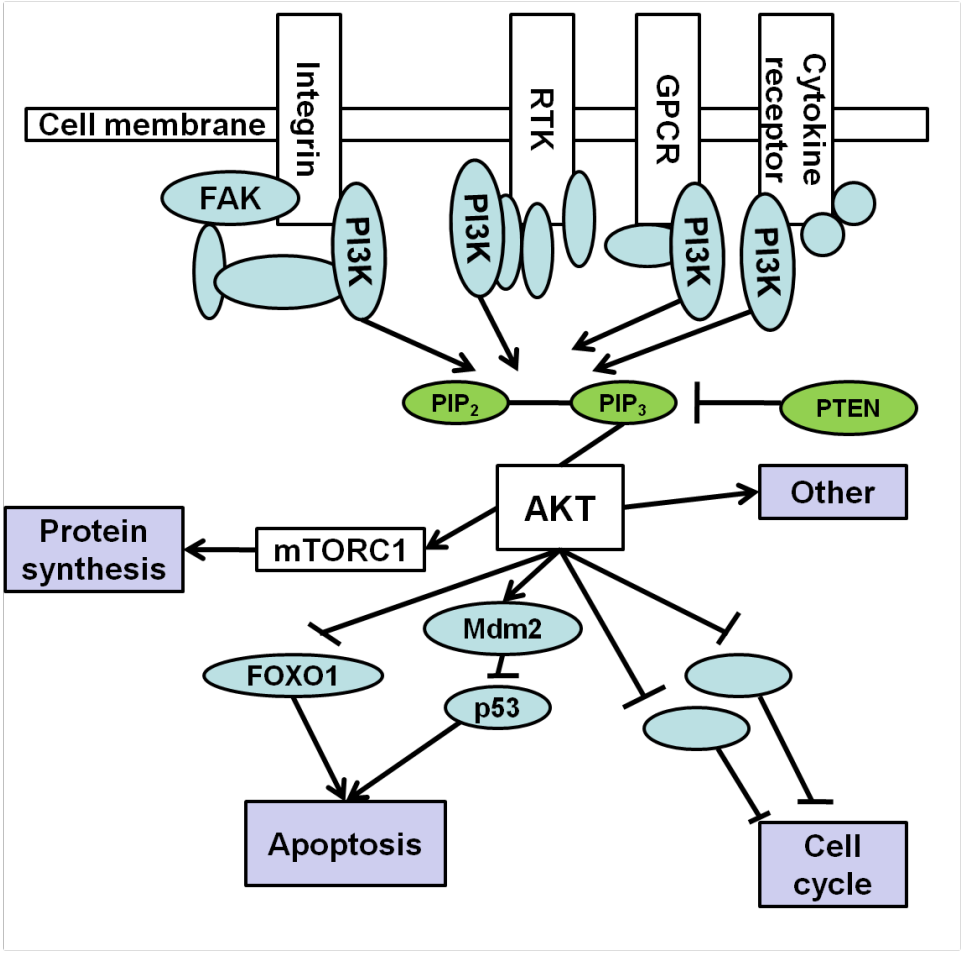

Figure 5.3: **Akt pathway.** Akt phosphorylation occurs downstream of PI3K, which phosphorylates PIP_2 to PIP_3. Loss of PTEN, which inhibits PIP3, allows increased activation of Akt. Downstream signals of Akt include increased protein synthesis, protection from apoptosis, and increased proliferation.

loss-of-function mutations in cancers of the brain, breast, prostate, and other organs (Wang et al., 2003; Li et al., 1997). We chose to cross the PTEN$^{flox/flox}$ mouse with a MyH11-Cre mouse to generate a VSMC-specific, inducible PTEN-deficient model. This model, when crossed with our SPRR3$^{-/-}$ ApoE$^{-/-}$ mice, will allow us to induce PTEN loss of function and subsequent Akt activation specifically in the VSMCs at time points of interest, such as at initiation of high fat diet (2 months of age) and after atherosclerosis has become established (4 months of high fat diet). We will then evaluate atheroma burden, VSMC apoptosis, and features of atheroma stability as described in Chapters 2 and 3 to determine whether forced upregulation of Akt activation is sufficient to rescue or reverse the SPRR3-deficient ApoE$^{-/-}$ phenotype.

5.2.2 SPRR3$^{-/-}$ ApoE$^{-/-}$ Mouse as a Novel Animal Model of Atheroma Vulnerability

As described in Chapter 1, data available from human atherosclerosis has limited value in dissecting the mechanisms driving atheroma rupture. Longitudinal studies are not feasible with histologic samples, which severely limits the possibilities for differentiating correlations from cause and effect relationships. Despite advances in live imaging technology such as computed tomography (CT), positron emission tomography (PET), and intravascular ultrasound, they lack the resolution to distinguish detailed information on atheroma cellular and molecular activity, can increase risk of adverse events, and is cost-prohibitive for sample size frequency of testing (Cocker et al., 2012; Stone et al., 2011).

Animal models, however, provide their own set of limitations. Mouse models are least costly and most easily genetically manipulated, allowing for larger sample sizes and more experimental opportunities. Yet they also have key physiological differences from humans

that have limited their use particularly in the study of initiation and of complications of advanced stage atherosclerosis such as rupture. Mice do not naturally develop atherosclerosis and must be induced through genetic manipulation of plasma lipid levels. Unlike humans, they have very thin intimas consisting of a single layer of endothelial cells and devoid of vascular smooth muscle cells. And due to their small size, they are hypothesized to undergo dramatically reduced mechanical strains across their arterial tree. Various models have been developed to achieve a more human-like atherosclerotic phenotype. At least two have been shown to cause spontaneous myocardial infarction, possibly due to a high degree of stenosis observed in the coronary vasculature or to a combination of vascular dysfunction and hypertension (Braun et al., 2002; Nakata et al., 2008). Several others have used aging, mechanical, or genetic means in an attempt to replicate the human plaque rupture phenotype of frank breakdown of the fibrous cap, contact of the circulation with the lipid-rich core, and resulting thrombosis (Johnson and Jackson, 2001; Johnson et al., 2005; Williams et al., 2002; Calara et al., 2001; Chen et al., 2013; Gough et al., 2006). While some studies have successfully demonstrated rare instances of thrombus formation or have shown fissuring of the atheroma, no one has yet replicated atheroma rupture in a mouse.

In Chapter 3, we described the consequences of SPRR3 loss in atherogenic mice on aspects of atheroma vulnerability. We found one instance of thrombus formation, though being unassociated with a plaque rupture we cannot rule out thrombosis due to plaque erosion or other causes. We also identified microinfarctions in the left ventricle of ApoE-null mice lacking SPRR3 that were not detected in ApoE-null controls. Of great interest, we observed uniquely complex coronary artery atherosclerosis, including an instance of intraplaque hemorrhage, which has not been previously reported for other models. These

data highlight the critical nature of VSMC function in atheroma progression and stability and suggest that intervention to rescue atheroma VSMC function may be of great utility in modulating human disease. Future studies will utilize assessment of coronary artery atherosclerosis as a measure of disease severity and effectiveness of interventions.

Much of our data characterizing vulnerable lesions in Chapter 3 was measured in the brachiocephalic artery. This artery feeds into the right carotid artery and from there to the brain. Any consequences of atheroma instability in the brachiocephalic artery would therefore be expected to be found in the brain. While our mice did not demonstrate evidence of severe stroke, it is possible that microinfarctions similar to those observed in the left ventricle of the SPRR3$^{-/-}$ ApoE$^{-/-}$ mice may occur without resulting in observable alterations in behavior or function. TTC (2,3,5-triphenyltetrazolium chloride) staining for focal cerebral ischemia of grossly cross-sectioned brains SPRR3$^{-/-}$ ApoE$^{-/-}$ brains would therefore complement our study of embolic vascular disease in the SPRR3-deficient mouse.

5.2.3 Using SPRR3 to Delay Atherosclerosis Progression and Instability

If SPRR3 or its pathway members are to be used as a tool for delaying atherosclerosis progression, evidence is needed that increased expression in animals with moderate to advanced atherosclerosis will halt or reverse the phenotype. In order to test this, we will generate a conditional mouse model in which SPRR3 will be overexpressed specifically within the VSMCs. We will then evaluate whether, on an atherogenic background, SPRR3 overexpression in atheroma VSMCs is sufficient to delay atheroma progression and reduce features of atheroma vulnerability. This model will also help to identify potential problems with induction of SPRR3 in VSMCs throughout the vasculature. It is possible that con-

stitutive activation of SPRR3 may promote early onset of arterial wall thickening due to accumulation of VSMCs and ECM at sites of stress or another clinically relevant phenotype. Methods for targeted drug delivery have been described that are effective in endothelial cells or bone-marrow derived cells but have not been well characterized for VSMCs, which do not have direct contact with the circulation. Tissue factor-targeted nanoparticles have been successfully used to bind VSMCs in carotid arteries after stretch induced injury (Lanza et al., 2000). These have not been investigated in uninjured arteries, however, and likely will demonstrate reduced efficacy under conditions where the VSMCs are not exposed to the circulation. However, since normal SPRR3 expression patterns are atheroma-specific, a more targeted approach to therapy may yet be found if downstream effectors could be used.

5.3 Closing

Most myocardial infarctions occur due to complications of atherosclerosis. These studies highlight the importance of VSMC function in atherosclerosis pathophysiology. Specifically, our work shows that VSMC survival and collagen synthesis as regulated by SPRR3 are critical mediators of atheroma progression and stability *in vivo*. As the first atheroma- and VSMC-specific atheroprotective protein, SPRR3 has the potential for use as a powerful preventative tool in delaying vulnerable atheroma development.

BIBLIOGRAPHY

Abifadel, M., Varret, M., Rabes, J., Allard, D., Ouguerram, K., Devillers, M., Cruaud, C., Benjannet, S., Wickham, L., Erlich, D., et al. (2003). Mutations in pcsk9 cause autosomal dominant hypercholesterolemia. *Nature Genetics*, 34:154–156.

Ait-Oufella, H., Salomon, B., Potteaux, S., Robertson, A., Gourdy, P., Zoll, J., Merval, R., Esposito, B., Cohen, J., Fisson, S., et al. (2006). Natural regulatory t cells control the development of atherosclerosis in mice. *Nature Medicine*, 12:178–180.

Alfaro, M., Vincent, A., Saraswati, S., Thorne, C., Hong, C., Lee, E., and Young, P. (2010). sfrp2 suppression of bone morphogenic protein (bmp) and wnt signaling mediates mesenchymal stem cell (msc) self-renewal promoting engraftment and moyocardial repair. *The Journal of Biological Chemistry*, 285:35645–35653.

Allard, D., Figg, N., Bennett, M., and Littlewood, T. (2008). Akt regulates the survival of vascular smooth muscle cells via inhibition of foxo3a and gsk3. *The Journal of Biological Chemistry*, 283:19739–19747.

Ambrose, J., Tannenbaum, M., Alexopoulos, D., Hjemdahl-Monsen, C., Leavy, J., Weiss, M., Borrico, S., Gorlin, R., and Fuster, V. (1988). Angiographic progression of coronary artery disease and the development of myocardial infarction. *Journal of the American College of Cardiology*, 12:56–62.

Amento, E., Ehsani, N., Palmer, H., and Libby, P. (1991). Cytokines and growth factors positively and negatively regulate interstitial collagen gene expression in human vascular smooth muscle cells. *Arteriosclerosis, Thrombosis, and Vascular Biology*, 11:1223–1230.

Andres, V., Gascon-Irun, M., Pandolfi, P., and Gonzalez-Navarro, H. (2006). Atheroma development in apoe-null mice is not affected by partial inactivation of pten. *Frontier in Biosciences*, 11:2739–2745.

Arbab-Zadeh, A., Nakano, M., Virmani, R., and Fuster, V. (2012). Acute coronary events. *Circulation*, 125:1147–1156.

Association, A. H. (2001). 2001 heart and stroke statistical update. *Dallas, Texas: American Heart Association*.

Association, A. H. (2002). 2002 heart and stroke statistical update. *Dallas, Texas: American Heart Association*.

Babaev, V., Yancey, P., Ryzhov, S., Kon, V., Breyer, M., Magnuson, M., Fazio, S., and Linton, M. (2005). Conditional knockout of macrophage ppar(1) increases atherosclerosis in c57bl/6 and low-density lipoprotein receptor-deficient mice. *Arteriosclerosis, Thrombosis, and Vascular Biology*, 25:1647–1653.

Barter, P., Caulfield, M., Eriksson, M., Grundy, S., Kastelein, J., Komajda, M., Lopez-Sendon, J., Mosca, L., Tardif, J., Waters, D., et al. (2007). Effects of torcetrapib in patients at high risk for coronary events. *The New England Journal of Medicine*, 357:2109–2122.

Bass, A. and Berk, B. (1995). Differential activation of mitogen-activated protein kinases by h2o2 and o2- in vascular smooth muscle cells. *Circulation Research*, 77:29–36.

Belmadani, S., Zerfaoui, M., Boulares, H., Palen, D., and Matrougui, K. (2008). Microvessel vascular smooth muscle cells contribute to collagen type i deposition through erk1/2 map kinase, alphavbeta3-integrin, and tgf-beta1 in response to ang ii and high glucose. *American Journal of Physiology - Heart and Circulatory Physiology*, 295:H69–H76.

Bennett, M. and Boyle, J. (1998). Apoptosis of vascular smooth muscle cells in atherosclerosis. *Atherosclerosis*, 138:3–9.

Bennett, M., Evan, G., and Schwartz, S. (1995). Apoptosis of human vascular smooth muscle cells derived from normal vessels and coronary atherosclerotic plaques. *The Journal of Clinical Investigation*, 95:2266–2274.

Birjmohun, R., Hutten, B., Kastelein, J., and Stroes, E. (2005). Efficacy and safety of high-density lipoprotein cholesterol-increasing compounds: A meta-analysis of randomized controlled trials. *Journal of the American College of Cardiology*, 45:185–197.

Blom, N., Sicheritz-Ponten, T., Gupta, R., Gammeltoft, S., and Brunak, S. (2004). Prediction of post-translational glycosylation and phosphorylation of proteins from the amino acid sequence. *Proteomics*, 4:1633–1649.

Boden, W., Probstfield, J., Anderson, T., Chaitman, B., Desvignes-Nickens, P., Koprowics, K., McBride, R., Teo, K., and Weintraub, W. (2011). Niacin in patients with low hdl cholesterol levels receiving intensive statin therapy. *The New England Journal of Medicine*, 365:2255–2267.

Boucher, P., Wi, W., Matz, R., Takayama, Y., Auwerx, J., Anderson, R., and Herz, J. (2007). Lrp1 functions as an atheroprotective integrator of tgfbeta and pdfg signals in the vascular wall: implications for marfan syndrome. *PLoS ONE*, 2:e448.

Braun, A., Trigatti, B., Post, M., Sato, K., Simons, M., Edelberg, J., Rosenberg, R., Schrenzel, M., and Krieger, M. (2002). Loss of sr-bi expression leads to the early onset of occlusive atherosclerotic coronary artery disease, spontaneous myocardial infarctions, severe cardiac dysfunction, and premature death in apolipoprotein e-deficient mice. *Circulation Research*, 90:270–276.

Brownlee, M. (2001). Biochemistry and molecular cell biology of diabetic complications. *Nature*, 414:813–820.

Brugts, J., Yetgin, T., Hoeks, S., Gotto, A., Shepherd, J., Westendorp, R., de Craen, A. M., Knopp, R., Nakamura, H., Ridker, P., et al. (2009). The benefits of statins in people

without established cardiovascular disease but with cardiovascular risk factors: meta-analysis of randomised controlled trials. *BMJ*, 338:b2376.

Cabral, A., Voskamp, P., Cleton-Jansen, A., South, A., Nizetic, D., and Backendorf, C. (2001). Structural organization and regulation of the small proline-rich family of cornified envelope precursors suggest a role in adaptive barrier function. *The Journal of Biological Chemistry*, 276:19231–19237.

Cai, H. and Harrison, D. (2000). Endothelial dysfunction in cardiovascular diseases: the role of oxidant stress. *Circulation Research*, 10:840–844.

Calara, F., Silvertre, M., Casanada, F., Yuan, N., Napoli, C., and Palinski, W. (2001). Spontaneous plaque rupture and secondary thrombosis in apolipoprotein e-deficient and ldl receptor-deficient mice. *The Journal of Pathology*, 195:257–263.

Candi, E., Schmidt, R., and Melino, G. (2005). The cornified envelope: a model of cell death in the skin. *Nature Reviews Molecular Cell Biology*, 6:328–340.

Chen, D., Krasinski, K., Chen, D., Sylvester, A., Chen, J., Nisen, P., and Andréas, V. (1997). Downregulation of cyclin-dependent kinase 2 activity and cyclin a promoter activity in vascular smooth muscle cells by p27 ^{KIP1}, an inhibitor of neointima formation in the rat carotid artery. *The Journal of Clinical Investigation*, 99:1334–1341.

Chen, Y., Bui, A., Diesch, J., Manasseh, R., Hausding, C., Rivera, J., Haviv, I., Agrotis, A., Htun, N., Jowett, J., et al. (2013). A novel mouse model of atherosclerotic plaque instability for drug testing and mechanistic/therapeutic discoveries using gene and microrna expression profiling. *Circulation Research*, 113:252–265.

Chèvre, R., González-Granado, J., Megens, R., Sreeramkumar, V., Silvertre-Roig, C., Molina-Sánchez, P., Weber, C., Soehnlein, O., Hidalgo, A., and Andrés, V. (2014). High-resolution imaging of intravascular atherogenic inflammation in live mice. *Circulation Research*, 114:770–779.

Cho, D., Jo, Y., Roh, S., Na, Y., Kim, T., Jang, S., Kim, Y., and Kim, J. (2010). Upregulation of sprr3 promotes colorectal tumorigenesis. *Molecular Medicine*, 16:271–277.

Choi, E., Collins, E., Marine, L., Uberti, M., Uchida, H., Leidenfrost, J., Khan, M., Boc, K., Abendschein, D., and Parks, W. (2005). Matrix metalloproteinase-9 modulation by resident arterial cells is responsible for injury-induced accelerated atherosclerotic plaque development in apolipoprotein edeficient mice. *Arteriosclerosis, Thrombosis, and Vascular Biology*, 25:1020–1025.

Clarke, E., Thompson, R., Allam, A., Wann, L., Lombardi, G., Sutherland, M., Sutherland, J., Cox, S., Soliman, M., Abd el-Maksoud, G., et al. (2014). Is atherosclerosis fundamental to human aging? lessons from ancient mummies. *Journal of Cardiology*, 63:329–334.

Clarke, M., Figg, N., Maguire, J., Davenport, A., Goddard, M., Littlewood, T., and Bennett, M. (2006). Apoptosis of vascular smooth muscle cells induces features of plaque vulnerability in atherosclerosis. *Nature Medicine*, 12:1075–1080.

Clarke, M., Littlewood, T., Figg, N., Maguire, J., Davenport, A., Goddard, M., and Bennett, M. (2008). Chronic apoptosis of vascular smooth muscle cells accelerates atherosclerosis and promotes calcification and medial degeneration. *Circulation Research*, 102:1529–1538.

Clarke, M., Talib, S., Figg, N., and Bennett, M. (2010). Vascular smooth muscle cell apoptosis induces interleukin-1directed inflammation: Effects of hyperlipidemia-mediated inhibition of phagocytosis. *Circulation Research*, 106:363–372.

Cocker, M., McArdle, B., Spence, J., Lum, C., Hammond, R., Ongaro, D., McDonald, M., deKemp, R., Tardif, J., and Beanlands, R. (2012). Imaging atherosclerosis with hybrid [18f]fluorodeoxyglucose positron emission tomography/computed tomography imaging: What leonardo da vinci could not see. *Journal of Nuclear Cardiology*, 19:1211–1225.

Cohen, J., Boerwinkle, E., Mosley Jr., T., and Hobbs, H. (2006). Sequence variations in *PCSK9*, low ldl, and protection against coronary heart disease. *The New England Journal of Medicine*, 354:1264–1272.

Dai, G., Vaughn, S., Zhang, Y., Wang, E., Garcia-Cardena, G., and Gimbrone, M. J. (2010). Biomechanical forces in atherosclerosis-resistant vascular regions regulate endothelial redox balance via phosphoinositol 3-iinase/akt dependent activation of nrf2. *Molecular Medicine*, 16:271–277.

Davies, M., Bland, J., Hangartner, J., Angelini, A., and Thomas, A. (1989). Factors influencing the presence or absence of acute coronary artery thrombi in sudden ischaemic death. *European Heart Journal*, 10:203–208.

De la Cruz, O., Wen, X., Ke, B., Song, M., and Nicolae, D. (2010). Gene, region and pathway level analyses in whole-genome studies. *Genetic epidemiology*, 34:222–231.

Deguchi, J., Yamazaki, H., Aikawa, E., and Aikawa, M. (2009). Chronic hypoxia activates the akt and beta-catenin pathways in human macrophages. *Arteriosclerosis, Thrombosis, and Vascular Biology*, 29:1664–1670.

DiCorleto, P. and Soyombo, A. (1993). Role of the endothelium in atherogenesis. *Current Opinion in Lipidology*, 4:364–372.

Dimmeler, S., Haendeler, J., Galle, J., and Zeiher, A. (1997). Oxidized low-density lipoprotein induces apoptosis of human endothelial cells by activation of cpp32-like proteases. *Circulation*, 95:1760–1763.

Dimmeler, S. and Zeiher, A. (2003). Exercise and cardiovascular health: get active to "aktivate" your endothelial nitric oxide synthase. *Circulation*, 107:3118–3120.

Ding, L., Biswas, S., Morton, R., Smith, J., Hay, N., Byzova, T., Febbraio, M., and Podrez, E. (2012). Akt3 deficiency in macrophages promotes foam cell formation and atherosclerosis in mice. *Cell Metabolism*, 15:861–872.

Doran, A., Lehtinen, A., Meller, N., Lipinski, M., Slayton, R., Oldham, S., Skaflen, M., Yeboah, J., Rich, S., Bowden, D., and McNamara, A. (2010). Id3 is a novel atheroprotective factor containing a functionally significant single-nucleotide polymorphism associated with intima-media thickness in humans. *Circulation Research*, 106:1303–1311.

Döring, Y., Drechsler, M., Wantha, S., Kemmerich, K., Lievens, D., Vijayan, S., Gallo, R., Weber, C., and Soehnlein, O. (2012). Lack of neutrophil-derived cramp reduces atherosclerosis in mice. *Circulation Research*, 110:1052–1056.

Durante, W., Liao, L., Reyna, S., Peyton, K., and Schafer, A. (2001). Transforming growth factor-beta1 stimulates l-arginine transport and metabolism in vascular smooth muscle cells. *Circulation*, 103:1121–1127.

Fernández-Hernando, C., Ackah, E., Yu, J., Suárez, Y., Murata, T., Iwakiri, Y., Prendergast, J., Miao, R., Birnbaum, M., and Sessa, W. (2007). Loss of akt1 leads to severe atherosclerosis and occlusive coronary artery disease. *Cell Metabolism*, 6:446–457.

Fernández-Hernando, C., József, L., Jenkins, D., Di Lorenzo, A., and Sessa, W. (2009). Absence of akt1 reduces vascular smooth muscle cell migration and survival and induces features of plaque vulnerability and cardiac dysfunction during atherosclerosis. *Arteriosclerosis, Thrombosis, and Vascular Biology*, 29:2033–2040.

Finegold, J., Asaria, P., and Francis, D. (2013). Mortality from ischaemic heart disease by country, region, and age: Statistics from world health organisation and united nations. *International Journal of Cardiology*, 168:934–945.

Fischer, D., Sark, M., Lehtola, M., Gibbs, S., van de Putte, P., and Backendorf, C. (1999). Structure and evolution of the human sprr3 gene: implications for function and regulation. *Genomics*, 55:88–99.

Galis, Z., Sukhova, G., Lark, M., and Libby, P. (1994). Increased expression of matrix metalloproteinases and matrix degrading activity in vulnerable regions of human atherosclerotic plaques. *The Journal of Clinical Investigation*, 94:2493–2503.

Geng, Y., Henderson, L., Levesque, E., Muszynski, M., and Libby, P. (1997). Fas is expressed in human atherosclerotic intima and promotes apoptosis of cytokine-primed human vascular smooth muscle cells. *Arteriosclerosis, Thrombosis, and Vascular Biology*, 17:2200–2208.

Geng, Y., Wu, Q., Muszynski, M., G.K, H., and Libby, P. (1996). Apoptosis of vascular smooth muscle cells induced by *in vitro* stimulation with interferongamma, tumor necrosis factor-alpha, and interleukin-1 beta. *Arteriosclerosis, Thrombosis, and Vascular Biology*, 16:19–27.

Getz, G. and Reardon, C. (2004). Paraoxonase, a cardioprotective enzyme: continuing issues. *Current Opinions in Lipidology*, 15:261–267.

Giroud, D., Li, J., Urban, P., Meier, B., and Rutishauser, W. (1992). Relation of the site of acute myocardial infarction to the most severe coronary arterial stenosis at prior angiography. *The American Journal of Cardiology*, 69:729–732.

Giugliano, R., Desai, N., Kohli, P., Rogers, W., Somaratne, R., Huang, F., Liu, T., Mohanavelu, S., Hoffman, E., McDonald, S., et al. (2012). Efficacy, safety, and tolerability of a monoclonal antibody to proprotein convertase subtilisin/kexin type 9 in combination with a statin in patients with hypercholesterolaemia (laplace-timi 57): a randomised, placebo-controlled, dose-ranging, phase 2 study. *The Lancet*, 380:2007–2017.

Glaser, R., Selzer, F., Faxon, D., Laskey, W., Cohen, H., Slater, J., Detre, K., and Wilensky, R. (2005). Clinical progression of incidental, asymptomatic lesions discovered during culprit vessel coronary intervention. *Circulation*, 111:143–149.

Gojova, A., Brun, V., Esposito, B., Cottrez, F., Gourdy, P., Ardouin, P., Tedgui, A., Mallat, Z., and Groux, H. (2003). Specific abrogation of transforming growth factor-beta signaling in t cells alters atherosclerotic lesion size and composition in mice. *Blood*, 102:4052–4058.

Gough, P., Gomez, I., Wille, P., and Raines, E. (2006). Macrophage expression of active mmp-9 induces acute plaque disruption in apoe-deficient mice. *The Journal of Clinical Investigation*, 116:59–69.

Gupta, S., Pablo, A., Jiang, X., Wang, N., Tall, A., and Schindler, C. (1997). Ifn-gamma potentiates atherosclerosis in apoe knock-out mice. *The Journal of Clinical Investigation*, 99:2752–2761.

Hahn, C., Orr, A., Sanders, J., Jhaveri, K., and Schwartz, M. (2009). The subendothelial extracellular matrix modulates jnk activation by flow. *Circulation Research*, 104:995–1003.

Hahn, C. and Schwartz, M. (2009). Mechanotransduction in vascular physiology and atherogenesis. *Nature Reviews Molecular Cell Biology*, 10:53–62.

Hara-Kaonga, B., Gao, Y., Havrda, M., Harrington, A., Berqquist, I., and Liaw, L. (2006). Variable recombination efficiency in responder transgenes activated by cre recombinase in the vasculature. *Transgenic Research*, 15:101–106.

Harada-Shiba, M., Kinoshita, M., Kamido, H., and Shimokado, K. (1998). Oxidized low density lipoprotein induces apoptosis in cultured human umbilical vein endothelial cells by common and unique mechanisms. *The Journal of Biological Chemistry*, 273:9681–9687.

Heidenreich, P., Trogdon, J., Khavjou, O., Butler, J., Dracup, K., Ezekowitz, M., Finkelstein, E., Hong, Y., Johnston, S., Khera, A., et al. (2011). Forecasting the future of

cardiovascular disease in the united states: A policy statement from the american heart association. *Circulation*, 123:933–944.

Hellings, W., Peeters, W., Moll, F., Piers, S., van Setten, J., Van der Spek, P., de Vries, J., Seldenrijk, K., De Bruin, P., Vink, A., et al. (2010). Composition of carotid atherosclerotic plaque is associated with cardiovascular outcome. *Circulation*, 121:1941–1950.

Hergenreider, E., Heydt, S., Tréguer, K., Boettger, T., Horrevoets, A., Zeiher, A., Scheffer, M., Frangakis, A., Yin, X., Mayr, M., et al. (2012). Atheroprotective communication between endothelial cells and smooth muscle cells through mirnas. *Nature Cell Biology*, 14:249–256.

Hetterich, H., Jaber, A., Gehring, M., Curta, A., Bamberg, F., Filipovic, N., and Rieber, J. (2015). Coronary computed tomography angiography based assessment of endothelial shear stress and its association with atherosclerotic plaque distribution *in-vivo*. *PLoS ONE*, 10:e0115408.

Hibi, K., Ishigami, T., Tamura, K., Mizushima, S., Nyui, N., Fujita, T., Ochiai, H., Kosuge, M., Watanabe, Y., Yoshii, Y., et al. (1998). Endothelial nitric oxide synthase gene polymorphism and acute myocardial infarction. *Hypertension*, 32:521–526.

Hobbs, H., Brown, M., and Goldstein, J. (1992). Molecular genetics of the ldl receptor gene in familial hypercholesterolemia. *Human Mutations*, 1:445–466.

Hohl, D., de Viragh, P., Arniguet-Barras, F., Gibbs, S., Backendorf, C., and Huber, M. (1995). The small proline-rich proteins constitute a multigene family of differentially regulated cornified cell envelope precursor proteins. *Journal of Investigative Dermatology*, 104:902–909.

Hong, M., Mintz, G., Lee, C. W., Kim, Y., Lee, S., Song, J., Han, K., Kang, D., Song, J., Kim, J., et al. (2004). Comparison of coronary plaque rupture between stable angina and acute myocardial infarction: A three-vessel intravascular ultrasound study in 235 patients. *Circulation*, 110:928–933.

Huber, S., Sakkinen, P., Conze, D., Hardin, N., and Tracy, R. (1999). Interleukin-6 exacerbates early atherosclerosis in mice. *Arteriosclerosis, Thrombosis, and Vascular Biology*, 19:2364–2367.

Ip, J., Fuster, V., Badimon, L., Badimon, J., Taubman, M., and Chesebro, J. (1990). Syndromes of accelerated atherosclerosis: role of vascular injury and smooth muscle cell proliferation. *Journal of the American College of Cardiology*, 15:1667–1687.

Johnson, J., Carson, K., Williams, H., Karanam, S., Newby, A., Angelini, G., and Jackson, S. G. C. (2005). Plaque rupture after short periods of fat feeding in the apolipoprotein eknockout mouse: Model characterization and effects of pravastatin treatment. *Circulation*, 111:1422–1430.

Johnson, J., Dwivedi, A., Somerville, M., George, S., and Newby, A. (2011). Matrix metalloproteinase (mmp)-3 activates mmp-9 mediated vascular smooth muscle cell migration and neointima formation in mice. *Arteriosclerosis, Thrombosis, and Vascular Biology*, 31:e35–e44.

Johnson, J. and Jackson, C. (2001). Atherosclerotic plaque rupture in the apolipoprotein e knockout mouse. *Atherosclerosis*, 154:399–406.

Karas, R., van Eickels, M., Lydon, J., Roddy, S., Kwoun, M., Aronovitz, M., Baur, W., Conneely, O., O'Malley, B., and Mendelsohn, M. (2001). A complex role for the progesterone receptor in the response to vascular injury. *The Journal of Clinical Investigation*, 108:611–618.

Kato, H., Suzuki, H., Tajima, S., Ogata, Y., Tominaga, T., Sato, A., and Saruta, T. (1991). Angiotensin ii stimulates collagen synthesis in cultured vascular smooth muscle cells. *Journal of Hypertension*, 9:17–22.

Khanicheh, E., Qi, Y., Xie, A., Mitterhuber, M., Xu, L., Mochizuki, M., Daali, Y., Jaquet, V., Krause, K., Ruggeri, Z., et al. (2001). Molecular imaging reveals rapid reduction of endothelial activation in early atherosclerosis with apocynin independent of antioxidative properties. *Arteriosclerosis, Thrombosis, and Vascular Biology*, 108:611–618.

Kim, J., Yu, J., Cho, Y., Jung, C., Ahn, S., Gong, G., Kim, Y., and Cho, D. (2012). Expression of sprr3 is associated with tumor cell proliferation in less advanced stages of breast cancer. *Breast Cancer Research and Treatment*, 133:909–916.

Kirii, H., Tamikazu, N., Yamada, Y., Wada, H., Saito, K., Iwakura, Y., Asano, M., Moriwaki, H., and Seishima, M. (2003). Lack of interleukin-1beta decreases the severity of atherosclerosis in apoe-deficient mice. *Arteriosclerosis, Thrombosis, and Vascular Biology*, 23:656–660.

Koren, M., Scott, R., Kim, J., Knusel, B., Liu, T., Lei, L., Bolognese, M., and Wasserman, S. (2012). Efficacy, safety, and tolerability of a monoclonal antibody to proprotein convertase subtilisin/kexin type 9 as monotherapy in patients with hypercholesterolaemia (mendel): a randomised, double-blind, placebo-controlled, phase 2 study. *The Lancet*, 380:1995–2006.

Kulkarni, A., Ward, J., Yaswen, L., Mackall, C., Bauer, S., Huh, C., Gress, R., and Karlsson, S. (1995). Transforming growth factor-beta 1 null mice. an animal model for inflammatory disorders. *The American Journal of Pathology*, 146:264–275.

Kwon, G., Schroeder, J., Amar, M., Remaley, A., and Balaban, R. (2008). Contribution of macromolecular structure to the retention of low-density lipoprotein at arterial branch points. *Circulation*, 117:2919–2927.

Kyaw, T., Tay, C., Krishnamurthi, S., Kanellakis, P., Agrotis, A., Tipping, P., Bobik, A., and Toh, B. (2011). B1a b lymphocytes are atheroprotective by secreting natural igm that increases igm deposits and reduces necrotic cores in atherosclerotic lesions. *Circulation Research*, 109:830–840.

Laine, J., Künstle, G., Obata, T., and Noguchi, M. (2002). Differential regulation of akt kinase isoforms by the members of the tcl1 oncogene family. *The Journal of Biological Chemistry*, 277:3743–3751.

Laine, J., Künstle, G., Obata, T., Sha, M., and Noguchi, M. (2000). The protooncogene tcl1 is an akt kinase coactivator. *Molecular Cell*, 6:395–407.

Langheinrich, A., Michniewicz, A., Sedding, D., Walker, G., Beighley, A., Rau, W., Bohle, R., and Ritman, E. (2006). Correlation of vasa vasorum neovascularization and plaque progression in aortas of apolipoprotein $e^{-}/^{-}$/ low-density lipoprotein$^{-}/^{-}$ double knock-out mice. *Arteriosclerosis, Thrombosis, and Vascular Biology*, 26:347–352.

Langlois, D., Forcheron, F., Li, J., del Carmine, P., Neggazi, S., and Beylot, M. (2011). Increased atherosclerosis in mice deficient in perilipin1. *Lipids in Health and Disease*, 10:169.

Lanza, G., Abendschein, D., Hall, C., Scott, M., Scherrer, D., Houseman, A., Miller, J., and Wickline, S. A. (2000). In vivo molecular imaging of stretch-induced tissue factor in carotid arteries with ligand-targeted nanoparticles. *Journal of the American Society of Echocardiography*, 13:608–614.

Law, R., Meehan, W., Xi, X., Graf, K., Wuthrich, D., Coats, W., Faxon, D., and Hsueh, W. (1996). Troglitazone inhibits vascular smooth muscle cell growth and intimal hyperplasia. *The Journal of Clinical Investigation*, 98:1897–1905.

Lehoux, S., Esposito, B., Merval, R., Loufrani, L., and Tedgui, A. (2000). Pulsatile stretch-induced extracellular signal-regulated kinase $\frac{1}{2}$ activation in organ culture of rabbit aorta involves reactive oxygen species. *Arteriosclerosis, Thrombosis, and Vascular Biology*, 20:2366–2372.

Li, J., Yen, C., Liaw, D., Podsypanina, K., Bose, S., Wang, S., Puc, J., Miliaresis, C., Rodgers, L., McCombie, R., et al. (1997). Pten, a putative protein tyrosine phosphatase gene mutated in human brain, breast, and prostate cancer. *Science*, 275:1943–1947.

Li, T., Tian, H., Zhao, Y., An, F., Zhang, L., Zhang, J., Peng, J., Zhang, Y., and Guo, Y. (2011). Heme oxygenase-1 inhibits progression and destabilization of vulnerable plaques in a rabbit model of atherosclerosis. *European Journal of Pharmacology*, 672:143–152.

Libby, P. (2013). Mechanisms of acute coronary syndromes and their implications for therapy. *The New England Journal of Medicine*, 368:2004–2013.

Lindner, V. and Reidy, M. (1991). Proliferation of smooth muscle cells after vascular injury is inhibited by an antibody against basic fibroblast growth factor. *Proceedings of the National Academy of Sciences*, 88:3739–3743.

Lindner, V. and Reidy, M. (1993). Expression of basic fibroblast growth factor and its receptor by smooth muscle cells and endothelium in injured rat arteries. an *en face* study. *Circulation Research*, 73:589–595.

Linsel-Nitschke, P., Gotz, A., Erdmann, J., Braenne, I., Braund, P., Hengstenberg, C., Stark, K., Fischer, M., Schreiber, S., El Mokhtari, N., et al. (2008). Lifelong reduction of ldl cholesterol related to a common variant in the ldl receptor gene decreases the risk of coronary artery disease a mendelian randomisation study. *PLoS One*, 3:e2986.

Linton, M., Atkinson, J., and Fazio, S. (1995). Prevention of atherosclerosis in apolipoprotein e-deficient mice by bone marrow transplantation. *Science*, 267:1034–1037.

Lutgens, E., de Muinck, E., Kitslaar, P., Tordoir, J., Wellens, H., and Daemen, M. (1999). Biphasic pattern of cell turnover characterizes the progression from fatty streaks to ruptured human atherosclerotic plaques. *Cardiovascular Research*, 41:473–479.

Lutgens, E., Gijbels, M., Smook, M., Heeringa, P., Gotwals, P., Koteliansky, V., and Daemon, M. (2002). Transforming growth factor-beta mediates balance between inflammation and fibrosis during plaque progression. *Arteriosclerosis, Thrombosis, and Vascular Biology*, 22:975–982.

Mallat, Z., Corbaz, A., Scoazec, A., Besnard, S., Lesèche, G., Chvatchko, Y., and Tedgui, A. (2001). Expression of interleukin-18 in human atherosclerotic plaques and relation to plaque instability. *Circulation*, 104:1598–1603.

Mann, J. and Davies, M. (1996). Vulnerable plaque: Relation of characteristics to degree of stenosis in human coronary arteries. *Circulation*, 94:928–931.

Mann, J. and Davies, M. (1999). Mechanisms of progression in native coronary artery disease: role of healed plaque disruption. *Heart*, 82:265–268.

Martínez-Hervás, S., Vinué, A., Núnez, L., Andrés-Blasco, I., Piqueras, L., Real, J., Ascaso, J., Burks, D., Sanz, M., and González-Navarro, H. (2014). Insulin resistance aggravates atherosclerosis by reducing vascular smooth muscle cell survival and increasing cx_3cl1/cx_3cr1 axis. *Cardiovascular Research*, 103:324–336.

Matsui, T., Li, L., Wu, J., Cook, S., Nagoshi, T., Picard, M., Liao, R., and Rosenzweig, A. (2002). Phenotypic spectrum caused by transgenic overexpression of activated akt in the heart. *The Journal of Biological Chemistry*, 277:22896–22901.

Mercer, J., Figg, N., Stoneman, V., Braganza, D., and Bennett, M. (2005). Endogenous p53 protects vascular smooth muscle cells from apoptosis and reduces atherosclerosis in apoe knockout mice. *Circulation Research*, 96:667–674.

Mifune, M., Sasamura, H., Shimizu-Hirota, R., Miyazaki, H., and Saruta, T. (2000). Angiotensin ii type 2 receptors stimulate collagen synthesis in cultured vascular smooth muscle cells. *Hypertension*, 36:845–850.

Mizuguchi, Y., Specht, S., Lunz, J. r., Isse, K., Corbitt, N., Takizawa, T., and Demetris, A. (2012). Sprr2a enhances p53 deacetylation through hdac1 and down regulates p21 promoter activity. *BMC Molecular Biology*, 13:20.

Morray, B., Goldenberg, O., Moss, A., Zareba, W., Ryan, D., McNitt, S., Eberly, S., Glazko, G., and Matthew., J. (2007). Polymorphisms in the paraoxonase and endothelial nitric oxide synthase genes and the risk of early-onset myocardial infarction. *American Journal of Cardiology*, 99:1100–1105.

Moulton, K., Vakili, K., Zurakowski, D., Soliman, M., Butterfield, C., Sylvin, E., Lo, K., Gillies, S., Javaherian, K., and Folkman, J. (2003). Inhibition of plaque neovascularization reduces macrophage accumulation and progression of advanced atherosclerosis. *Proceedings of the National Academy of Sciences*, 100:4736–4741.

Mozaffarian, D., Benjamin, E., Go, A., Arnett, D., Blaha, M., Cushman, M., deFerranti, S., Despres, J., Fullerton, H., and Howard, V. (2014). Heart disease and stroke statistics - 2015 update: a report from the american heart association. *Circulation*, 131:e29–e322.

Murphy, S., Xu, J., and Kochanek, K. (2013). Deaths: Final data for 2010. *National Vital Statistics Report*, 61:4.

Myocardial Infarction Genetics Consortium (2009). Genome-wide association of early-onset myocardial infarction with common single nucleotide polymorphsims, common copy number variants, and rare copy number variants. *Nature Genetics*, 41:334–341.

Nahrendorf, M., Zhang, H., Hembrador, S., Panizzi, P., Sosnovik, D., Aikawa, E., Libby, P., Swirski, F., and Weissleder, R. (2008). Nanoparticle pet-ct imaging of macrophages in inflammatory atherosclerosis. *Circulation*, 117:379–387.

Nakamura, H. and Ohtsubo, K. (1992). Ultrastructure appearance of atherosclerosis in human and experimentally-induced animal models. *Electron Microscopy Reviews*, 5:129–170.

Nakata, S., Tsutsui, M., Shimokawa, H., Suda, O., Morishita, T., Shibata, K., Yatera, Y., Sabanai, K., Tanimoto, A., Nagasaki, M., et al. (2008). Spontaneous myocardial infarction in mice lacking all nitric oxide synthase isoforms. *Circulation*, 117:2211–2223.

Napoli, C., Crudele, V., Soricelli, A., Al-Omran, M., Vitale, N., Infante, T., and Mancini, F. (2012). Primary prevention of atherosclerosis: A clinical challenge for the reversal of epigenetic mechanisms? *Circulation*, 125:2363–2373.

Napoli, C., D'Armiento, F., Mancini, F., Postiglione, A., Witztum, J., Palumbo, G., and Palinski, W. (1997). Fatty streak formation occurs in human fetal aortas and is greatly enhanced by maternal hypercholesterolemia. *The Journal of Clinical Investigation*, 100:2680–2690.

Navab, M., Reddy, S., Van Lenten, B., and Fogelman, A. (2011). Hdl and cardiovascular disease: atherogenic and atheroprotective mechanisms. *Nature Reviews Cardiology*, 8:222–232.

Nemenoff, R., Horita, H., Ostriker, A., Furgeson, S., Simpson, P., VanPutten, V., Crossno, J., Offermanns, S., and Weiser-Evans, M. (2011). Sdf-1alpha induction in mature smooth

muscle cells by inactivation of pten is a critical mediator of exacerbated injury-induced neointima formation. *Arteriosclerosis, Thrombosis and Vascular Biology*, 31:1300–1308.

Nemenoff, R., Simpson, P., Furgeson, S., Kaplan-Albuquerque, N., Crossno, J., Garl, P., Cooper, J., and Weiser-Evans, M. (2008). Targeted deletion of pten in smooth muscle cells results in vascular remodeling and recruitment of progenitor cells through induction of stromal cell-derived factor-1alpha. *Circulation Research*, 102:1036–1045.

Ni, C., Qiu, H., Rezvan, A., Kwon, K., Nam, D., Son, D., Visvader, J., and Jo, H. (2010). Discovery of novel mechanosensitive genes *in vivo* using mouse carotid artery endothelium exposed to disturbed flow. *Blood*, 14:e66–e73.

NIH (2000). Working group on atheroprotective genes. NIH Heart, Lung, and Blood Institute.

Paigen, B., Morrow, A., Holmes, P., Mitchell, D., and Williams, R. (1987). Quantitative assessment of atherosclerotic lesions in mice. *Atherosclerosis*, 68:231–240.

Park, J., Yoo, J., Jeong, S., Choi, J., Lee, M., Lee, M., Lee, J. H., Kim, H., Jo, H., Yu, D., et al. (2011). Peroxiredoxin 2 deficiency exacerbates atherosclerosis in apolipoprotein e-deficient mice. *Circulation Research*, 109:739–749.

Ponticos, M., Partridge, T., Black, C., Abraham, D., and Bou-Gharios, G. (2004). Regulation of collagen type i in vascular smooth muscle cells by competition between nkx2.5 and delta-ef1/zeb1. *Molecular Cell Biology*, 24:6151–6161.

Pozzi, A., Moberg, P., Miles, L., Wagner, S., Soloway, P., and Gardner, H. (2000). Elevated matrix metalloprotease and angiostatin levels in integrin knockout mice cause reduced tumor vascularization. *Proceedings of the National Academy of Sciences*, 97:2202–2207.

Pradervand, S., Yasukawa, H., Muller, O., Kjekshus, H., Nakamura, T., St. Amand, T., Yajima, T., Matsumura, K., Duplain, H., Iwatate, M., et al. (2004). Small proline-rich protein 1a is a gp130 pathway- and stress-inducible cardioprotective protein. *The EMBO Journal*, 23:4517–4525.

Pyle, A., Atkinson, J., Pozzi, A., Reese, J., Eckes, B., Davidson, J., Crimmins, D., and Young, P. (2008). Regulation of the atheroma-enriched protein, sprr3, in vascular smooth muscle cells through cyclic strain is dependent on integrin $\text{alpha}_1\text{beta}_1$/collagen interaction. *American Journal of Pathology*, 173:1577–1588.

Pyle, A., Li, B., Maupin, A., Guzman, R., Crimmins, D., Olson, S., Atkinson, J., and Young, P. (2010). Biomechanical stress induces novel arterial intima-enriched genes: implications for vascular adaptation to stress. *Cardiovascular Pathology*, 19:e13–e20.

Raal, F., Scott, R., Somaratne, R., Bridges, I., Li, G., Wasserman, S., and Stein, E. (2012). Low-density lipoprotein cholesterollowering effects of amg 145, a monoclonal antibody

to proprotein convertase subtilisin/kexin type 9 serine protease in patients with heterozygous familial hypercholesterolemia: The reduction of ldl-c with pcsk9 inhibition in heterozygous familial hypercholesterolemia disorder (rutherford) randomized trial. *Circulation*, 126:2408–2417.

Reid, V., Brabbs, C., and Mitchinson, M. (1992). Cellular damage in mouse peritoneal macrophages exposed to cholesteryl linoleate. *Atherosclerosis*, 92:251–260.

Reif, S., Lang, A., Lindquist, J., Yata, Y., Gabele, E., Scanga, A., Brenner, D., and Rippe, R. (2002). The role of focal adhesion kinase-phosphatidylinositol 3-kinase-akt signaling in hepatic stellate cell proliferation and type i collagen expression. *Journal of Biological Chemistry*, 278:8083–8090.

Rensing, K., de Jager, S., Stroes, E., Vos, M., Twickler, M., Dallinga-Thie, G., de Vries, C., Kuiper, J., Bot, I., and von der Thüsen, J. (2014). Akt2/ldlr double knockout mice display impaired glucose tolerance and develop more complex atherosclerotic plaques than ldlr knockout mice. *Cardiovascular Research*, 101:277–287.

Richardson, P., Davies, M., and Born, G. (1989). Influence of plaque configuration and stress distribution on fissuring of coronary atherosclerotic plaques. *The Lancet*, 2:941–944.

Risch, N. (2000). Searching for genetic determinants in the new millennium. *Nature*, 405:847–856.

Ritchie, M., Denny, J., Crawford, D., Ramirez, A., Weiner, J., Pulley, J., Basford, M., Brown-Gentry, K., Balser, J., Masys, D., et al. (2010). Robust replication of genotype-phenotype associations across multiple diseases in an electronic medical records. *American Journal of Human Genetics*, 86:560–572.

Roger, V., Go, A., Lloyd-Jones, D., Benjamin, E., Berry, J., Borden, W., Bravata, D., Dai, S., Ford, E., Fox, C., et al. (2012). Heart disease and stroke statistics2012 update: a report from the american heart association. *Circulation*, 125:e2–e220.

Ross, R., Glomset, J., and Harker, L. (1977). Response to injury and atherogenesis. *American Journal of Pathology*, 86:675–684.

Sandirasegarane, L. and Kester, M. (2001). Enhanced stimulation of akt-3/protein kinase b-gamma in human aortic smooth muscle cells. *Biochemical and Biophysical Research Communications*, 283:158–163.

Sawada, N., Itoh, H., Ueyama, K., Yamashita, J., Doi, K., Chun, T., Inoue, M., Masatsugu, K., Saito, T., Fukunaga, Y., et al. (2000). Inhibition of rho-associated kinase results in suppression of neointimal formation of balloon-injured arteries. *Circulation*, 101:2030–2033.

Schapira, K., Lutgens, E., de Fougerolles, A., Sprague, A., Roemen, A., Gardner, H., Koteliansky, V., Daemen, M., and Heeneman, S. (2005). Genetic deletion or antibody

blockade of alpha1beta1 integrin induces a stable plaque phenotype in apoe$^{-/-}$ mice. *Arteriosclerosis, Thrombosis, and Vascular Biology*, 25:1917–1924.

Schaub, F., Han, D., Liles, W., Adams, L., Coats, S., Ramachandran, R., Seifert, R., Schwartz, S., and Bowen-Pope, D. (2000). Fas/fadd-mediated activation of a specific program of inflammatory gene expression in vascular smooth muscle cells. *Nature Medicine*, 6:790–796.

Schaub, F., Liles, W., Ferri, N., Sayson, K., Seifert, R., and Bowen-Pope, D. (2003). Fas and fas-associated death domain protein regulate monocyte chemoattractant protein-1 expression by human smooth muscle cells through caspase- and calpain-dependent release of interleukin-1alpha. *Circulation Research*, 93:515–522.

Schunkert, H., Konig, I., Kathiresan, S., Reilly, M., Assimes, T., Holm, H., Preuss, M., Stewart, A., Barbalic, M., Geiger, C., Absher, D., et al. (2011). Large-scale association analysis identifies 13 new susceptibility loci for coronary artery disease. *Nature Genetics*, 43:333–338.

Schwartz, S., Galis, Z., Rosenfeld, M., and Falk, E. (2007). Plaque rupture in humans and mice. *Arteriosclerosis, Thrombosis, and Vascular Biology*, 27:705–713.

Segedy, A., Pyle, A., Li, B., Zhang, Y., Babaev, V., Jat, P., Fazio, S., Atkinson, J., Linton, M. F., and Young, P. (2014). Identification of small proline-rich repeat protein 3 as a novel atheroprotective factor that promotes adaptive akt signaling in vascular smooth muscle cells. *Arteriosclerosis, Thrombosis, and Vascular Biology*, 34:2527–2536.

Seimon, T., Wang, Y., Han, S., Senokuchi, T., Schrijvers, D., Kuriakose, G., Tall, A., and Tabas, I. (2009). Macrophage deficiency of p38-alpha mapk promotes apoptosis and plaque necrosis in advanced atherosclerotic lesions in mice. *The Journal of Clinical Investigation*, 119:886–898.

Shah, P. (2001). Link between infection and atherosclerosis: Who are the culprits: Viruses, bacteria, both, or neither? *Circulation*, 103:5–6.

Shi, W., Wang, X., Wang, N., McBride, W., and Lusis, A. (2000). Effect of macrophage-derived apolipoprotein e on established atherosclerosis in apolipoprotein e-deficient mice. *Arteriosclerosis, Thrombosis, and Vascular Biology*, 20:2261–2266.

Shioi, T., Kang, P., Douglas, P., Hampe, J., Yballe, C., Lawitts, J., Cantley, L., and Izumo, S. (2000). The conserved phosphoinositide 3-kinase pathway determines heart size in mice. *The EMBO Journal*, 19:2537–2548.

Silence, J., Lupu, F., Collen, D., and Lijnen, H. (2001). Persistence of atherosclerotic plaque but reduced aneurysm formation in mice with stromelysin-1 (mmp-3) gene inactivation. *Arteriosclerosis, Thrombosis, and Vascular Biology*, 21:1440–1445.

Stary, H., Chandler, A., Dinsmore, R., Fuster, V., Glagov, S., Rosenfeld, M., Schwartz, C., Wagner, W., and Wissler, R. (1995). A definition of advanced types of atherosclerotic

lesions and a histological classification of atherosclerosis: A report from the committee on vascular lesions of the council on arteriosclerosis. *Arteriosclerosis, Thrombosis, and Vascular Biology*, 15:1512–1531.

Stary, H., Chandler, A., Glagov, S., Guyton, J., Insull, W., Rosenfeld, M., Schaffer, S., Schwartz, C., Wagner, W., and Wissler, R. (1994). A definition of initial, fatty streak, and intermediate lesions of atherosclerosis: A report from the committee on vascular lesions of the council on arteriosclerosis, american heart association. *Arteriosclerosis, Thrombosis, and Vascular Biology*, 14:840–856.

Steinert, P., Candi, E., Tarcsa, E., Marekov, L., Sette, M., Paci, M., Ciani, B., Guerrieri, P., and Melino, G. (1999). Transglutaminase crosslinking and structural studies of the human small proline rich 3 protein. *Cell Death and Differentiation*, 6:916–930.

Stone, G., Maehara, A., Lansky, A., de Bruyne, B., Cristea, E., Mintz, G., Mehran, R., McPherson, J., Farhat, N., Marso, S., et al. (2011). A prospective natural-history study of coronary atherosclerosis. *The New England Journal of Medicine*, 364:226–235.

Stronach, E., Chen, M., Maginn, E., Argarwal, R., Mills, G., Wasan, H., and Gabra, H. (2011). Dna-pk mediates akt activation and apoptosis inhibiton in clinically acquired platinum resistance. *Neoplasia*, 13:1069–1080.

Sullivan, D., Olsson, A., Scott, R., Kim, J., Xue, A., Gebski, V., Wassterman, S., and Stein, E. (2012). Effect of a monoclonal antibody to pcsk9 on low-density lipoprotein cholesterol levels in statin-intolerant patients: The gauss randomized trial. *The Journal of the American Medical Association*, 308:2497–2506.

Sun, J., Sukhova, G., Wolters, P., Yang, M., Kitamoto, S., Libby, P., MacFarlane, L., Clair, J. M., and Shi, G. (2007). Mast cells promote atherosclerosis by releasing proinflammatory cytokines. *Nature Medicine*, 13:719–724.

Surapisitchat, J., Hoefen, R., Pi, X., Yoshizumi, M., Yan, C., and Berk, B. (2001). Fluid shear stress inhibits tnf-alpha activation of jnk but not erk1/2 or p38 in human umbilical vein endothelial cells: Inhibitory crosstalk among mapk family members. *Proceedings of the National Academy of Science*, 98:6476–6481.

Tabas, I. (2002). Cholesterol in health and disease. *The Journal of Clinical Investigation*, 110:583–590.

Tabas, I., Williams, K., and Borén, J. (2007). Subendothelial lipoprotein retention as the initiating process in atherosclerosis. *Circulation*, 116:1832–1844.

Thim, T., Hagensen, M., Bentzon, J., and Falk, E. (2008). From vulnerable plaque to atherothrombosis. *Journal of Internal Medicine*, 263:506–516.

Thompson, R., Allam, A., Lombardi, G., Wann, L., Sutherland, M., Sutherland, J., Soliman, M., Frohlich, B., Mininberg, D., Monge, J., et al. (2013). Atherosclerosis across 4000 years of human history: the horus study of four ancient populations. *The Lancet*, 381:1211–1222.

Vengrenyuk, Y., Carlier, S., Xanthos, S., Cardoso, L., Ganatos, P., Virmani, R., Einav, S., Gilchrist, L., and Weinbaum, S. (2006). A hypothesis for vulnerable plaque rupture due to stress-induced debonding around cellular microcalcifications in thin fibrous caps. *Proceedings of the National Academy of Sciences*, 103:14678–14683.

Virmani, R., Burke, A., Kolodgie, F., and Farb, A. (2003). Pathology of the thin-cap fibroatheroma. *Journal of Interventional Cardiology*, 16:267–272.

Virmani, R., Kolodgie, F., Burke, A., Farb, A., and Schwartz, S. (2000). Lessons from sudden coronary death: A comprehensive morphological classification scheme for atherosclerotic lesions. *Arteriosclerosis, Thrombosis, and Vascular Biology*, 20:1262–1275.

Virmani, R., Kolodgie, F., Burke, A., Finn, A., Gold, H., Tulenko, T., Wrenn, S., and Narula, J. (2005). Atherosclerotic plaque progression and vulnerability to rupture angiogenesis as a source of intraplaque hemorrhage. *Arteriosclerosis, Thrombosis, and Vascular Biology*, 25:2054–2061.

Voight, B., Peloso, G., Orho-Melander, M., Frikke-Schmidt, R., Barbalic, M., Jensen, M., Hindy, G., Hólm, H., Ding, E., Johnson, T., et al. (2012). Plasma hdl cholesterol and risk of myocardial infarction: a mendelian randomisation study. *The Lancet*, 380:572–580.

Voloshenyuk, T., Landesman, E., Khoutorova, E., Hart, A., and Gardner, J. (2011). Induction of cardiac fibroblast lysyl oxidase by tgf-1 requires pi3k/akt, smad3, and mapk signaling. *Cytokine*, 55:90–97.

von der Leyen, H., Gibbons, G., Morishita, R., Lewis, N., Zhang, L., Nakajima, M., Kaneda, Y., Cooke, J., and Dzau, V. (1995). Gene therapy inhibiting neointimal vascular lesion: In vivo transfer of endothelial cell nitric oxide synthase gene. *Proceedings of the National Academy of Sciences*, 92:1137–1141.

Vuust, J., Sobel, M., and Martin, G. (1985). Regulation of type i collagen synthesis: Total pro-alpha-1(i) and pro-alpha-2(i) mrnas are maintained in a 2:1 ratio under varying rates of collagen synthesis. *European Journal of Biochemistry*, 151:449–453.

Wang, P., Xu, T., Guan, Y., Zhao, Y., Li, Z., Lan, X., Wang, X., Yang, P., Kang, Z., Vanhoutte, P., and Miao, C. (2014). Vascular smooth muscle cell apoptosis is an early trigger for hypothyroid atherosclerosis. *Cardiovascular Research*, 102:448–459.

Wang, S., Gao, J., Lei, Q., Rozengurt, N., Pritchard, C., Jiao, J., Thomas, G., Li, G., Roy-Burman, P., Nelson, P., et al. (2003). Prostate-specific deletion of the murine pten tumor suppressor gene leads to metastatic prostate cancer. *Cancer Cell*, 4:209–221.

Williams, H., Johnson, J., Carson, K., and Jackson, C. (2002). Characteristics of intact and ruptured atherosclerotic plaques in brachiocephalic arteries of apolipoprotein e knockout mice. *Arteriosclerosis, Thrombosis, and Vascular Biology*, 22:788–792.

Williams, K. and Tabas, I. (1995). The response-to-retention hypothesis of early atherogenesis. *Arteriosclerosis, Thrombosis, and Vascular Biology*, 15:551–561.

Williams, K. and Tabas, I. (1998). The response-to-retention hypothesis of atherogenesis reinforced. *Current Opinion in Lipidology*, 9:471–474.

Witztum, J. and Steinberg, D. (2001). The oxidative modification hypothesis of atherosclerosis: does it hold for humans? *Trends in Cardiovascular Medicine*, 11:93–102.

Woo, K., Qu, X., Babaev, V., Linton, M., Guzman, R., Fazio, S., and Baldwin, H. (2011). Tie1 attenuation reduces murine atherosclerosis in a dose-dependent and shear stressspecific manner. *The Journal of Clinical Investigation*, 121:1624–1635.

Xu, Q., Liu, Y., Gorospe, M., Udelsman, R., and Holbrook, N. (1996). Acute hypertension activates mitogen-activated protein kinases in arterial wall. *The Journal of Clinical Investigation*, 97:508–514.

Yang, X., Thomas, D., Zhang, X., Culver, B., Alexander, B., Murdoch, W., Rao, M., Tulis, D., Ren, J., and Sreejayan, N. (2006). Curcumin inhibits platelet-derived growth factor-stimulated vascular smooth muscle cell function and injury-induced neointima formation. *Arteriosclerosis, Thrombosis, and Vascular Biology*, 26:85–90.

Yap, C., Liu, X., and Pekkan, K. (2014). Characterization of the vessel geometry, flow mechanics and wall shear stress in the great arteries of wildtype prenatal mouse. *PLoS ONE*, 9:e86878.

Young, P., Modur, V., Teleron, A., and Ladenson, J. (2005). Enrichment of genes in the aortic intima that are associated with stratified epithelium: implications of underlying biomechanical and barrier properties of the arterial intima. *Circulation*, 111:2382–2390.

Zarins, C., Giddens, D., B.K, B., Sottiurai, V., Mabon, R., and Glagov, S. (1983). Carotid bifurcation atherosclerosis. quantitative correlation of plaque localization with flow velocity profiles and wall shear stress. *Circulation Research*, 53:502–514.

Zhou, X., Nicoletti, A., Elhage, R., and Hansson, G. (2000). Transfer of cd4$^+$ t cells aggravates atherosclerosis in immunodeficient apolipoprotein e knockout mice. *Circulation*, 102:2919–2922.